Micro-computed Tomography Validation of Cochlear Implant Electrode Position

Dr. Alon Taylor MD BE BSc (Adv)

A thesis submitted to fulfil the requirements of the degree of Master of Philosophy

Faculty of Medicine and Health

The University of Sydney

May 2026

Table of Contents

Statement of Originality

This is to certify that the content of this thesis is my own work. This thesis has not been submitted for any other degree or purpose.

I certify that all assistance received in preparing this thesis and all sources has been acknowledged.

Dr. Alon Taylor

Monday 27th April 2026

Acknowledgements

As the author I, Alon Taylor (AT), would like to make the following acknowledgements regarding assistance provided to me in the writing of this thesis:

Specimen preparation

The cadaveric specimens (including the expertise, equipment and lab costs associated with preparing these specimens), the cochlear implant electrodes and the facility required for microsurgical implantation of the bones were provided by Cochlear Ltd. (Macquarie Park, NSW). Please see the section 'Industry Support' for further details. Assistance was provided by several Cochlear Ltd employees with regards to the above:

- **Mr. Irfan Durmo**: procured and prepared the cadaveric temporal bones for implantation and undertook post-implantation post-processing of specimens to prepare them for clinical imaging.
- **Dr. Nick Pawsey** and **Dr. Zachary Smith**: assisted in the overall study direction and with the logistics of cadaveric temporal bone procurement.

MicroCT imaging

MicroCT imaging was undertaken at the Sydney Microscopy & Microanalysis (The University of Sydney, Camperdown, NSW) with assistance from **Dr. Matthew Foley** (Deputy Facility Manager, Analysis & X-Ray Microscopy Manager; Sydney Microscopy & Microanalysis)

Multidetector CT and cone-beam CT imaging

Multidetector and cone-beam CT imaging was undertaken at Castlereagh Imaging Westmead (Westmead, NSW) with assistance from **Mr. Stuart Allan** (Chief Radiographer, Castlereagh Imaging Westmead).

Mr. Christopher Nuzzo (CN) and Mr. Himath Siriniwasa (HS)

CN and HS are two University of Sydney School of Medicine (MD) students who undertook a related project as a part of their capstone MD project. Their work has been submitted separately to meet their MD project requirements.

CN and HS assisted in this thesis in two ways

1. Systematic Review - CN and HS separately and independently undertook the search strategy, reviewed and selected studies, and evaluated these against eligibility criteria, for the purposes of performing a systematic review (which forms Chapter 1 of this study). All data extraction, data analysis and subsequent writing of Chapter 1 was performed by the thesis author (AT).
2. Inter-observer variability assessment – CN and HS separately and independently performed the same measurements on the 12 implanted specimens for the purposes of their MD project. These measurements are used in this thesis to undertake an 'inter-observer variability assessment', against the measurements/results performed by the thesis author (AT).

A/Prof. Melville Da Cruz (MDC)

As my primary supervisor, A/Prof Da Cruz assisted with overall project direction, technical and subject matter support. MDC reviewed the draft thesis manuscript and provided feedback throughout the editing process.

A/Prof. Kerry Hitos (KH)

As my secondary supervisor, A/Prof. Hitos provided guidance, recommendations and proofing of the statistical methodology used in this project.

Author Attribution Statement

This thesis contains material that was created during the period 1st July 2022 – 31st December 2025.

List of Presentations

Findings of this project were presented as an:

1. e-Poster presentation at the 75th annual Australian Society of Otolaryngology-Head and Neck Surgery (ASOHNS) Annual Scientific Meeting (Friday 28th – Sunday 30th March 2025, Sydney NSW). Presented by *Dr. Alon Taylor*.
2. Oral presentation at the University of Sydney FMH HDR Conference (Wednesday 23rd July 2025, Westmead Hospital, Sydney). Presented by *Dr. Alon Taylor.*
3. e-Poster presentation at the 15th Asia Pacific Symposium on Cochlear Implants and Related Sciences (APSCI 2025) in Kuala Lumpur, Malaysia (Wednesday 12th – Saturday 15th November 2025). Presented by *A/Prof. Melville Da Cruz*.

Artificial Intelligence (AI)

During the preparation of this thesis, I used ChatGPT (OpenAI) and Google Gemini (Google) for the purpose of text enhancement, and in guiding the use of SPSS for the purposes of statistical analysis. The use of these generative AI tools included paraphrasing, sentence and paragraph structure. I confirm that where text was modified by generative AI, the content was reviewed for possible errors, inaccuracies and bias.

I take full responsibility for the submitted thesis, confirm the work is my own and declare that generative AI was used within the parameters as laid out in the 'University of Sydney, Generative-AI: Guidelines for researchers[*]'.

Australian Government Support

This research was supported by an Australian Government Research Training Program (RTP) Scholarship.

[*] Available at https://sydneyuni.service-now.com/sm?id=kb_article_view&sysparm_article=KB0031813

Industry Support

This thesis is based on research conducted with support of industry partnerships, as follows:

1. **Cochlear Ltd.** (Macquarie Park, NSW) provided material support for this project as follows: provision, storage and pre-preparation of human cadaveric temporal bone specimens; the facilities for cochlear implantation of these specimens under standard microsurgical laboratory conditions; all equipment required for electrode implantation; the cochlear implant electrodes themselves; post-implantation fixation and specimen preparation; all labour and facility costs associated with the above. The provision of this expertise, labour and all equipment was provided by Cochlear Ltd. as a part of a pre-arranged, investigator-initiated research agreement between my supervisor (A/Prof Melville Da Cruz) and Cochlear Ltd. This agreement stipulates issues pertaining to project data and tangible property, project intellectual property, confidentiality and publications.
2. **Castlereagh Imaging Westmead** (Westmead, NSW) undertook clinical CT imaging (specifically, multidetector CT and cone-beam CT imaging) of the specimens. All labour, scan time and expertise associated with scanning were provided by Castlereagh Imaging as support in-kind.

Glossary of Terms

Angular insertion depth (AID) – the angle, expressed in degrees, through which the intracochlear portion of a cochlear implant electrode array is inserted into the cochlea.

Bamford-Kowal-Bench Speech-in-Noise (BKB-SIN) test –– a standardised speech perception test that assesses sentence recognition in the presence of background noise using Bamford–Kowal–Bench sentence lists. Performance is expressed as the signal-to-noise ratio required for 50% sentence recognition. Test scores are commonly used to evaluate functional hearing in cochlear implant recipients.

Basal turn – the lowermost and widest segment of the cochlear spiral, located adjacent to the round window and corresponding to the high-frequency region of the cochlea. Following cochlear implantation, most electrode contacts are located within the basal turn.

Basilar membrane – a fibroelastic membrane that forms the floor of the scala media and separates it from the scala tympani. The organ of Corti rests upon its surface.

Cochlear aperture – the opening of the distal internal acoustic canal which transmits the cochlear nerve.

Cochlear implant – an implantable auditory prosthesis which provides electrical stimulation of the cochlear nerve to enable hearing. It consists of an external sound processor and an internal receiver-stimulator connected to an intracochlear electrode array.

Consonant-nucleus-consonant (CNC) word recognition test – a standardised speech perception assessment that evaluates monosyllabic word recognition using consonant-nucleus-consonant (CNC) word lists. Results are reported as the percentage of correctly identified words. CNC scores are commonly used to quantify auditory performance in cochlear implant recipients.

Computed tomography (CT) – an imaging modality that uses rotating x-ray beams and mathematical reconstruction algorithms to generate cross-sectional images representing the spatial distribution of x-ray attenuation within biological tissues.

Cone-beam CT (CBCT) – a clinical CT modality that uses a cone-shaped x-ray beam and flat-panel detector to acquire a volumetric dataset in a single rotation, most commonly in dental and otologic imaging.

Electrode array – the flexible, linear assembly of multiple electrode contacts and insulating segments that is inserted into the cochlea during cochlear implantation. It is a collective term referring to the assembled intracochlear device and its constituent components (i.e. electrode contacts, carrier or substrate, insulating material and lead wires).

Electrode contact – an individual conductive element on a cochlear implant electrode array that delivers electrical current to the surrounding perilymph and neural tissues. Each contact represents a discrete stimulation site and is spatially localised along the length of the array. The number and spacing of electrode contacts vary according to electrode array design and manufacturer.

Electrode to modiolus distance (EMD) – the radial, straight line distance between a given cochlear implant electrode contact and the modiolar axis.

Electrode-neural interface (ENI) – the spatial and functional relationship between a cochlear implant electrode array and the target neural elements of the auditory pathway (i.e. the spiral ganglion neurons within the modiolus).

Flat-panel volumetric CT (fpVCT) – a high-resolution CT technique implemented on angiographic or hybrid imaging systems that uses a flat-panel detector to generate isotropic volumetric data.

Frequency-to-place mismatch – a discrepancy between the frequency assigned to an electrode contact by the cochlear implant speech processor and the characteristic frequency of the cochlear location being stimulated. This can adversely affect pitch perception, speech understanding and adaptation following cochlear implantation.

Helicotrema – the small apical opening at the cochlear apex where the scala tympani and scala vestibuli communicate.

Homogeneity factor (HF) – a quantitative metric describing the variance in the electrode to modiolus distance along the length of the electrode array.

Hounsfield unit (HU) - a quantitative scale used in computed tomography to express tissue x-ray attenuation relative to water. Hounsfield units provide a standardised measure of tissue density.

Inserted electrode length (IEL) – the cumulative length of a cochlear implant electrode array that lies within the cochlea.

Intraclass correlation coefficient (ICC) – a statistical measure of reliability that quantifies the degree of agreement or consistency between repeated measurements of the same variable, either by different observers or across multiple measurement occasions.

Intracochlear electrode position index (ICPI) – a quantitative metric designed to summarise the intracochlear position of a cochlear implant electrode array relative to the modiolus and the lateral cochlear wall.

Lamina cribosa – a sieve-like bony plate at the fundus of the internal acoustic meatus, perforated by multiple openings that transmit cochlear nerve fibres and accompanying vessels between the cochlea and the internal acoustic canal.

Lateral wall length (LWL) – the curvilinear distance measured along the outer (lateral) wall of the cochlear spiral, extending from the round window to a defined apical endpoint.

Microcomputed tomography (microCT) – a non-clinical, high-resolution, small-field CT technique capable of achieving voxel sizes in the micron, providing near-histological visualisation of cochlear anatomy and serving as a reference modality for *ex vivo* assessment of intracochlear electrode position.

Modiolus – the central, conical bony core of the cochlea through which the spiral ganglion neurons and cochlear nerve fibres run.

Modiolar axis – an imaginary line running longitudinally through the centre of the modiolus, representing the geometric axis of the cochlear spiral and serving as a reference for metrics of intracochlear electrode position.

Multidetector CT (MDCT) – a clinical CT modality that uses multiple rows of energy-integrating detector elements to acquire volumetric data with thin collimation during continuous gantry rotation. It enables rapid volumetric imaging and is the standard clinical modality for temporal bone imaging.

Organ of Corti – the specialised sensory epithelium of the cochlea situated on the basilar membrane within the scala media. It contains inner and outer hair cells and supporting structures responsible for mechanoelectrical transduction of sound.

Photon counting CT (PCCT) – an emerging clinical CT modality that uses photon-counting detectors to register individual x-ray photons and their energies.

Reissner's membrane – a thin membranous partition separating the scala media from the scala vestibuli.

Signal-to-noise ratio (SNR, audiology) – a measure of the level of a desired acoustic signal relative to background noise, typically expressed in decibels. In speech perception testing, SNR represents the relative

intensity of speech compared with competing noise and determines the listening conditions required for accurate speech recognition.

Signal-to-noise ratio (SNR, imaging) – a quantitative measure of image quality defined as the ratio of the mean signal intensity within a region of interest to the standard deviation of background noise. Higher SNR indicates improved image quality and greater ability to resolve anatomical detail.

Scalar position – the location of a cochlear implant electrode within one of the cochlea's fluid-filled scalae, most commonly the scala tympani and less frequently the scala vestibuli or scala media.

Scala media – the central compartment of the cochlea, lying between the scala vestibuli superiorly and the scala tympani inferiorly.

Scala tympani – the inferior, perilymph-filled cochlear compartment that begins at the round window and extends to the helicotrema. It is the intended lumen for most cochlear implant electrode insertions.

Scala vestibuli – the superior, perilymph-filled cochlear compartment that begins at the oval window and spirals towards the helicotrema, where it becomes contiguous with the scala tympani.

Spearman's rho (ρ) – a non-parametric measure of rank correlation that assesses the strength and direction of a monotonic association between two variables. It is commonly used when relationships are ordinal rather than linear.

Synchrotron radiation phase contrast imaging (SR-PCI) – an advanced, non-clinical x-ray imaging technique that exploits the high brilliance, coherence, and collimation of synchrotron radiation to generate image contrast from x-ray phase shifts.

Wrapping factor (WF) – a dimensionless metric describing the proximity of the intracochlear portion of a cochlear implant electrode array to the medial and lateral walls of the cochlea.

Thesis Abstract

Introduction

Accurate characterisation of cochlear implant electrode position is increasingly recognised as a critical determinant of postoperative auditory outcomes. While computed tomography (CT) is routinely used for postoperative assessment, numerous quantitative CT-derived metrics have been proposed, with inconsistent definitions and limited validation against anatomical reference standards. This heterogeneity limits both clinical interpretation and progress in research correlating electrode position with auditory performance.

Aims

This thesis has two primary aims:

1. *To systematically evaluate the existing literature base regarding the validity of CT-derived metrics of cochlear electrode position.*
2. *To validate the accuracy and reproducibility of intracochlear electrode position metrics derived from clinical CT against a high-resolution radiological reference standard derived from microCT images of implanted human cadaveric temporal bones.*

Methods

This thesis comprises two methodological components.

Chapter 1 presents a systematic literature review conducted in accordance with PRISMA guidelines. The review identifies and critically appraises studies evaluating CT-derived metrics of intracochlear electrode position against histological or high-resolution imaging reference standards.

Chapter 2 reports an *ex vivo* cadaveric temporal bone validation study, in which implanted cadaveric temporal bones were imaged using multidetector CT (MDCT), cone-beam CT (CBCT), and micro-computed tomography (microCT). Whole array and electrode contact-level metrics were measured independently by three blinded raters using three-dimensional reconstruction imaging software. Inter-modality agreement and interobserver reliability were assessed using standard agreement and reliability analyses.

Results

Existing CT-derived metrics of intracochlear electrode position are supported by limited and methodologically heterogeneous validation studies. In the experimental validation component, intracochlear position metrics derived from clinical CT showed close agreement the radiological gold standard. Cone-beam CT (CBCT) showed consistently closer agreement with microCT than multidetector CT (MDCT) across most whole array and electrode contact-level metrics. Measurement discrepancies were small, typically within sub-millimetre or voxel-scale limits. Interobserver reliability was good to excellent for most metrics, particularly as measured on CBCT.

Conclusion

Clinical CT can accurately and reproducibly quantify intracochlear electrode position within clinically acceptable limits. Cone-beam CT shows the closest agreement with a radiological reference standard and demonstrates high interobserver reliability. Whole array-level metrics show strong agreement across imaging modalities, whereas electrode contact–level metrics are reliably represented on CBCT, but remain constrained on MDCT by spatial resolution and metal-related artefact. These findings establish clinical CT, particularly cone-beam CT, as a reliable tool for postoperative electrode assessment. The results also define a validated radiological framework to support future outcome studies and implant design research.

Chapter 1: *CT-derived metrics of cochlear implant electrode position: a systematic review*

Introduction

Cochlear implantation remains the standard of care in the treatment of patients with moderate to profound sensorineural hearing loss. Candidacy criteria have progressively expanded and now include selected patients with residual, low frequency hearing loss[1-3]. Large cohort studies and meta-analyses have identified several patient factors to account for some of the variance in auditory performance after cochlear implantation. These include the duration, degree and age of onset of hearing loss, time since implantation, age at surgery, pure tone average of the better hearing ear and hearing loss aetiology[4-8]. However, these studies estimate that clinical predictors account for no more than 22% of implant performance. Whilst preimplantation cognitive factors, neural plasticity and other variables are likely to play a role[9,10], a large percentage of performance variation remains unexplained by patient factors. Several surgical factors have been implicated in influencing post-implantation performance, including cochleostomy vs. round window and posterior tympanotomy vs. suprameatal approaches, electrode insertion speed, and the use of a soft tissue vs. fibrin glue seal of the cochleostomy site[11,12].

With regards to cochlear implantation, the electrode-neuron interface (ENI) refers to the functional 'meeting point' where the implant electrode interfaces with the auditory nerve fibres within the cochlea. The ENI is a multifaceted concept influenced by electrode position, electrode design, the mode of neural stimulation and the health and response of the neural pathway. The ENI varies between patients and characterising the influence of its components may explain part of the unaccounted variance of post-implantation performance. A growing of body evidence is examining how intracochlear electrode position relates to postoperative hearing outcomes through modulation of the ENI. Implantation of the electrode array entirely within the scala tympani with closer proximity to the target ganglion cell population predicts improved post-operative word recognition scores[13-15]. In addition, a greater array angular insertion depth has been associated with improved speech recognition scores[16-19]. Cochlear implant electrode design continues to evolve, and manufacturers market several arrays with different mechanical properties. The most prominent designs are the 'straight' (lateral wall) arrays and the 'precurved' (perimodiolar) arrays. Lateral wall arrays are designed to follow the natural curve of the scala tympani along its outer wall, maximising preservation of delicate cochlear structures[20]. Conversely, perimodiolar arrays are engineered to conform to the medial wall, closer to the modiolar axis, aiming to maximise neural proximity to provide focused electrical stimulation[21]. Although results are mixed, each electrode targets different patient cohorts with lateral wall electrodes associated with higher rates of hearing preservation[8,22], while perimodiolar electrodes often correlated with improved outcomes in post-lingually deaf patients[23,24].

Modern clinical assessment of postoperative electrode position *in vivo* relies primarily on computed tomography (CT). Owing to its high spatial resolution, three-dimensional depiction of fine bony and metallic

detail, rapid acquisition, widespread availability and device compatibility, CT remains the optimal modality for evaluating intracochlear electrode position. The two principal CT modalities used for postoperative evaluation of electrode position are multidetector CT (MDCT, also termed high-resolution CT (HRCT)) and cone-beam CT (CBCT). Whilst MDCT is widely available in clinical practice, it suffers from only moderate spatial resolution and can be dominated by metallic artefact. In contrast, cone-beam CT provides submillimetre spatial resolution with reduced metal artefact and lower radiation dose, but is slightly slower and less widely available.

A range of radiological metrics of intracochlear electrode position have been reported including scalar position, angular insertion depth (AID), wrapping factor (WF), electrode to modiolus distance (EMD), intracochlear position index (ICPI) and homogeneity factor (HF). These metrics aim to describe the *in-vivo* anatomical component of the electrode-neural interface. Whilst there is consensus regarding a cochlear coordinate system[25], no such research or clinical standard exists for radiological measures of the final intracochlear electrode position. No single metric is routinely reported in real-world radiology reports, and it is unclear the degree to which they are standardised and validated against anatomical or radiological gold standards. As a result, the extent to which these metrics capture the true spatial relationship between electrode contacts and their neural targets remains unclear. This limitation confers uncertainty into studies investigating an association between final electrode position and hearing outcomes. Assessing the validity of currently described metrics of intracochlear electrode position is the natural first step in developing a robust framework to explore the relationship between the electrode position and cochlear implant performance.

The following systematic review aims to evaluate the validity of metrics used to characterise intracochlear electrode position.

Materials and Methods

A systematic review of the literature was conducted in accordance with the Cochrane Handbook and the Preferred Reporting Items for Systematic Reviews and Meta-Analyses (PRISMA) guidelines[26].

Studies reporting English language, original patient data in peer-reviewed journals from inception to June 2024 were considered for inclusion. Review articles were excluded.

A literature search was conducted in June 2024 using the following electronic databases: PubMed via OVID, Embase, Cochrane Review and CINAHL. The systematic search was augmented by scanning reference lists for relevant articles. A combination of Medical Subject Heading ('MeSH') Terms and keywords (Appendix 1) were used to devise a search strategy.

Three authors (AT, CN, and HS) independently executed the search strategy, conducted study selection and assessed each study based on established eligibility criteria. Initial screening involved title review, followed by comprehensive evaluations of abstracts and full texts. Reference lists from identified articles were examined for potential additional studies, which also underwent title, abstract and full-text review if considered relevant. Any discrepancies among reviewers were resolved through discussion until consensus was reached.

Eligibility criteria were defined according to the PICOTS framework (populations, interventions, comparisons, timings and study design)[27]. Studies involving human temporal bones (*in vivo* or cadaveric) which had undergone cochlear implantation were included. The intervention of interest was the assessment of quantitative metrics of cochlear implant electrode position using any clinical CT modality. Eligible studies were required to report a comparator reference standard for electrode position, defined as either a CT-based reference modality or histological assessment. Outcomes of interest were the accuracy and concordance of electrode position metrics relative to the reference standard. No restrictions were placed on study timing. Only English-language, peer-reviewed studies reporting original patient data were included. Non-human studies, review articles, conference proceeding, editorials and letters were excluded. In addition, studies assessing cochlear implant positioning on plain radiograph, magnetic resonance imaging or ultrasound were excluded as these modalities are not routinely used to assess electrode position.

The quality of each study and concomitant bias assessment were appraised independently by each reviewer using the Quality Assessment of Diagnostic Accuracy Studies 2 (QUDAS-2) Tool[28]. Any discrepancies were reconciled by discussion. A designation of "low", "some concerns", "high" or "unclear" was assigned for each item of the tool. Robvis[29] was used to visually represent these results.

The following data were extracted from each included using a standardised template: study design, sample characteristics, cochlear implant model and electrode type, CT modality and acquisition parameters,

reference standard, intracochlear position metrics assessed and accuracy outcomes. Where reported, data on rater characteristics and the presence of independent review, blinding, and randomisation were extracted[†].

[†] 'Independent review' refers to whether raters assessed images independently of one another. 'Blinding' refers to whether raters were blinded to the images of the ground truth when assessing the intervention modality. 'Image randomisation' refers to whether images were presented to the raters in a randomised fashion.

Results

Study selection

The search strategy is summarised in Figure 1. The formal search strategy produced a total of 1239 records after removal of duplicates. Subsequent title and abstract review excluded a further 1179 articles yielding 62 studies for eligibility assessment by full text review. A further 4 studies were identified as potentially irrelevant after reference list review and individual searching. Of these 66 studies, a total of 26 studies met eligibility criteria and were included in the review.

Heterogeneity in imaging modalities and scanning protocols along with small samples sizes precluded a meta-analysis of results. As such, a descriptive analysis was performed.

Study characteristics

Characteristics of the included studies are summarised in Table 1.

Participants

A total of 280 cochlear implants were included. Sample sizes ranged from 1 to 30 participants with a mean of 11.2 and median of 10. One study did not state the number of implanted bones in their study. Implanted electrodes were from four manufacturers: Cochlear (n = 16), MED-EL (n = 8), Advanced Bionics (n = 4), and Oticon (n = 2). Whilst included studies employed a wide range of specific cochlear implant models, three broad types of electrode arrays were implanted: lateral wall (n = 15), perimodiolar (n = 13), and mid-scala (n = 2). Two studies did not specify the manufacturer or type of implanted electrodes.

Interventions

The 26 included studies evaluated three type of clinical CT modalities: multidetector CT, cone-beam CT and photon counting CT.

Multidetector CT (MDCT)

10 studies assessed intracochlear electrode position on MDCT against a comparator gold standard. Several generations of MDCT were utilised with varying number of detector rows, ranging from 1 to 192 slices/detector rows.

With regards to x-ray tube parameters in MDCT studies, kVp ranged from 100kV - 140kV (median 120kV and mAs ranged from 220mA - 1200mAs (median 400mAs). ‘Smart mA’ was used in 1 study, and exposure time was not specified in 2 studies.

Cone-beam CT (CBCT)

19 studies assessed electrode position on CBCT against a comparator gold standard. The CBCT setups utilised included a combination of standard dental/maxillofacial CBCT (n = 11), rotational/C-arm-based CBCT systems (n = 4) and gantry-based flat panel volume CBCT (n = 3).

With regards to x-ray tube parameters in CBCT studies, kVp ranged from 60kV - 125kV (median 110kV and mAs ranged from 71mAs - 4320mAs (median 172mAs). kVp was not specified in 3 studies, and mAs was not specified in 6 studies

Photon counting CT (PCCT)

1 study evaluated intracochlear electrode position on PCCT against a comparator gold standard. For tube parameters, the kVp was 120kV and mAs was 158mAs.

Comparators

The 26 studies used histology (n = 19), microCT (n = 5), MDCT (n = 3) and CBCT (n = 2) as ground truth anatomical reference standards.

Studies

The majority (n = 24) of studies were comparative, cadaveric temporal bone studies, with prospective (n = 1) and retrospective (n = 1) in vivo studies also included. Included studies were published in the peer-reviewed literature from 2002 – 2024.

With regards to review of the CT images, the median number of raters/reviewers utilised was 2 (range 2 - 10). The number of raters was unspecified in 6/26 studies. Raters tended to be comprised of groups of exclusively otolaryngologists (4/26), exclusively radiologists (7/26) or a mixture of the two (8/26). Credentialling of the raters were not specified in one study. Raters were independent in 14/26, blinded in 8/26 and image randomisation was specifically mentioned in 2/26 studies.

Findings across included studies

Reported findings across the included studies are summarised in Table 2.

Scalar position

Scalar position was the most frequently evaluated metric of intracochlear position, assessed in 24/26 included studies[30-54]. Median sample size was 10. Scalar position was assessed on a range on CT modalities including MDCT (n = 10[30-33,37,41,43-45,52]), standard dental/maxillofacial CBCT (n = 9[32,39,40,42,47-49,51,55]), rotational/C-arm-based CBCT systems (n = 5[30,31,34,41,50]) and gantry-based flat panel volume CBCT (n = 4[31,50,52,54]). Several reference standards were used including histology (n = 17), microCT (n = 7), CBCT (n = 1) and MDCT (n = 1).

The accuracy of CT for determining the correct scalar position of the electrode varied between approximately 78 - 100%, depending on the CT modality used. MDCT demonstrated the greatest variability, with Burck *et al.* (2021) reporting correct scalar localisation in 31/40 (77.5%) of specimens, whilst Teymouri *et al.* (2011) showed 94.9% concordance with histology, and 97% concordance with microCT. Carlson *et al.* (2017) reported superior visualisation and identification of individual electrodes with a 192-slice MDCT (vs. a 64-slice MDCT).

CBCT tended to perform better than MDCT. Standard CBCT performed slightly better with accuracies between 84-100%, including 11/13 (84.6%) in Kurzweig *et al.* (2010), 7/8 (88%) in Mosnier *et al.* (2017) and 100% sensitivity with 90% specificity in Marx *et al.* (2014). Rotational CBCT systems performed very well in determining scalar position, with 11/11 correct classification in Cushing et al. 2012, and correct identification

of 5/5 scalar tympani insertions and 3/3 scalar translocations in Schuman et al (2010). Zou et al. (2015) reported complete accuracy in all samples using a flat-panel CBCT set up. Husstedt *et al.* (2002), Iso-Mustajärvi *et al.* (2017), Karkas *et al.* (2023) and Zeitler *et al.* (2011) all made qualitative statements regarding close concordance between scalar position on CBCT compared with a reference standard.

Some studies noted a regional relationship with correct scalar position determination. Two studies reported that apical assessment was more challenging, with De Seta *et al.* (2016) demonstrating lower agreement in the apical region vs. basal turn (Cohen's κ = 0.54 vs. 0.31, pairwise agreement 78% vs. 50%; basal vs. apical), whilst Saeed *et al.* (2014) noted incorrect scalar localisation by one rater in 2/8 (25%) of specimens. Similarly, Helbig *et al.* (2012) noted that correct scalar position determination became worse beyond 270 degrees (i.e. beyond the basal turn).

Electrode to modiolus distance

Electrode to modiolus distance (EMD) was evaluated in 4/26 of the included studies[38,39,42,53]. Median sample size was 13. EMD was only assessed on CBCT, specifically standard CBCT (n = 2[39,42]), rotational CBCT (n = 1[38]) and flat-panel CBCT (n = 1[53]), with histology (n = 3) and microCT (n = 2) serving as the anatomical reference standard. Study methodology was heterogenous, however CBCT generally showed good agreement with an anatomical reference for measurement of the EMD. In the two studies employing standard CBCT, Kurzweig *et al.* (2010) reported a mean difference of 0.065mm between CBCT and histology in measurement of EMD, whilst Iso-Mustajärvi *et al.* (2017) found moderate concordance (ICC 0.697) between CBCT and histology in EMD measurement, when utilised a pre- and post-implantation fusion technique to counteract the detrimental effect of metallic artefact. Husstedt *et al.* (2002) and Zeitler *et al.* (2011) both made qualitative statements regarding the use of rotational and flat-panel CBCT respectively in measuring EMD, both reporting that CBCT gave similar information regarding EMD/electrode-modiolus proximity, when compared with histology.

Angular insertion depth

Angular insertion depth (AID) was evaluated in 2/26 studies, using flat-panel volume CBCT[53] and photon counting CT[56]. Zeitler *et al.* (2011) reported that AID measurement correlated well between CBCT and histology, although no numerical or statistical analysis was quoted. Rak *et al.* (2024) found no statistically significant difference between AID measurement when made on photon counting CT vs. CBCT ($p < 0.001$) however noted a significant difference when photon counting CT was compared with MDCT.

Inserted electrode length

Inserted electrode length (IEL) was assessed in 2/26 studies, using CBCT[48] and photon counting CT[56]. Razafindranaly *et al.* (2016) assessed IEL on standard CBCT in nine implanted specimens, using MDCT as a reference standard, and reported a mean difference of 0.66 mm between CBCT and MDCT. Rak *et al.* (2024) evaluated IEL in ten temporal bones across photon counting CT (PCCT), MDCT, and rotational CBCT, demonstrating a significant difference in IEL measurement accuracy between MDCT and PCCT ($p < 0.001$), while no significant difference was found between CBCT and PCCT.

Intracochlear position index, wrapping factor and homogeneity factor

Intracochlear position index (ICPI), wrapping factor (WF) and homogeneity factor (HF) were all evaluated in a single study[55]. Ramos de Miguel *et al.* (2019) assessed these metrics on standard CBCT in three implanted cadaveric temporal bones against a histological reference standard. ICPI showed the highest concordance with no statistical difference in ICPI measurement on CBCT and histology noted on 3/3 specimens. HF and WF showed a lower concordance rate between CBCT and histology, with HF and WF showing no statistical difference in measurement in 2/3 and 1/3 specimens respectively.

Electrode to medial wall distance

The distance from the electrode contact to the medial wall of the cochlea duct was evaluated on flat panel volume CBCT against a microCT reference standard on a single study[54]. Zou *et al.* (2015) found a mean difference of 0.154mm in measurement of this distance between CBCT and microCT.

Risk of Bias Assessment

The risk of bias of included studies was assessed using the QUADAS-2 tool and is summarised in Figure 2. Overall, the methodological quality of the included data was variable. No study was judged to be low risk of bias across all domains. Sixteen studies were rated as having “some concerns”, most commonly due to incomplete reporting of sampling methods, rater blinding or reference standard procedures. Ten studies were rated as high risk of bias, mostly due to small cadaveric sample sizes, lack of blinding during CT or reference standard interpretation, or the use of an inadequate reference standard such as another CT modality (rather than microCT or histology). The flow and timing domain consistently showed low concern across the studies, as almost all specimens underwent index and reference assessments without missing data.

Discussion

This systematic review is the first to evaluate the validity of CT-derived metrics of intracochlear electrode position. Although CT assessment of implant electrode position is routine, this review highlights a clear gap between the number of available quantitative metrics and the limited evidence supporting their accuracy. It identifies that validation of quantitative metrics is limited to a small number of methodologically heterogenous studies which are generally insufficient to support confident interpretation.

Previous work has shown the importance of the intracochlear electrode position for implant recipients. The scalar position of the electrode array is known to influence speech outcomes, with scala tympani insertions associated with better consonant-nucleus-consonant word scores in moderate sample sized studies[13,14,57-59]. Scalar position was the most consistently evaluated metric in this review, assessed in 24 of the 26 included studies – 10 using MDCT and 18 using CBCT. Concordance between clinical CT modalities and the reference standard for scalar position was generally high (78–100%), with CBCT achieving the highest rates (84–100 This strong performance likely reflects the ability of both modalities to delineate scalar boundaries and the binary nature of the visual assessment. Because scalar localisation does not require submillimetre resolution and remains assessable despite metallic artefact, MDCT achieves comparatively strong performance in this metric. However, the evidence base is constrained by methodological limitations, including small median sample sizes (10 patients), heterogeneity in CT protocols, and limited quantitative reporting of concordance outcomes. Accordingly, although scalar localisation is the best-validated quantitative metric, its validation is tempered by limited methodological quality of the supporting studies.

The literature analysing the relationship between other quantitative metrics and patient outcomes is growing. A recent systematic review by Hasan *et al.* (2024) identified 30 studies (n = 2530) reporting correlations between electrode-modiolar distance, angular insertion depth and wrapping factor, with audiologic outcomes[60]. Results were mixed with greater electrode-modiolar distance tending to either have no impact or negatively impact outcomes, a smaller wrapping factor showing no correlation with outcomes and the effect of angular insertion depth differing between straight and perimodiolar arrays. Importantly, the authors also noted marked heterogeneity in methodology and outcome reporting of the included studies.

Included studies assessing electrode to modiolus distance, angular insertion depth, and composite metrics such as intracochlear position index, wrapping factor and homogeneity factor generally reported good agreement with anatomical standards. However, the key finding of this review is the marked heterogeneity across studies. The risk of bias assessment judged 16/26 studies as exhibiting “some concerns of bias” and 10/26 as “high risk of bias”. This variability and risk of bias dilutes the accuracy of metrics and limits the ability to amalgamate results and draw generalisable conclusions. For this reason, a meta-analysis was not performed.

There was a wide array of CT modalities used in the included studies. Scanner technology spanned early-generation MDCT, modern MDCT with improved detector configurations, several classes of CBCT (standard dental/ENT, C-arm rotational and flat panel systems) and an emerging clinical modality in photon-counting CT. There were marked differences in CT acquisition parameters including slice thickness, tube voltage and current, reconstruction kernels and the use of pre- and post-implantation image fusion techniques.

Another source of heterogeneity was in the reporting of the agreement between clinical CT and the ground truth. Some studies provided quantitative comparisons, such as mean differences and correlation coefficients. Others reported solely qualitative statements of “close agreement” or “good correspondence” without numerical data. This significantly limits interpretability and precludes comparison across studies. A minority of studies incorporated formal statistical analysis, which when performed, were inconsistent and often underpowered. Taken together with the small number of studies evaluating each metric (electrode to modiolus distance being the most frequently examined in only four studies) and the consistently small sample sizes, the evidence base remains deficient. As a result, clinical CT can be considered only partially validated for assessing gross electrode position (such as scalar position) and remains poorly validated for finer-grained quantitative metrics.

Reference standards varied with histology, microCT, and clinical CT comparators used, each with diverse methodological constraints. Differences in sectioning planes, sectioning intervals, histological preparation, microCT resolution and anatomical alignment procedures introduce significant uncertainty in drawing overall conclusions. These inconsistencies weaken confidence in reported accuracy values and highlight the need for rigorous, standardised use of anatomical reference standards in future studies. Verbist *et al.* established a three-dimensional co-ordinate system for the human cochlea, which aims to facilitate consistent comparisons across studies and disciplines in cochlear research[25]. Notably, none of the included studies referenced or applied this cochlear coordinate system, underscoring the lack of standardisation of anatomical landmarks across studies. Furthermore, studies used different definitions or measurement conventions for the same metric. Angular insertion depth reference points varied, modiolar distance and the position of the modiolar axis was inconsistently defined, and composite indices lacked standardised definitions. An illustrative example is intracochlear position index (ICPI). Intracochlear position index is a composite metric intended to summarise the relative intracochlear position of an electrode array with respect to the modiolus and lateral cochlear wall. This literature survey identified ambiguities in the definition of ICPI between studies. Ramos de Miguel *et al.*[55] introduced the concept of ICPI in a study included in this review, defined as the ratio between the distance from a given electrode contact to the medial wall, and the distance between the modiolar axis and the lateral wall. However, Lee *et al*.[61] define ICPI differently, in which the numerator is the distance between a given electrode contact and the *modiolar axis*[‡]. Whilst subtle, this definitional discrepancy underscores the interstudy inconsistencies that limit the ability to draw meaningful conclusions from pooled findings.

Two clinical CT modalities dominated this review – multidetector CT (MDCT) and cone-beam CT (CBCT). Conventional multidetector CT (MDCT) has historically been the workhouse of temporal bone imaging. It provides excellent spatial resolution of the inner ear osseous anatomy and is widely used in the preoperative workup of CI candidates[62]. It is inexpensive, widely available and has a rapid acquisition time, minimising patient motion artefact. Ten out of 26 studies assessed intracochlear electrode position on MDCT against a comparator gold standard, all of which evaluated scalar position. MDCT is intrinsically limited in its ability to accurately represent fine grain, individual electrode level metrics due to several well recognised constraints.

[‡] See Appendix 1 for pictorial explanations of ICPI as defined by Ramos de Miguel and Lee.

The high atomic number platinum-iridium contacts produce substantial beam hardening artefact, whilst the combination of the dense otic capsule and the metallic electrodes results in photon starvation[63]. The combined effect of these artefacts is to generate prominent ‘streaking’, which masks local anatomy and makes accurate determination of precise intracochlear anatomy difficult. Additionally, metallic electrode contacts generate substantial Compton x-ray scatter that is poorly modelled by filtered back projection and only partially addressed by basic iterative reconstruction[63]. This scattered radiation contaminates the raw projection data, producing incoherent streaks and signal degradation, particularly across the basal and middle turns of the cochlea where interactions are most frequent. Furthermore, the small size and close spacing of electrode contacts promote partial volume averaging and blurred expansion of the electrode. Collectively, these factors restrict MDCT’s ability to resolve key intracochlear relationships.

CBCT is now generally regarded as the modality of choice in imaging the post-implantation patient. In this review, 19 out of 26 studies assessed electrode position on CBCT against a comparator gold standard. Cone-beam CT employs a divergent cone-shaped x-ray beam to acquire an entire cylindrical volume in a single gantry rotation, generating isotropic voxels with high spatial resolution and relatively low scatter-induced artefact[64]. These small, isotropic voxels substantially reduce partial volume averaging and blooming, enabling clearer delineation of individual contacts and adjacent cochlear boundaries[65]. Because CBCT acquires all projections during a single circular rotation, it avoids the z-axis interpolation and cone-angle artefacts inherent to helical MDCT, preserving geometric accuracy along the cochlear spiral[32]. In addition, projection-domain metal artefact reduction algorithms commonly implemented on CBCT systems more effectively correct for artefact arising from the small, closely spaced electrode contacts[66]. Furthermore, CBCT achieves these benefits at a lower radiation dose compared with conventional MDCT[67-69].

With regards to the next generation of clinical CT, photon-counting CT (PCCT) is an emerging modality. PCCT was assessed in a single study of 10 specimens and showed close agreement with CBCT for measurement of angular insertion depth and inserted electrode length. PCCT employs direct conversion semiconductor detectors (typically cadmium telluride or cadmium zinc telluride) to convert incident x-ray photos into electronic pulses, which are then sorted into distinct energy bins based on pulse height[70]. This energy-discriminating detection improves signal-to-noise ratio, dose efficiency and spatial resolution with reduced blooming and beam-hardening artefact. Recently published series of implanted cadaveric temporal bone specimens examined with PCCT demonstrated highly precise postoperative electrode contact determination, with overall improved image quality and fewer metal artefacts at a lower radiation dose compared with conventional clinical CT modalities[56,71]. As it becomes more affordable and clinically available, we are likely to see a shift towards PCCT as the modality of choice in imaging cochlear implants. As such, future investigators should seek to incorporate PCCT into their studies.

Conclusion

This systematic literature review identifies as significant gap in the validation of CT-derived metrics of intracochlear electrode position. Scalar localisation is the sole metric with supportive validation evidence to date, demonstrating generally good agreement with anatomical reference standards, particularly on CBCT. Nevertheless, the available evidence is limited by small sample sizes, heterogeneous imaging protocols, and incomplete statistical reporting. In comparison, other commonly cited metrics, such as electrode to modiolius distance, angular insertion depth, wrapping factor and the intracochlear position index, are only validated by isolated studies. These studies exhibit considerable methodological inconsistencies regarding CT modalities, reference standards, analytical methods and operational definitions of the metrics themselves. Notably, no single study was judged to be at low risk of bias across all domains.

This limited validation and poor standardisation across the literature constrain synthesis of findings and undermines efforts to correlate CT-derived metrics to postoperative auditory outcomes. To support more meaningful use of these metrics in clinical practice and research, rigorous methodological standardisation against a high-resolution anatomical gold standard is required.

Accordingly, the following chapter presents a robust radiological validation study quantifying the agreement of clinical CT modalities against a microCT reference standard to establish a validated framework for future clinical and research applications.

Chapter 2: *Validation of cochlear implant electrode position metrics derived from clinical imaging against microCT reference standards.*

Introduction

As outlined in Chapter 1, a comprehensive review of the literature demonstrates a significant gap in high quality, quantitative validation studies of metrics of intracochlear electrode position. The current evidence base is limited by small sample sizes, heterogenous methodologies and inconsistencies in reference standards. As a result, quantitative metrics of intracochlear position remain inadequately validated for application to clinical CT imaging.

The validation of these metrics is essential within both clinical and research settings. In clinical practice, the accurate determination of angular insertion depth is central to anatomy-based fitting, a strategy shown to reduce frequency-to-place mismatch and improve speech perception[72,73]. Additionally, metrics such as electrode to modiolus distance and wrapping factor are increasingly employed to account for variability in stimulation thresholds and channel interaction[8,74]. From a research standpoint, the validity of large-scale investigations correlating electrode position with clinical outcomes depends on the assumption that CT-derived metrics accurately reflect biological conditions. In the absence of ground-truth validation, a degree of uncertainty will persist in all subsequent studies.

The central challenge in accurately quantifying intracochlear electrode position stems from intrinsic limitations of clinical CT modalities. Beam-hardening, photon starvation and partial volume averaging represent the primary artefactual sources of error when imaging cochlear implant electrodes with CT[75]. The high atomic number platinum-iridium electrode contacts create significant beam-hardening in which lower energy x-ray photons are preferentially absorbed. The reconstruction algorithm subsequently misinterprets the detected beam quality, resulting in ‘streaking artefact’, in which dark bands appear along the long axis of the electrode contact. Photon starvation degrades the image further as high x-ray attenuation results in small number of photons reaching the detector, decreasing the signal-to-noise ratio, also resulting in distinct, severe streaks in the image. Partial volume artefact occurs when a single voxel must represent the averaged X-ray attenuation of two or more materials with widely different densities, such as a metallic electrode pad and surrounding perilymph. The averaging process raises the Hounsfield units of the structures around the electrode. This effect manifests as a pervasive ‘blooming artefact’ which can artificially inflates the radiological diameter of the electrode by up to 50 – 70%[76,77]. These limitations necessitate robust validation studies to quantify any resulting discrepancies and determine the accuracy of these metrics as measured on clinical imaging modalities.

To overcome these shortcomings and establish the true reliability of these radiological metrics, a ground-truth validation framework is required. A logical avenue to achieve this is

with cadaveric temporal bone models, which allow for standardised electrode insertion and post-implantation imaging with ultra-high-resolution imaging. The gold standard for this radiological validation is micro-computed tomography (microCT), with offers spatial resolution 30 – 100 times greater than clinical CT[78]. This improvement all but eliminates the partial volume effect allowing for precise, artefact-minimised measurement of radiological metrics of electrode position[54]. By directly comparing the measurements derived from clinical CT modalities against this high-fidelity ground truth, the accuracy and interobserver variability of these increasingly utilised radiological metrics can be quantitatively assessed.

Aims and Hypothesis

The principal objective of this study is to address the current knowledge gap by undertaking a comprehensive radiological validation of quantitative intracochlear electrode position metrics derived from clinical CT imaging, using high-resolution microCT as an anatomical reference standard.

The objectives of this study are as follows:

1. Quantify the magnitude and direction of measurement error for CT-derived intracochlear electrode position metrics on clinical CT modalities, relative to a microCT reference standard.
2. Evaluate the influence of electrode type and intracochlear position (basal versus apical) on inter-modality measurement agreement between clinical CT and microCT.
3. Assess interobserver variability in measurements to determine agreement and reproducibility across independent observers.

More broadly, an expanded data will be obtained which will provide a robust, normative dataset for future studies investigating the electrode position on clinical imaging.

The present study hypothesises that agreement between metrics of intracochlear electrode position derived from clinical imaging modalities and a radiological gold standard will fall within a clinically acceptable range, with low measurement variance and good interobserver reliability.

Methodology

Experimental design

An *ex-vivo,* comparative validation study using cadaveric human temporal bones was performed. Ethics approval was obtained through the Western Sydney Local Health District Human Research Ethics Committee (ID: 2022/PID01475).

Specimen preparation

Twelve human cadaveric temporal bones were supplied to the investigators by Cochlear Ltd. via their established human tissue procurement pipeline. Specimens were acquired by via Science Care, Inc. (Phoenix, AZ, USA)[§]. Specimen preparation, surgical implantation and post-implantation histological sectioning were performed at the Cochlear Ltd. Temporal Bone Laboratory (Macquarie Park, NSW) in compliance with the Human Tissue Act 1983 and Cochlear Ltd.'s anatomy licence.

Stored, frozen bones were thawed prior to implantation. Once suitably thawed, a single experienced surgeon with over 30 years surgical experience (MDC) performed cochlear implantation of each bone with one of two electrodes - CI622 Slim Straight Electrode[79] and CI632 Slim Modiolar Electrode[80]. Implantation was performed under standard microsurgical conditions. Following posterior tympanotomy, the round window niche was identified and overhang drilled as required. The electrode was then carefully advanced through the round window membrane under direct vision.

Following implantation, each electrode was fixed at the facial recess or round window with cyanoacrylate glue to prevent subsequent electrode translocation. Any excess cryoacrylate glue was removed from the facial recess and the stapes footplate using a 0.5mm burr surgical drill. The stapes footplate was then removed, and the specimen dehydrated through sequential ethanol baths (from 70%, to 100% ethanol) to eliminate moisture and minimise anatomical distortion. Once dehydrated, each bone was immersed in degassed epoxy resin for acrylic embedding and placed under vacuum to ensure complete resin infiltration and removal of air bubbles. Finally, surplus bone and resin was trimmed to remove irrelevant extracochlear anatomy.

All 12 bones underwent imaging on multidetector CT, cone-beam CT and microCT imaging.

Imaging

Multidetector CT imaging (MDCT)

Multidetector CT (MDCT) imaging was performed on a SOMATOM X.cite scanner 128-slice CT scanner (Siemens, Erlangen, Germany) with commercially available software (syngo VB10A, Siemens Healthineers) at a private clinical imaging facility (Castlereagh Imaging, Westmead, Sydney). For scanning, specimens were oriented supine, and a standard petrous temporal bone scanning protocol was used to mimic a clinical scenario. No metal artefact reduction algorithm was used as this was found to reduce electrode edge definition. Final MDCT scanning parameters were as follows: tube voltage 130kVp, effective mAs 445, pitch 0.45, beam collimation 64 x 0.6mm (z-sharp), rotation time 1s, field of view ≤ 16 cm. Reconstruction was

[§] Science Care, Inc is a U.S. based, non-transplant, anatomical organisation accredited by the American Association of Tissue Banks (AATB accreditation 00124/7)

performed using the Hr60uA1n3 kernel with a slice thickness of 0.5 – 1.0mm. Following imaging, MDCT data were exported in DICOM format.

Cone-beam CT imaging (CBCT)

Cone-beam CT (CBCT) imaging was performed on a Carestream CS9600 scanner (Carestream Dental, Atlanta, USA) at a private clinical imaging facility (Castlereagh Imaging, Westmead, Sydney). For scanning, specimens were oriented in the erect position to mimic a clinical scenario. A purpose built 'cochlear implant' protocol was used, which was devised by MDC and the Castlereagh Imaging Westmead chief radiographer, for use in post-operative cochlear implant patients. No metal artefact reduction algorithm was used. Final CBCT scanning parameters were as follows: tube voltage 130kVp, tube current 5mA, effective acquisition time 19s, field of view 6 x 6cm, voxel size 0.075mm, filtration Cu 0.15mm with automatic noise reduction turned on. Following imaging, CBCT data were exported in DICOM format.

MicroCT imaging

MicroCT imaging of the implanted temporal bones was performed on a SKYSCAN 2214 (Bruker, Kontich, Belgium) at Sydney Microscopy & Microanalysis (University of Sydney, Camperdown, Sydney). For scanning, specimens were oriented such that the x-ray beam was perpendicular to the plane of the basal turn of the cochlea. This was done to reduce the angle-dependent components of metallic artefact (beam hardening and photon starvation) in the plane parallel to the basal turn. The optimum scanning parameters were determined through a combination of multiple test runs (to produce images with acceptable resolution and contrast with a favourable metallic artefact profile) and agreement with the literature[54,81,82]. Final microCT scanning parameters were as follows: 110kVp tube potential, 110mA tube current, exposure time 1487ms, Al 1mm + Cu 0.075mm, voxel size 10µm, rotation step 0.4 degrees. Following imaging, microCT data were exported in TIFF and BMP format with the associated imaging parameter log file.

Data management/storage

Once all imaging and histological data were obtained, these were uploaded to the University of Sydney, password-protected Research Data Storage (RDS) repository. Access was restricted to the primary investigator (AT), senior investigator (MDC) and named research associates (CN and HS).

Measurement

Following scanning, the primary rater (AT) assessed image quality, metal artefact, and anatomical visibility across modalities to determine which intracochlear electrode position metrics could be measured accurately and reliably.

Metrics of intracochlear electrode position

As identified in Chapter 1, several radiological metrics of intracochlear electrode position are in clinical and research use. Where adequate spatial resolution, image contrast and acceptable metallic artefact allowed, specific measurements were taken for each specimen, on each modality. These included whole array-level metrics (i.e. metrics calculated/measured on an entire array level) and electrode contact-level metrics (i.e. metrics calculated/measured on an individual electrode basis). The measured metrics are summarised in Table 3. Specific definitions for these metrics are found in Table 10. Scalar position was not assessed, as

during the preparation and fixation of the fresh-frozen cadavers, there was degradation of Reisnner's and the basilar membrane such that scalar localisation was not possible.

Table 3.
Metrics of intracochlear electrode position measured in this study.

Whole array-level metrics	Electrode contact-level metrics
1. Angular insertion depth (AID) 2. Inserted electrode length (IEL) 3. Lateral wall length (LWL) 4. Wrapping factor (WF)	1. Electrode to modiolus distance (EMD) 2. Medial wall to electrode distance. 3. Lateral wall to medial wall distance 4. Lateral wall to modiolus distance. 5. Intracochlear position index (ICPI) via two methods: a. ICPI by the methodology described in Ramos de Miguel[55] i. $ICPI_{i,\ RdM}$ ii. $\overline{ICPI}_{RdM}$ b. ICPI by the methodology described in Lee[61] i. $ICPI_{i,\ Lee}$ ii. $\overline{ICPI}_{Lee}$

Measurement process

Imaging data were imported into 3D Slicer (Version 5.8.1, http://www.slicer.org) for visualisation and measurement of relevant metrics[83] 3D Slicer is a free, open-source software platform for the analysis and visualisation of biomedical images, including in studies evaluating the cochlea and/or cochlear implants[84-86].3D Slicer facilitated submillimetre linear and path measurements in two and three dimensions, angular measurements, multiplanar reconstruction and voxel intensity (i.e. Hounsfield unit) measurements in all three CT modalities. Loading of the MDCT and CBCT DICOM data into 3D Slicer were performed using 3D Slicer's in-built DICOM import function, whilst MicroCT data were loaded with the SlicerMorph extension via the SkyscanReconImport module[87].

All measurements were performed individually by the primary rater (AT) and by the two secondary raters (CN and HS). All raters performed measurements independently of each other and were blinded to other rater's results. The primary rater (AT) was a RANZCR radiology trainee with prior ENT surgery experience, whilst the secondary raters were medical students trained in the recognition of the cochlear anatomical structures required for accurate measurement.

Calibration of 3D Slicer

To verify the accuracy of linear measurements obtained in 3D Slicer, a microCT scan was performed on a small calibration phantom containing four elements of known physical thickness. The resulting dataset was imported into 3D Slicer, and each element was measured using the same segmentation and distance-measurement workflow applied in the main study. These measurements were compared with the known physical dimensions to confirm that the workflow accurately reproduced real-world distances before its application to the study specimens.

Statistical analysis

Statistical analysis was performed using IBM SPSS Statistics Version 31 (IBM Corp., Armonk, NY, USA)[88]. Descriptive statistics as measured by the primary rater (AT) were calculated. Normality of continuous variables was assessed using Shapiro-Wilk tests and inspection of Q-Q plots. Normally distributed data were subjected to repeated-measures ANOVA testing and post-hoc pairwise t-tests to assess modality-dependent differences in electrode position measures. Non-normally distributed data underwent Friedman testing and Wilcoxon signed rank testing. Bland-Altman analysis was performed to calculate the mean difference in pairwise measurement of metrics of intracochlear position between MicroCT, CBCT by calculating mean bias and 95% limits of agreement (mean difference ± 1.96 x standard deviation). To evaluate whether measurement concordance between modalities differed by electrode type, mean absolute differences in measurements were compared between perimodiolar and lateral wall electrodes for each metric. To evaluate whether concordance between modalities varies systematically along the length of the array, Spearman's rank correlation was calculated between the absolute inter-modality difference for each metric and the electrode number (representing array position from basal to apical). Interobserver variability assessment was performed to evaluate the consistency of measurements between the three independent raters across all imaging modalities. Intraclass correlation coefficients (ICC) were calculated using a two-way mixed-effects model for absolute agreement of single measurements (denoted as ICC(3,1)) with 95% confidence intervals. Interpretation of ICC values followed conventional thresholds where values < 0.50 denote poor reliability, 0.50 – 74 moderate, 0.75 – 0.89 good and ≥ 0.90 excellent[89]. All tests were two-tailed, and a significance threshold of $p < 0.05$ was applied.

Results

A total of 12 cadaveric temporal bones were implanted with cochlear implant electrodes. Two different electrode types were used: a lateral wall electrode (Slim Straight Electrode (CI622), *n* = 8) and a perimodiolar electrode (Slim Modiolar Electrode (CI632), *n* = 4).

Assessment of image quality and resolution

The primary rater (AT) assessed electrode contact resolution and metal-related anatomical distortion on all specimens and modalities. MicroCT and CBCT reliably resolved individual electrode contacts with acceptable metal artefact, permitting visualisation of the medial and lateral cochlear duct walls and the modiolar axis (Figure 3). As such, all electrode contact-level measures and whole-array level metrics (Table 3), were measured on these two modalities.

MDCT *did not yield* sufficient image quality to reliably resolve adjacent electrode pads and often obscured the medial and lateral cochlea walls. This was primarily due to blooming artefact (Figure 4). As such, only AID, IEL, LWL and WF could be confidently and reliably measured on MDCT imaging. The remaining metrics were not measured on MDCT.

Post-implantation damage was noted in specimen 6, in which electrode contacts 12-17 were inadvertently removed from the specimen (Figure 5). As a result, IEL, LWL and WF could not be measured on this specimen. The remaining measures were calculated based on the 16 visible electrode contacts in this specimen.

3D Slicer workflow calibration

3D Slicer measurements showed excellent agreement with the phantom dimensions. The mean bias (between 3D Slicer and reference measurements) was 0.20 µm, with 95% limits of agreement from −7.2 µm to +7.6 µm, indicating only micron-level variation. The mean absolute error was 2.9 µm, and regression analysis demonstrated near-perfect linearity (slope 0.97, intercept 4.0 µm, R^2 0.9998). These findings confirm the high accuracy of the measurement workflow.

Descriptive statistics

A diagrammatic summary of the descriptive statistics for all intracochlear electrode position markers, as measured by the primary rater (AT), is presented in Figures 6A-C. A complete tabulated summary of the descriptive statistics is found in Table 4.

Normality testing

Shapiro-Wilk testing with review of Q-Q plots were used to assess normality of the datasets obtained. AID, LWL, WF, lateral wall – medial wall distance, electrode – modiolus distance, modiolus – lateral wall distance, $ICPI_{i,\,Lee}$ and $\overline{ICPI}_{Lee}$ met normality assumptions across all modalities in which each were measured. As such, parametric methods were used to assess these metrics. Conversely, IEL, medial – wall to electrode distance,

$ICPI_{i,\ RdM}$ and $\overline{ICPI}_{RdM}$ violated normality in at least one modality in which they were measured. Accordingly, these metrics were assessed using non-parametric tests.

Measurement concordance by modality

Concordance of parametric and non-parametric metrics of intracochlear electrode position as measured across CT modalities by the primary rater (AT), as summarised in Table 4A-B.

Table 4A.
Parametric metrics. Concordance analyses across CT modalities.

Metric	Statistical test	p value	Summary of findings
AID	Repeated-measures ANOVA	0.21	No significant difference across 3 CT modalities
LWL	Repeated-measures ANOVA	*< .01*	Measured as slightly longer on CBCT and MDCT compared with microCT.
WF	Repeated-measures ANOVA	0.17	No significant difference across 3 CT modalities
Electrode to modiolus distance	Paired t-test	*< .001*	Slightly longer on CBCT vs. microCT; mean difference 140μm
Medial wall to electrode distance	Paired t-test	*0.027*	Slightly longer on CBCT vs. microCT; mean difference 30μm
Lateral wall to medial wall distance	Paired t-test	*< .001*	Slightly longer on CBCT vs. microCT; mean difference 160μm
Modiolus to lateral wall distance	Paired t-test	*< .001*	Slightly longer on CBCT vs on microCT; mean difference 260μm

Table 4B.
Non – parametric metrics. Concordance analyses across CT modalities.

Metric	Statistical test	p value	Summary of findings
IEL	Friedman test	*< .001*	IEL measured longer on CBCT and MDCT compared with microCT.
$ICPI_{i,\ RdM}$	Wilcoxon signed-rank	*< .001*	CBCT calculated as slightly lower than MicroCT
$ICPI_{i,\ Lee}$	Wilcoxon signed-rank	*< .001*	CBCT calculated as slightly lower than MicroCT
$\overline{ICPI}_{RdM}$	Wilcoxon signed-rank	*.003*	CBCT calculated as slightly lower than MicroCT
$\overline{ICPI}_{Lee}$	Wilcoxon signed-rank	.06	No significant difference between CBCT and MicroCT

AID, IEL, LWL, WF

Repeated measures ANOVA indicated no significant difference in measurement of AID across all three CT modalities ($F(2,22) = 1.67$, $p = .021$). Similarly, repeated measures ANOVA indicated no difference in measurement of WF across all 3 modalities ($F(2,20) = 1.94$, $p = 0.17$)

Non-parametric Friedman testing showed a significant effect of modality on the measurement of IEL, with post-hoc Wilcoxon signed-rank testing demonstrating IEL tended to be measured to be longer on CBCT ($p = .005$) and MDCT ($p = .003$) when compared with the microCT gold standard. IEL was measured as significantly shorter on CBCT when compared with MDCT ($p = .026$).

LWL measurements differed significantly when measured across modalities ($F(2,20) = 16.07$, $p < .01$). Post-hoc pairwise comparisons showed that LWL measured significantly shorted on microCT when compared with CBCT (mean difference = -1.54mm, 95% CI -1.99 to -1.08mm, $p < .001$, Cohen's d = -2.28) and when compared with MDCT (mean difference = -2.01mm, 95% CI -2.98 to -1.06, $p < .001$, Cohen's d = -1.32). No significant difference was found between CBCT and MDCT measurement of LWL (mean difference –0.48 mm, 95% CI –1.45 to 0.49, p = .30, Cohen's d = –0.31).

Electrode to modiolus distance, medial wall to electrode distance, lateral wall to medial wall distance and modiolus to lateral wall distance

Across these measurements, CBCT differed significantly from microCT, with all distances measuring slightly longer on CBCT. Specifically, electrode to modiolus distance (mean difference −0.14 mm, $t(254) = −9.78$, $p < 0.001$, $d = −0.23$), medial wall to electrode distance (−0.03 mm, $t(246) = −2.22$, $p = 0.027$, $d = −0.21$), lateral wall to medial wall distance (−0.16 mm, $t(246) = −9.43$, $p < 0.001$, $d = −0.27$), and modiolus to lateral wall distance (−0.24 mm, $t(246) = −13.06$, $p < 0.001$, $d = −0.29$) all showed statistically significant differences. In all cases, mean differences were small (< 300μm).

Intracochlear position index (ICPI)

Non-parametric Wilcoxon signed-rank testing showed significant differences in ICPI as measured on an individual electrode basis, according to both the de Miguel and Lee methodologies. On CBCT, $ICPI_{i,\text{ de Miguel}}$ ($Z = -8.656$, $p < .001$) and $ICPI_{i,\text{ Lee}}$ ($Z = -5.834$, $p < .001$) were calculated as smaller when compared with MicroCT gold standard. When averaged over the entire electrode array, $\overline{ICPI}_{de\ Miguel}$ were significantly lower on CBCT than on microCT ($Z = -2.98$, $p = .003$), $\overline{ICPI}_{Lee}$ calculations did not differ significantly between CBCT and MicroCT ($Z = -1.88$, $p = .06$).

Inter-modality agreement (Bland-Altman analysis)

Mean bias across intracochlear electrode position metrics was small and centred close to zero (Figures 7A–C). Agreement was strongest for whole array–level metrics. Wall and distance-based metrics demonstrated consistently negative bias relative to microCT, indicating slightly larger measurements on CBCT. Intracochlear electrode position indices showed minimal mean bias with comparable limits of agreement across index definitions. Full Bland-Altman results are found in Table 5.

Figure 7A.
Bland-Altman summarised of mean bias and 95% limits of agreement for whole array-level intracochlear electrode position metrics across imaging modalities.

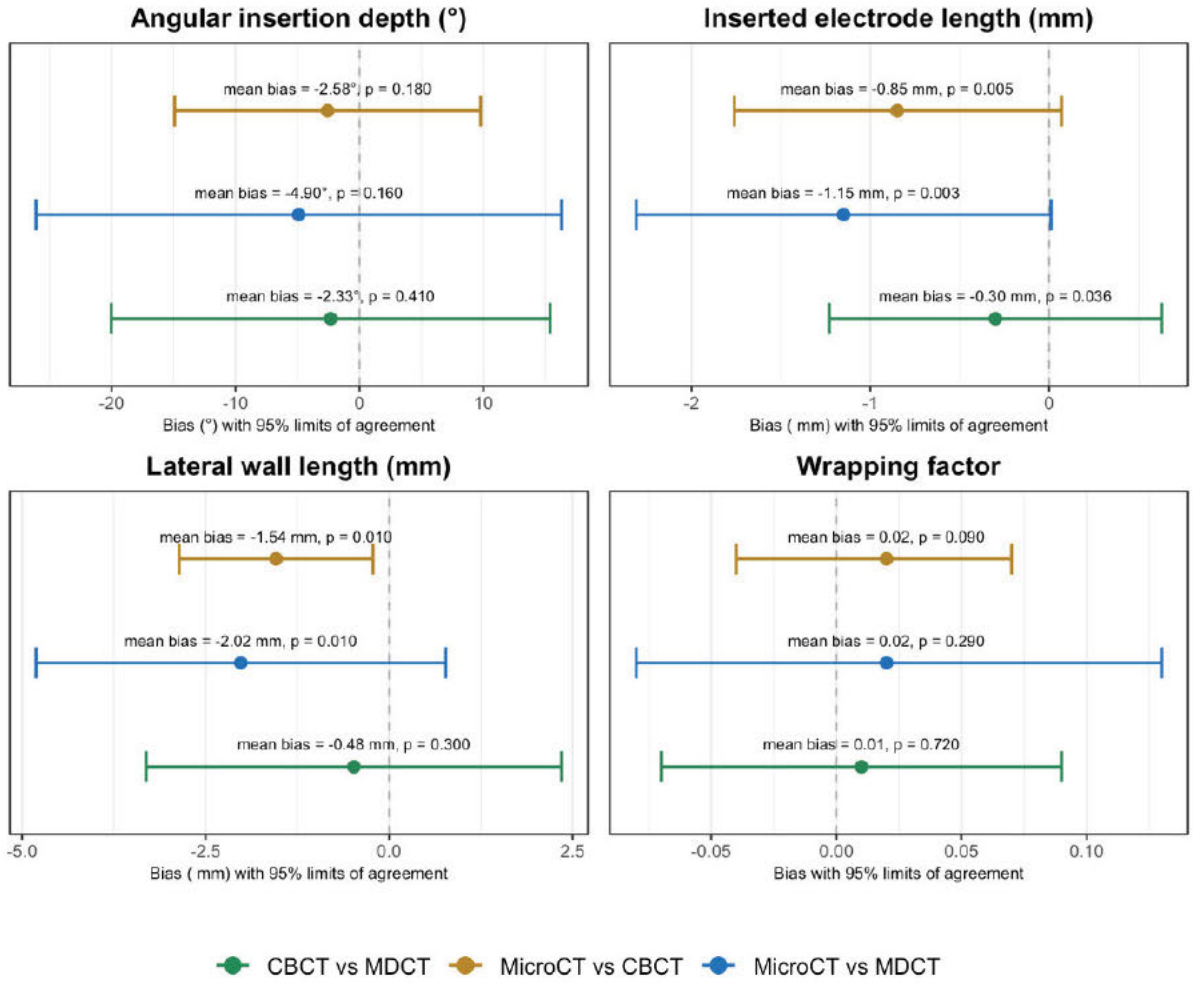

Figure 7B.

Bland-Altman summaries of inter-modality agreement for wall and distance-based intracochlear electrode position metrics.

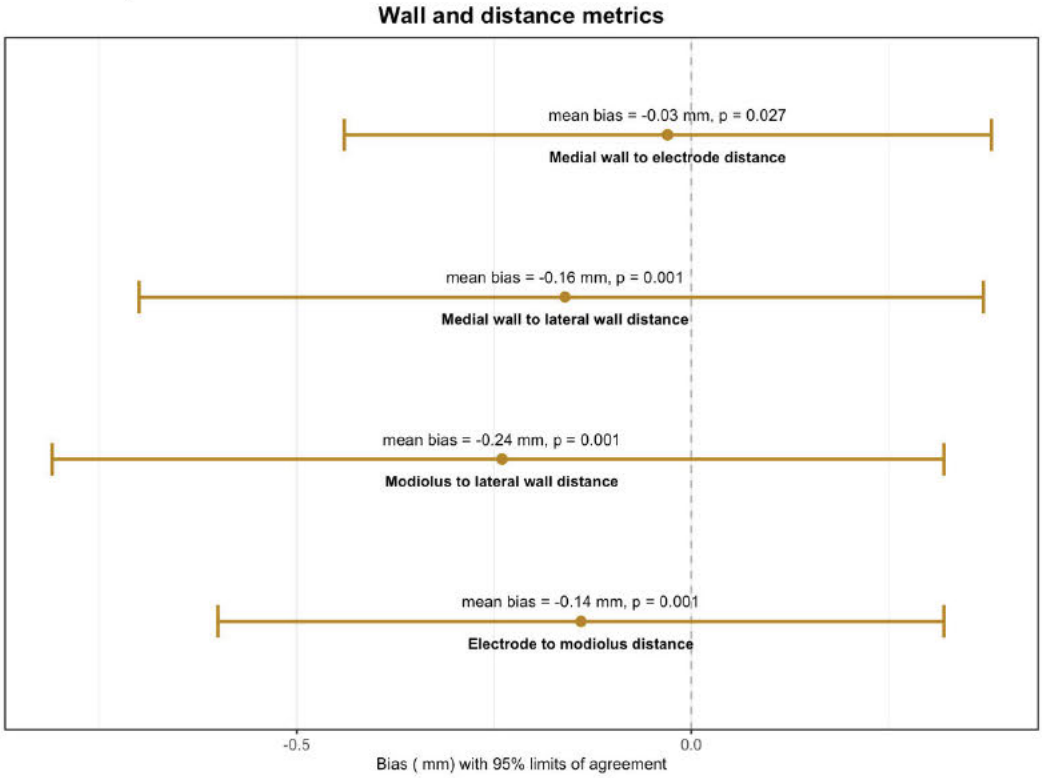

Figure 7C.

Bland-Altman summarises of inter-modality agreement for intracochlear electrode position indices (ICPI)

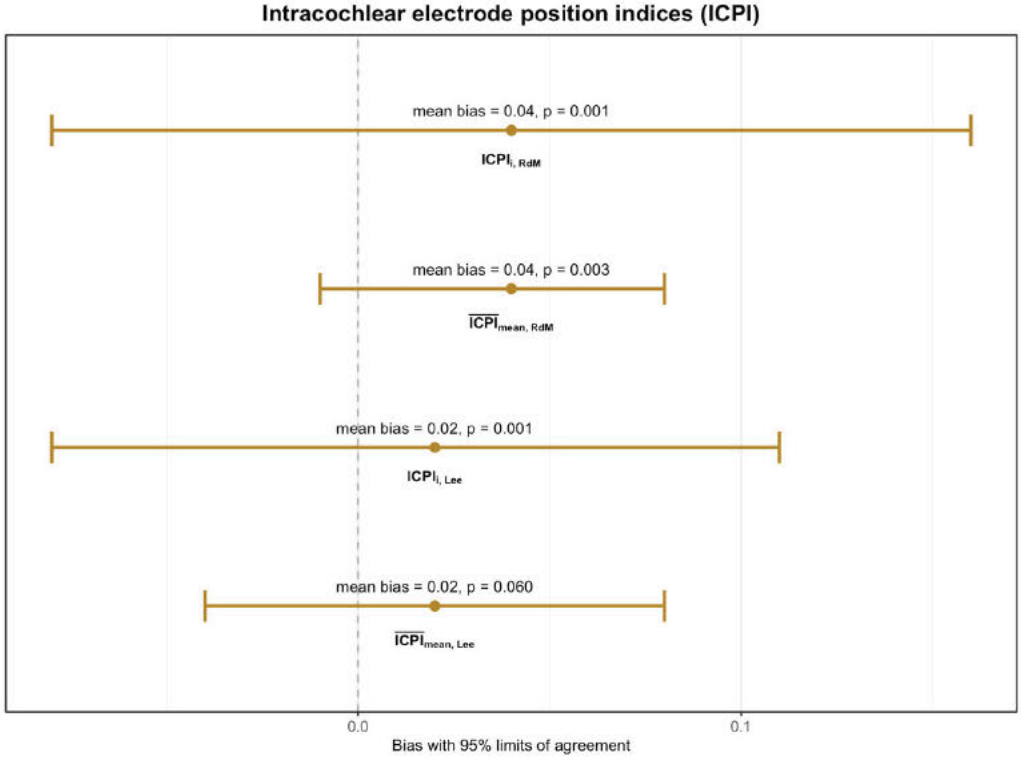

Measurement concordance by electrode type

Pairwise concordance between modalities for perimodiolar and lateral wall electrodes demonstrated broadly similar mean absolute differences across most metrics (Table 6). For AID, IEL, WF and several of the modiolus and wall-based distance measures, differences between electrode types were generally small and did not reach statistical significance. Significant differences were observed for LWL in the MicroCT-MDCT comparison (p = .03) and the CBCT-MDCT comparison (p < .01), and for medial wall–lateral wall distance in the MicroCT-CBCT comparison (p = .001). All other comparisons showed non-significant differences between perimodiolar and lateral wall arrays.

Measurement concordance along the electrode array

Measurement concordance along the electrode array was assessed using Spearman's correlation is summarised in Table 7. Medial wall to electrode distance and medial wall to lateral wall distance showed no significant variation in discrepancy along the array. Modiolus to lateral wall distance (ρ = –0.183, p = .004) and electrode–modiolus distance (ρ = –0.157, p = .012) demonstrated small but statistically significant correlations. Both ICPI metrics also showed significant positive correlations (ICPIi_{RdM} (ρ = 0.198, p = .002) and ICPIi_{Lee} (ρ = 0.396, p < .001), indicating greater discrepancy toward the apical end of the array, although the strength of this correlation was weak – modest.

Measurement concordance along the electrode array by electrode type (perimodiolar vs. lateral wall) is summarised in Table 8. For medial wall to electrode distance, neither array type showed significant variation in discrepancy along the array. Electrode to modiolus distance showed statistically significant, weak-modest strength correlation between electrode position and measurement discrepancy, with PM and LW arrays both showing a trend towards greater measurement discrepancy in basal most electrodes. Measurement discrepancy of both ICPI metrics demonstrated a statistically significant correlation with electrode position of weak to modest strength, with both electrode types showing a trend towards greater measurement discrepancy in apical most electrodes.

Interobserver variability assessment

Interobserver variability assessment across the 3 raters is summarised in Table 9. Interobserver reliability across all metrics was high overall, with ICC values ranging from 0.54-0.99 (moderate to excellent), depending on the metric and imaging modality. AID, IEL, WF and electrode to modiolus distance all demonstrated excellent reliability on across microCT and CBCT, with MDCT. Measurements involving the medial and lateral cochlear walls showed greater variability, with ICCs spanning moderate to excellent across modalities. Both definitions of the ICPI exhibited excellent reliability on CBCT. All ICC values were statistically significant at p > 0.001.

Discussion

This cadaveric temporal bone study aimed to validate metrics of intracochlear electrode position on clinical CT modalities against a microCT reference standard. Our results establish a robust radiological dataset demonstrating the accuracy, agreement, and reproducibility of CBCT and MDCT for determining cochlear implant electrode position. Consistent with our primary hypothesis, CBCT and MDCT enabled accurate measurement of intracochlear electrode position and showed close agreement with the radiological gold standard. Inter-modality discrepancies were small and clinically acceptable, often at the submillimetre or sub-voxel scale. Interobserver agreement among three independent trained raters was high, suggesting that the metrics are robust to observer variation.

The data show that CBCT demonstrates greater concordance with the ground truth, can resolve finer electrode contact-level and sub-cochlea level anatomical detail and lower interobserver variability, compared with MDCT. This finding is mirrored by prior studies, reinforcing CBCT as the preferred modality for post-implantation assessment of electrode position[30,32,41,48,65,68]. While both clinical modalities performed well for whole array-level metrics, CBCT offered higher spatial resolution and reduced metal artefact, enabling more accurate assessment of electrode contact-level metrics. *Our findings support the use of CBCT as the standard of care in imaging post-operative cochlear implant patients where the aim is to most accurately and comprehensively image the anatomical aspects of the electrode-neural interface*.

Key findings

Among whole array-level metrics, angular insertion depth (AID) and wrapping factor (WF) showed no statistically significant differences across the three CT modalities. Both metrics were also normally distributed. This is consistent with prior morphometric studies reporting that key cochlear dimensions vary approximately normally across populations[90,91]. Together, these findings suggest that AID and WF behave as stable descriptors of cochlear anatomy, with limited sensitivity to modality-specific factors such as spatial resolution or metal artefact. This robustness is particularly relevant for AID. A recent systematic review by Hasan *et al.* (2024) found that greater insertion depth was frequently associated with improved postoperative auditory outcomes[91]. In this context, the consistent measurement behaviour and cross-modality agreement of AID support its use as a reproducible anatomical descriptor that can be derived from clinical CT imaging.

In contrast, inserted electrode length (IEL) and lateral wall length (LWL) showed small but consistent measurement differences on CBCT and MDCT compared with microCT. In both cases, the clinical modalities tended to yield slightly longer distance measurements. MDCT showed greater discordance, with a mean IEL discrepancy of 1.15 mm (7.3%) relative to microCT. This observed error is comparable with results from other cadaveric validation studies of IEL length[48], as well as impedance telemetry-based estimations[92]. The mean LWL and IEL on MDCT was 22.5mm and 16.8mm respectively. Measurement of these path lengths require accurate tracing of the lateral wall and electrode contour through their ascent into the cochlea. Given limitations in spatial resolution, metal visualisation, and partial volume artefact, particularly on MDCT, small measurement errors can accumulate along the paths used to measure LWL and IEL. This erroneous accumulation increases discordance and interobserver variability for these whole array-level metrics.

Amongst individual electrode contact-level metrics, most demonstrated statistically significant differences between CBCT and microCT measurement. However, these differences were small, ranging between 30-240μm, representing between 2.7-8.1% of the mean values measured on microCT. This range is on the order of the spatial sampling limitations of CBCT, which in this study produced a voxel size of 75μm. Given that the voxel edge defines the smallest resolvable unit of distance, the discrepancies observed in this study (approximately 0.5-3.2 voxels) are consistent with the intrinsic uncertainty of CBCT imaging and the limitations imposed by voxel-based boundary definition and partial volume artefact[93,94]. Future refinements in metal artefact reduction techniques, the establishment of optimised scanning protocols, minimising motion artefact through shorter acquisition times or motion correction techniques and advances in iterative and AI-based reconstruction algorithms are likely to enhance the image quality of CBCT, further minimising measurement discrepancy of key electrode contact-level metrics.

Furthermore, these discrepancies are small on a clinical scale. Chakravorti *et al.* published a series 220 implanted ears modelling variance in audiological scores as a function of electrode position, calculating that an average deviation of 500μm of the electrode array from the modiolus was associated with a 21.7% reduction in CNC word recognition and 5.75 dB deterioration in BKB-SIN performance[15]. An approximately 8% change in CNC score[95] and a 3 dB deterioration in signal-to-noise ratio are commonly taken to correspond with a minimal clinically significant change[96]. Accordingly, measurement discrepancies below 300μm are unlikely to translate into meaningful changes in electrode-neural efficiency or associated hearing outcomes.

The intracochlear position index (ICPI) was calculated via two different methodologies quoted in the literature - according to Ramos de Miguel (2019)[55] and Lee[61], which, as discussed in Chapter 1, are defined differently. Our results show that the Lee methodology produced marginally less discordance between CBCT and microCT when compared with the de Miguel method (20μm, p = .06 vs. 40μm, p = .003; $\overline{ICPI}_{Lee}$ vs. $\overline{ICPI}_{RdM}$) and marginally lower interobserver variability (ICC (3,1) 0.96 (0.89 – 0.99) vs. ICC (3,1) 0.93 (0.81 – 0.98); $\overline{ICPI}_{Lee}$ vs. $\overline{ICPI}_{RdM}$ on CBCT). This small discrepancy is likely explained by the requirement to identify the medial wall of the cochlea duct in the Ramos de Miguel methodology, which is not required in the Lee calculation. The medial cochlea wall incorporates the osseous spiral lamina, which has an irregular perforated surface and relatively fine structure. After specimen preparation (which includes removal of cellular elements and dehydration) the osseous lamina is degraded into a porous bony matrix with an ill-defined margin. This margin is subsequently difficult to sharply define on CT and is subject to partial-volume averaging (Figure 8). As a result, there is uncertainty in identifying a defined medial wall cut-off point. It is conceivable that this discrepancy may be reduced *in vivo* or in fresh cadaveric specimens which avoid the destructive specimen preparation regimen used in this study, however some uncertainty is unavoidable due to the resolution capabilities of the current generation of CT.

Calculation of both ICPI metrics and determination of the electrode to modiolus distance requires identification of the modiolar axis on CT. Of the small number of cadaveric studies which have measured the EMD on CT, a definition of the position of the modiolus and/or modiolar axis is loosely defined and often omitted[55,61]. Verbist *et al.* established a cylindrical co-ordinate system in their consensus paper on a cochlear coordinate system applicable in histological, physiological and radiological studies of the human cochlea[25]. They defined a ‘z-axis’ as running perpendicular to a plane through the basal turn of the cochlea, passing through the centre of the modiolus. This definition introduces ambiguity as it assumes, rather than defining, the position of the modiolus. In this study, we applied a slightly different criteria for the modiolar axis, as the

line joining the helicotrema to the cochlear aperture/lamina cribosa[97]. This definition strictly defines the modiolus at each point along the length of the cochlea and is discernible from reproducible landmarks on CT. This likely resulted in increased cross-modality concordance and reduce error associated with landmark identification. Other computational strategies such as semi-automated fiducial, surface and intensity-based registration approaches have been used in radiological studies of cochlea anatomy[86,98]. These techniques could be evaluated in future post-implantation validation studies to reduce operator-related error related to landmark identification.

This study found that electrode to modiolus distances were normally distributed, whereas intracochlear position indices were not. This distinction is methodologically relevant as EMD directly measures a single, continuous anatomical relationship, whilst ICPI integrates multiple anatomical references with a mathematical transformation as a composite index. ICPI depends on consistent visualisation of the medial cochlea wall beyond the basal turn, where landmark definition on clinical CT is limited. These factors increase susceptibility to systematic measurement error and observer variability. The non-normal distribution of ICPI may therefore reflect measurement variability related to reliance on several, inconsistently visualised landmarks, rather than genuine anatomical variability. Normality alone does not establish anatomical validity. However, the different distributional patterns of EMD and ICPI suggest that simple metrics provide more stable and reproducible representations of electrode position on clinical CT. This may indicate that measurement paradigms may benefit from greater emphasis on simple, anatomically direct metrics, such as electrode to modiolus distance. These metrics demonstrate stable statistical behaviour and are likely to be robust and practically applicable in routine imaging workflows.

The correlation between electrode position (i.e. basal to apical-most electrodes) and measurement discrepancy between CBCT and MicroCT for electrode contact-level metrics was mixed. Correlations were found between electrode position and electrode to modiolus and modiolus to lateral wall distances, with both showing slightly increased discrepancies associated with the basal electrodes. Conversely, $IPCI_{i,RdM}$ *and* $IPCI_{i,Lee}$ both showed a trend toward greater discrepancy at the apical-most electrodes. Stratification by electrode type (perimodiolar vs. lateral wall) produced similarly heterogenous results, with measurement discrepancies vary along the array, but without systematic tendency towards either electrode design or cochlear position. Overall, correlation strength was predominantly very weak to weak, and only occasionally modest, suggesting that much of the observed heterogeneity is likely to be statistically artefactual.

Interobserver variability between the three independent raters was generally high, with ICC values indicating excellent agreement (> 0.90) for most metrics across all modalities. Variability was the least for microCT, followed by CBCT, and greatest for MDCT. Moderate agreement was found in measurement of LWL and medial – lateral wall length across modalities, reflecting uncertainty of identifying the lateral wall in some instances, and the potential for cumulative measurement error. However, the generally excellent interobserver variability observed is encouraging, suggesting that the bony landmarks and metric measurement definitions used were clear, objective and consistently identifiable across CT modalities, and that variance is primarily attributable to intrinsic imaging factors. This result provides a solid foundation for future imaging validation studies and raises the possibility of an automated or semi-supervised algorithmic approach to electrode position quantification for postoperative patients. Interestingly, two of the three raters

were medically trained but did not have specific neuroradiological expertise. Rather, they were instructed only in identifying the relevant anatomical landmarks required for measurement. Measurement performance was nonetheless comparable across raters with differing levels of experience. This suggests that reliable measurements may be obtained without subspecialty expertise and that future studies may be feasible with a single rater.

Limitations

There are several limitations to acknowledge. Imaging was performed on isolated temporal bones, which marginally improves image quality compared with *in vivo* conditions. Agreement with the microCT gold standard may therefore have been slightly overestimated. *In vivo* artefact burden is greater and expected to have a greater impact on MDCT than CBCT. While absolute accuracy may decrease, the performance difference between clinical modalities may increase, with MDCT likely more adversely affected. Although larger than most prior validation studies, the sample size remains modest, and larger cohorts are required to confirm these findings and assess subtle sources of bias. Fellowship-trained neuroradiologists were not included as raters, which may limit real-world clinical applicability. Although microCT is regarded as a radiological gold standard, it remains susceptible to metal-related artefacts, including beam hardening, photon starvation, and metallic bloom. Whilst modest, these drawbacks introduce uncertainty in the bony cochlea anatomy surrounding the electrode and may misrepresent the true magnitude of measurement discrepancy between modalities. The use of thawed temporal bones degraded fine cochlear structures, including the basilar membrane, Reissner's membrane and the spiral limbus. As a result, scalar translocation could not be assessed, and uncertainty was introduced in medial cochlear wall localisation. Fresh-frozen specimens may have mitigated these effects but were not feasible within the practical constraints of the study.

Future work

Future work could address the above limitations by integrating radiological data with histological thin-section microphotography of the implanted cochlea. Histology offers substantially higher spatial resolution than CT and permits accurate visualisation of bony landmarks obscured by X-ray–related artefacts. As an anatomical reference standard, a complementary histological dataset would mitigate microCT-related bias, enable comparison with true *ex vivo* anatomy and provide more complete validation of clinical CT metrics of electrode position.

In this and other cadaveric studies, the modiolus is commonly used as a radiological surrogate for the neural elements, with the electrode to modiolus distance serving as an approximation for electrode-neural proximity. However, the spiral ganglion follows a non-uniform helical course within the osseous spiral lamina that does not precisely conform to the radiological boundary of the modiolus. Consequently, electrode–modiolus distance is a geometric approximation that may not reflect true physiological electrode – neural separation. More important for studies of the ENI, is the spatial relationship between electrode contacts and the neural structures. Histological sectioning with neuronal staining would allow direct identification of the spiral ganglion neurons. This approach has been demonstrated in histopathological studies of implanted human temporal bones, where serial sectioning and neural staining have visualised spiral ganglion neurons within Rosenthal's

canal and their relationship to the intracochlear electrode array[99,100]. Advanced research-only alternatives to microCT and histology as ground truth references are emerging. Synchrotron radiation phase-contrast imaging exploits phase shifts in highly coherent monochromatic X-rays to visualise cochlear cytoarchitecture non-destructively, with superior spatial resolution and contrast-to-noise ratio and without beam-hardening artefact[101-104]. Incorporating these components will enable a more physiologically grounded validation of intracochlear electrode position metrics and give a better idea of the effect of electrode position on efficiency of the ENI and associated hearing outcomes.

More broadly, this study establishes a comprehensive radiological normative dataset of intracochlear electrode position with clear relevance for future research and implant design. By defining quantitative whole-array and electrode contact-level metrics, it provides a benchmark for future clinical imaging studies and a set of surrogate imaging endpoints for correlating electrode position with implant performance. These data also inform next-generation implant design, offering a reference standard against which emerging electrode prototypes can be evaluated.

Conclusion

This study addresses the methodological gap identified in the systematic review by validating quantitative CT-derived metrics of intracochlear electrode position. Findings demonstrate that clinical CT, particularly cone-beam CT, can determine cochlear implant electrode position with high accuracy, predictable error characteristics and strong reproducibility.

In relation to the first aim, pairwise comparisons showed that measurement error between modalities was small for all whole array-level metrics. For electrode contact-level metrics, discrepancies were consistently confined to sub-millimetre or voxel-scale limits. Secondly, inter-modality agreement did not differ significantly between perimodiolar and lateral wall electrodes across most metrics. Systematic variation along the array was generally weak, indicating consistent performance across electrode designs and cochlear positions. Thirdly, interobserver variability analysis showed good-to-excellent reliability across almost all metrics on microCT and CBCT, suggesting minimal operator-dependent variability when clear anatomical landmarks are used.

Collectively, the results substantiate the study's primary hypothesis. Agreement between clinical CT modalities and the microCT reference standard was consistently within clinically acceptable bounds and is supported by minimal variance and robust interobserver reliability.

By providing a detailed, modality-specific characterisation of measurement accuracy and reproducibility, this study establishes a foundational radiological dataset for postoperative electrode assessment. It defines the technical capabilities and practical limitations of current CT imaging, furnishing a framework upon which future clinical outcome studies, implant-design research and automated measurement algorithms may be built.

Appendix 1. Tables and Figures

Medical Subject Heading ('MeSH') Terms and Keywords used in systematic review

Cochlear implants

(1) Cochlear implants/ or Cochlear implantation/

Computed tomography (CT)

(2) Cone-beam computed tomography/ or Tomography, X-Ray Computed/ or X-Ray Microtomography/ or Multidetector computed tomography/

(3) (1) AND (2)

(4) Remove duplicates from (3)

(5) Limit 4 to English language

Figure 1. PRISMA flow diagram of study selection.

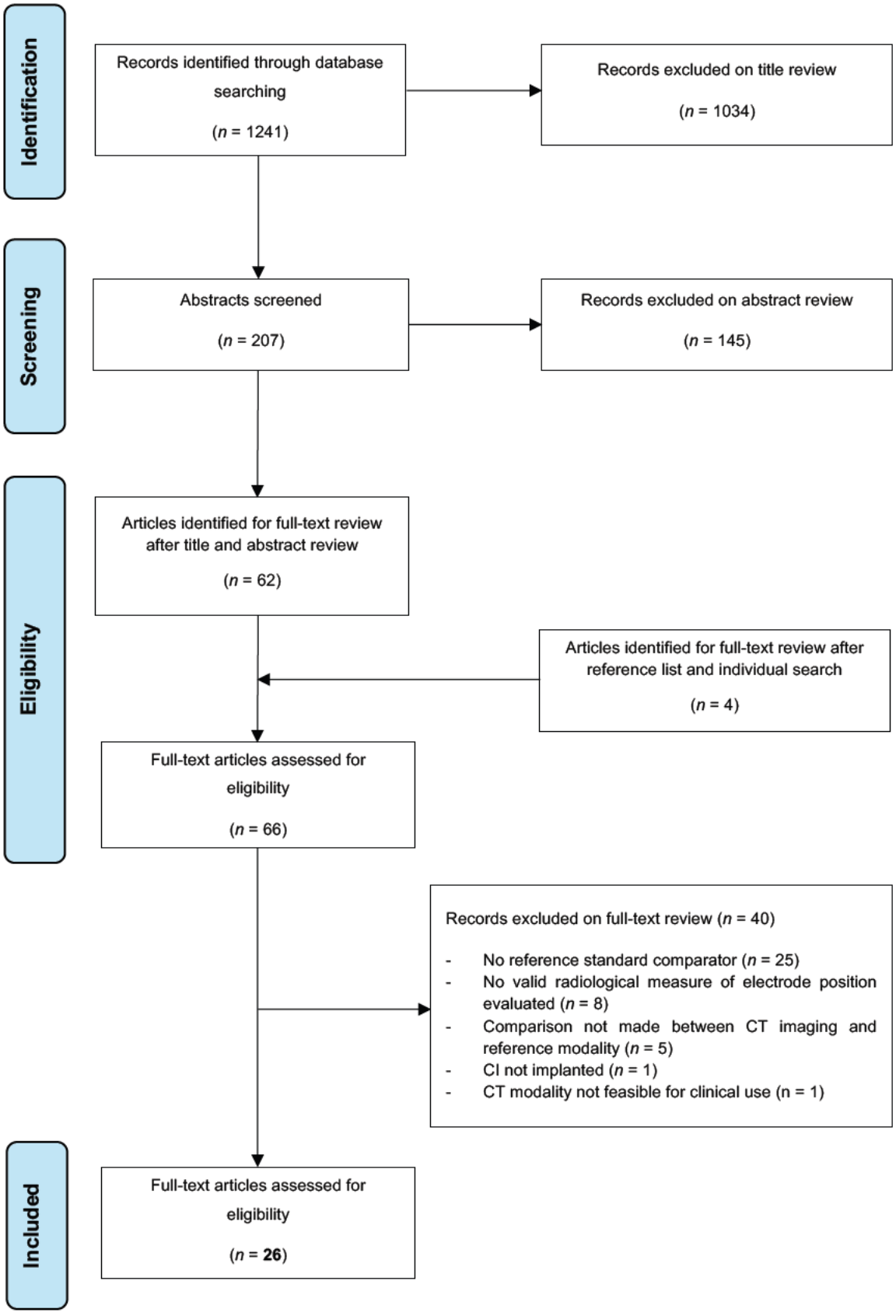

Figure 2. QUADAS-2 risk of bias assessment for included studies across four domains and overall judgement.

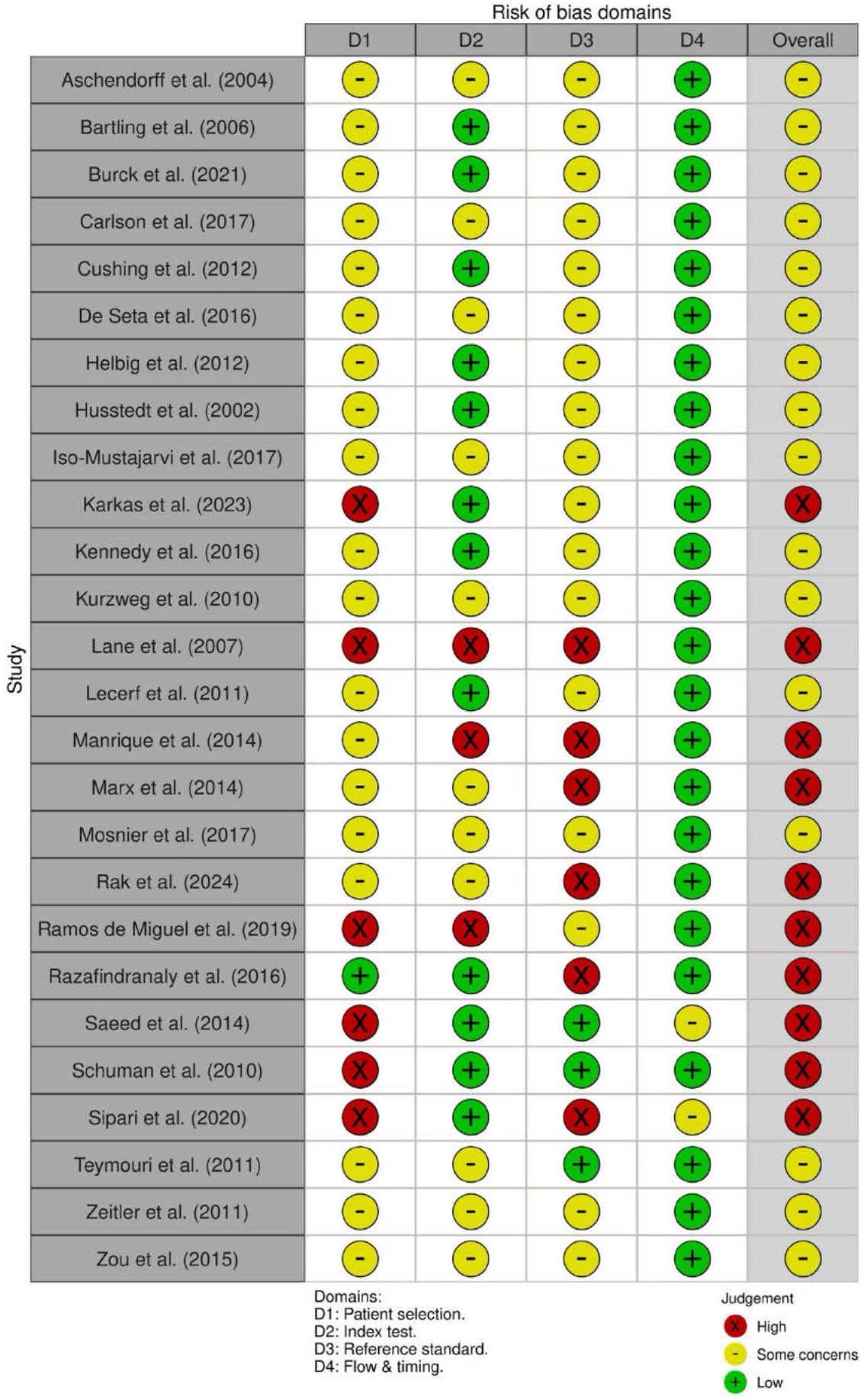

D1 – patient selection; D2 – index test; D3 – reference standard; D4 – flow and timing

Figure 3.
Representative microCT and CBCT images demonstrating clear separation of individual electrode contacts with acceptable metal artefact, allowing confident delineation of relevant bony anatomy, including the modiolar axis and the medial and lateral cochlear duct walls. **(A)** Specimen 8 in the basal turn view on microCT. **(B)** Specimen 8 in the basal turn view on CBCT. **(C)** Specimen 5 in the transmodiolar view on microCT. **(D)** Specimen 5 in the transmodiolar view on CBCT.

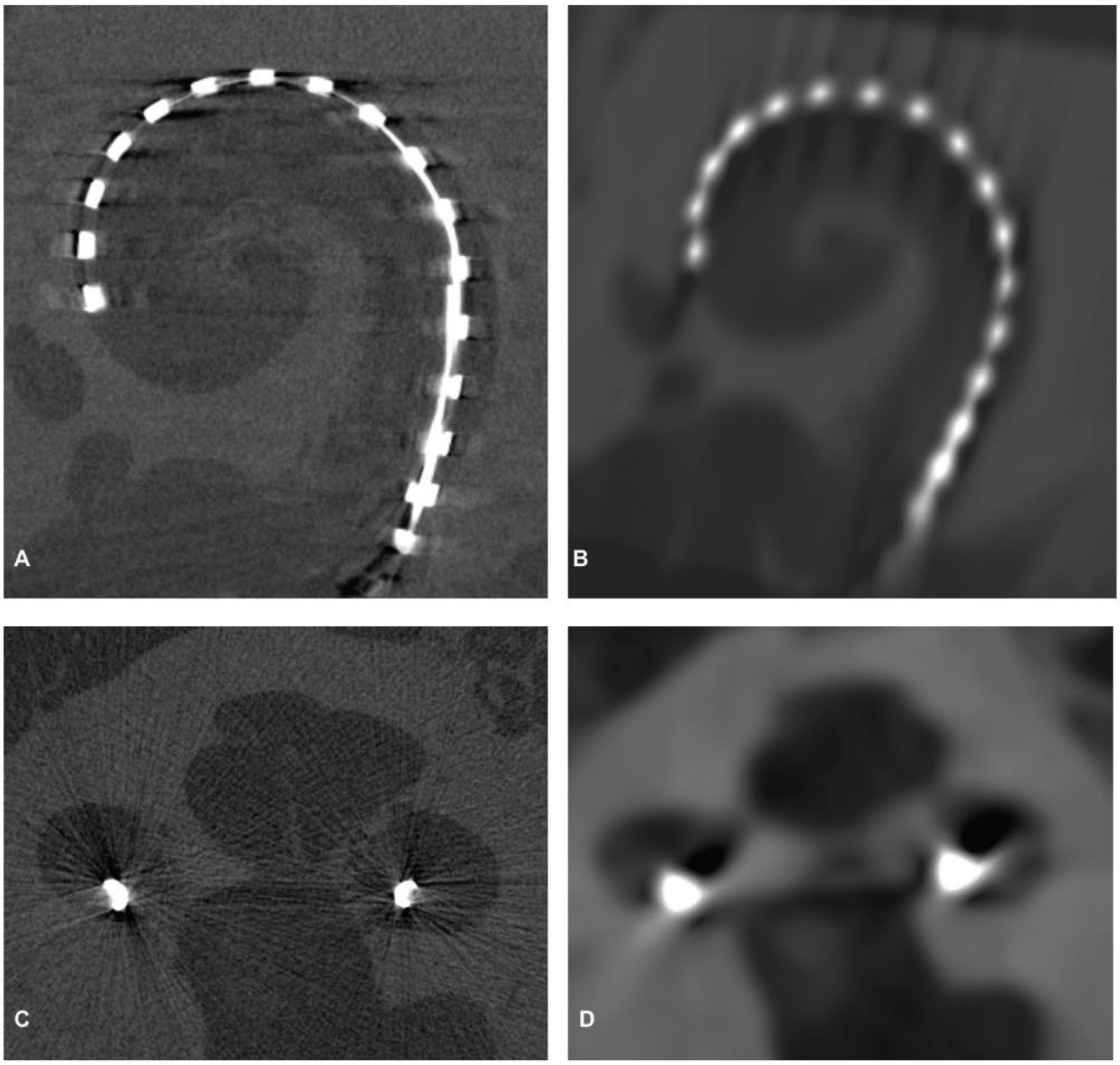

Figure 4.
Representative images illustrating prominent metallic blur with MDCT imaging. Blooming results in the inability to resolve adjacent electrodes and obscured cochlear duct walls.
(A) Specimen 8 in the basal turn view. **(B)** Specimen 5 in the transmodiolar view.

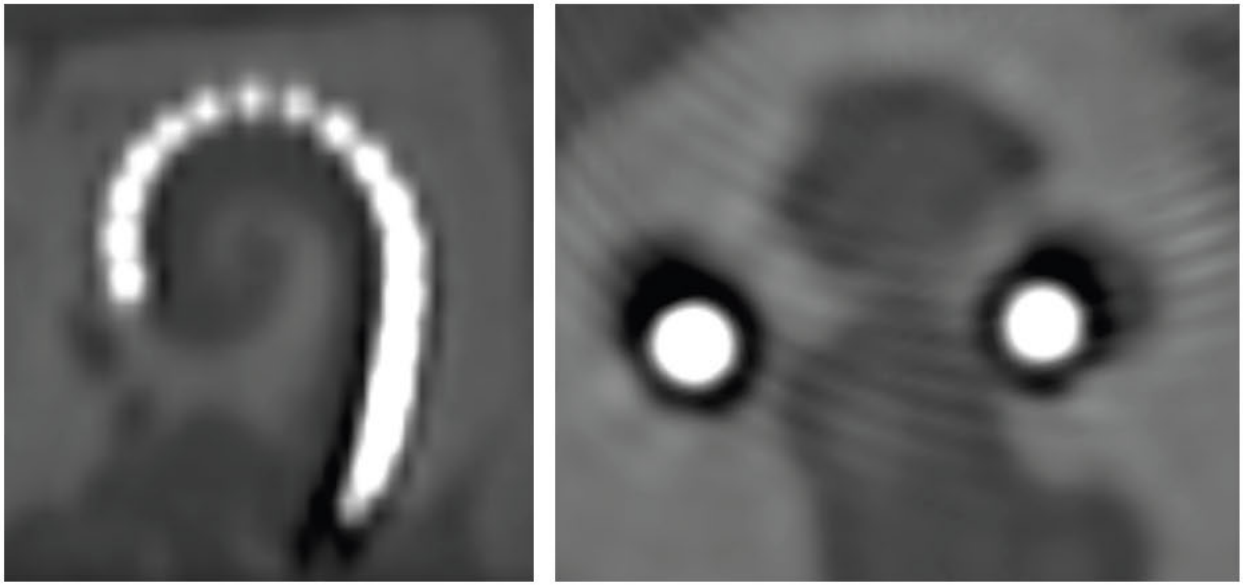

Figure 5.
MicroCT image of specimen 6 showing with electrode contacts 12–17 absent following inadvertent removal.

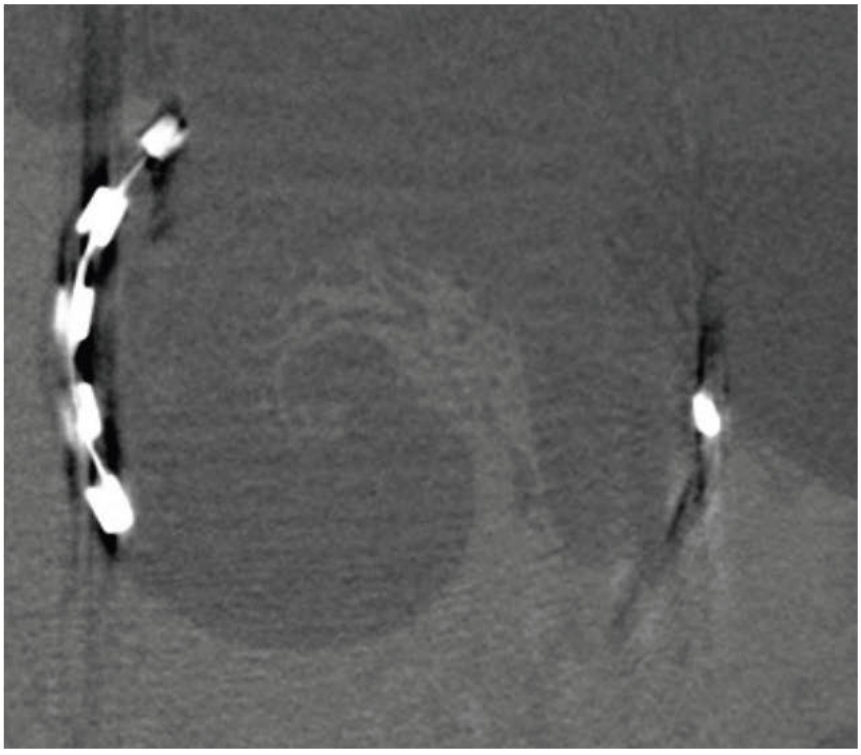

Figure 6A.
Graphical summary of descriptive statistics for whole-array–level intracochlear electrode position metrics. Mean values with 95% confidence intervals are shown for angular insertion depth, inserted electrode length, lateral wall length, and wrapping factor across microCT, CBCT, and MDCT.

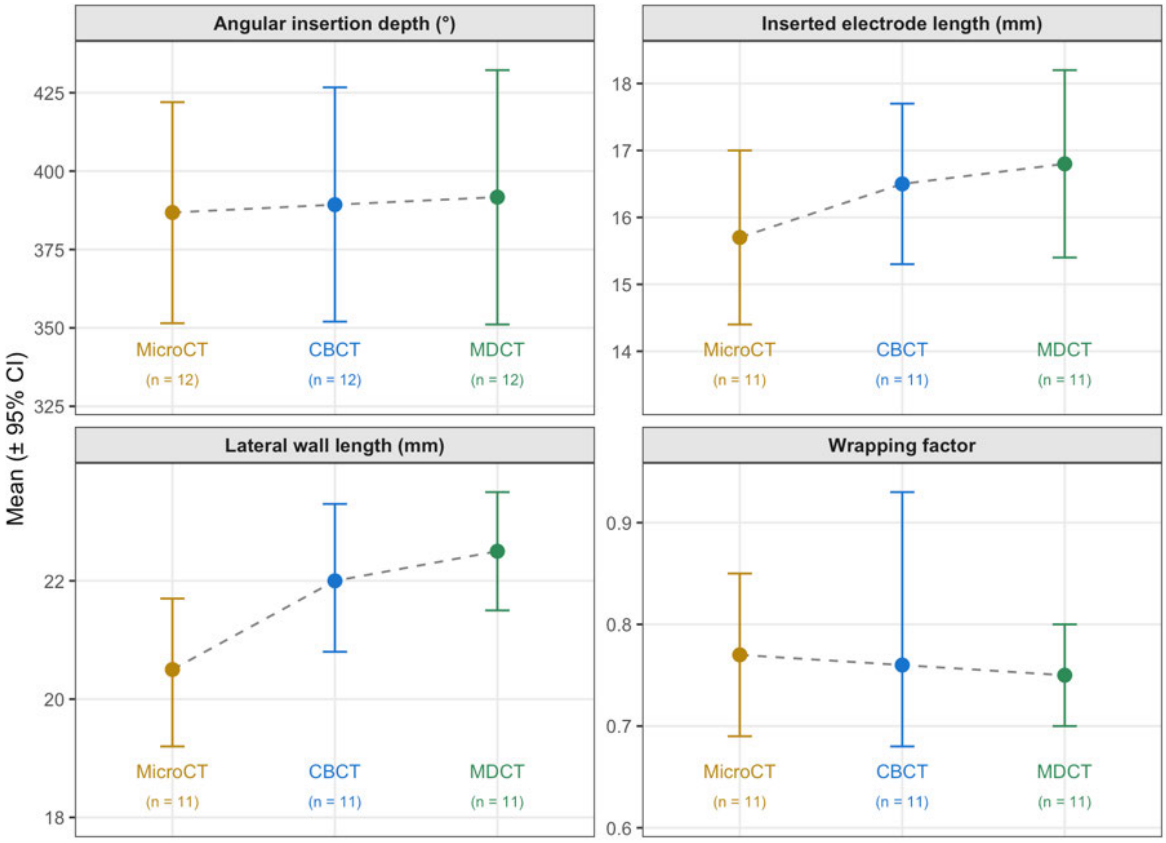

Figure 6B.
Descriptive statistics for wall and distance-based intracochlear electrode position metrics across microCT and CBCT (mean± 95% confidence intervals).

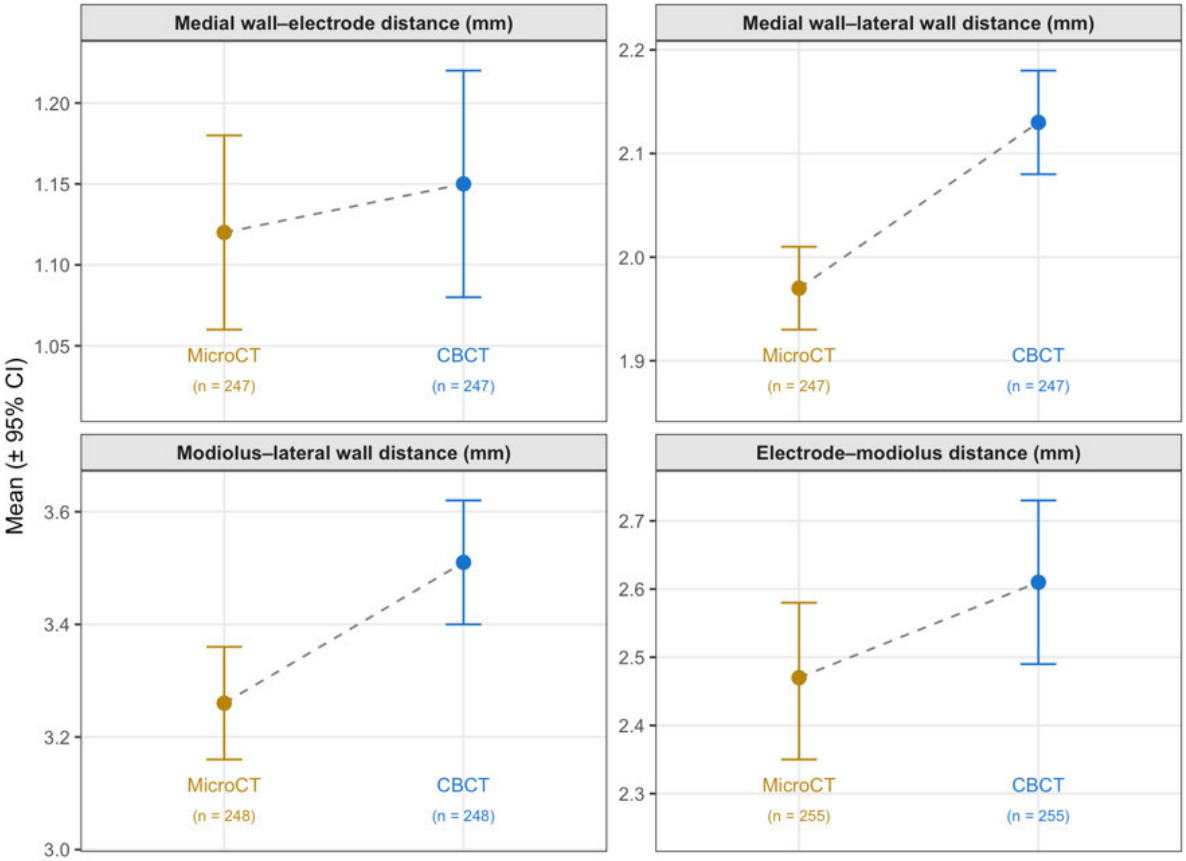

Figure 6C.
Descriptive statistics for intracochlear position indices across microCT and CBCT (mean± 95% confidence intervals).

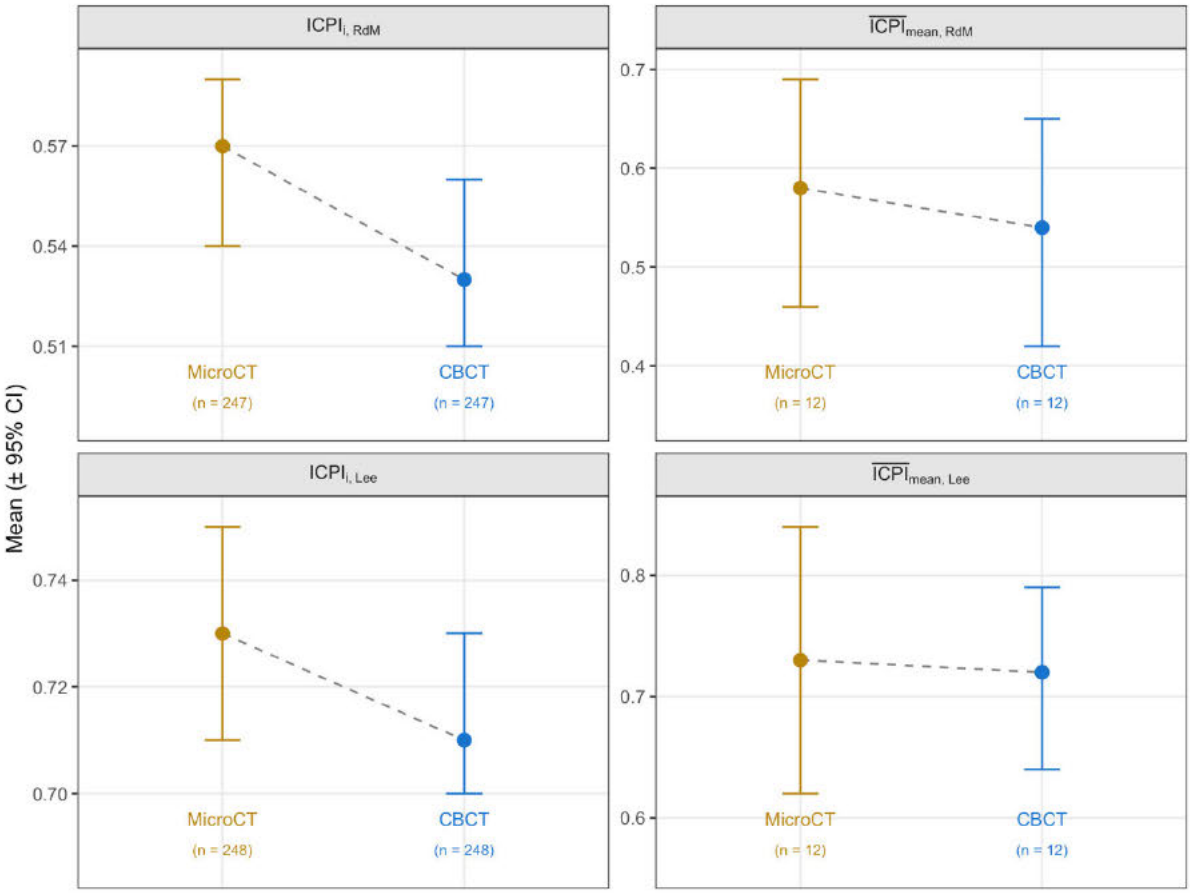

Table 1.
Characteristics of included studies.

Author (year)	Study Design	Sample	Electrode model (manufacturer)	Electrode type	CT modality(s)	Reference	Electrode position metric evaluated
Aschendorff *et al.* (2004) [30]	Cadaveric	2	Nuclear 22 (Cochlear)	LW	MDCT (1 slice) MDCT (16 slice) CBCT (rotational, biplane)	Histology	Scalar position
Bartling *et al.* (2006) [31]	Cadaveric	4	Contour Advance (Cochlear)	PM	MDCT (4 slice) CBCT (fpVCT)	Histology	Scalar position
Burck *et al.* (2021) [32]	Cadaveric	20	Hi-Focus Mid-Scala (Advanced Bionics)	MS	MDCT (128 slice) CBCT (standard)	Histology	Scalar position
Carlson *et al.* (2017) [33]	Cadaveric	8	Unspecified	N/A	MDCT (64 slice) MDCT (192 slice)	MicroCT	Scalar position
Cushing *et al.* (2012) [34]	Cadaveric	11	Research array (Cochlear)	LW	CBCT (rotational)	Histology	Scalar position Number of intracochlear electrodes Electrode kinking Electrode contact direction (medial vs. lateral) Electrode array ascension
De Seta *et al.* (2016) [35]	Cadaveric	14	FLEX28 (MED-EL)	LW	CBCT (standard)	Histology	Scalar position
Helbig *et al.* (2012) [37]	Cadaveric	20	FLEX-SOFT (MED-EL)	LW	MDCT (4 slice)	Histology	Scalar position
Husstedt *et al.* (2002) [38]	Cadaveric	Unspecified	CI24M (Cochlear) CI24RE (Cochlear)	LW, PM	CBCT (rotational)	Histology	Scalar position Electrode to modiolus distance
Iso- Mustajärvi *et al.* (2017) [39]	Cadaveric	20	CI532 (Cochlear)	PM	CBCT (standard)	Histology	Scalar position Electrode to modiolus distance
Karkas *et al.* (2023) [40]	Cadaveric	10	FLEX-26 (MED-EL)	LW	CBCT (standard)	MicroCT	Scalar position
Kennedy *et al.* (2016) [41]	Cadaveric	11	FLEX24 (MED-EL)	LW	MDCT (16 slice) CBCT (rotational)	MicroCT	Scalar position
Kurzweg *et al.* (2010) [42]	Cadaveric	13	Contour Advance (Cochlear)	PM	CBCT (standard)	Histology	Scalar position Electrode to modiolus distance
Lane *et al.* (2007) [43]	Cadaveric	1	Softtip Contour (Cochlear)	PM	MDCT (64 slice)	Histology MicroCT	Scalar position
Lecerf *et al.* (2011) [44]	Cadaveric	18	Contour Advance (Cochlear)	PM	MDCT (40 slice)	Histology	Scalar position
Manrique *et al.* (2014) [45]	Cadaveric	10	HiFocus 1J (Advanced Bionics) HiFocus Helix (Advanced Bionics)	LW, PM	MDCT (64 slice)	Histology	Scalar position

LW – lateral wall; PM – perimodiolar; MS – mid scala; MDCT – multidetector CT; CBCT – conebeam CT; fpVCT – flat-panel volumetric CT; microCT – microcomputed

Author (year)	Study Design	Sample	Electrode model (manufacturer)	Electrode type	CT modality(s)	Reference	Electrode position metric evaluated
Marx *et al.* (2014) [46]	Cadaveric	10	Modiolar Research Array (Cochlear)	PM	CBCT (standard)	Histology	Scalar position
Mosnier *et al.* (2017) [47]	Cadaveric	8	Slim Straight (Cochlear)	LW	CBCT (standard)	Histology	Scalar position
Rak *et al.* (2024) [56]	Cadaveric	10	FLEX28 (MED-EL)	LW	Photon counting CT	CBCT (rotational) MDCT (128 slice)	Angular insertion depth Inserted electrode length
Ramos de Miguel (2019) [55]	Cadaveric	3	CI532 (Cochlear)	PM	CBCT (standard)	Histology	Intracochlear electrode position index Homogeneity factor Wrapping factor
Razafindranaly *et al.* (2016) [48]	Prospective, randomised, *in vivo*	9	Electrode models not stated Nucleus CI24RE (Cochlear) Concerto (MED-EL) DigisonicSP (Oticon)	Unspecified	CBCT (standard)	MDCT 64-slice	Scalar position Inserted electrode length
Saeed *et al.* (2014) [49]	Cadaveric	8	Contour Advance (Cochlear) Slim Straight (Cochlear)	LW, PM	CBCT (standard)	Histology	Scalar position
Schuman *et al.* (2010) [50]	Cadaveric	7	Contour Advance (Cochlear)	PM	CBCT (fpVCT, with microCT)	Histology	Scalar position
Sipari *et al.* (2020) [51]	Retrospective cohort, *in vivo*	30	FLEX28 (MED-EL) Hi-Focus Mid-Scala (Advanced Bionics) HiFocus SlimJ (Advanced Bionics) Slim Modiolar (Cochlear) Slim Straight (Cochlear) EVO (Oticon)	LW, PM, MS	CBCT (standard, with image fusion technique)	CBCT alone	Scalar position
Teymouri *et al.* (2011) [52]	Cadaveric	18	HiFocus 1J (Advanced Bionics) Nucleus 24 (Cochlear)	LW, PM	MDCT (4 slice) MDCT (64 slice)	MicroCT Histology	Scalar position
Zeitler *et al.* (2011) [53]	Cadaveric	6	Not stated	PM, LW.	CBCT (fpVCT)	MDCT Histology	Scalar position Angular insertion depth Electrode to modiolus distance
Zou *et al.* (2015) [54]	Cadaveric	9	FLEX24, FLEX28, Experimental array (MED-EL)	LW	CBCT (fpVCT)	MicroCT	Scalar position Electrode to medial wall distance

Table 2.
Summary of reported findings across included studies.

Author (year)	CT modality(s)	CT parameters	Metric evaluated	Rater characteristic	Results
Aschendorff *et al.* (2004) [30]	MDCT (1-slice) MDCT (16-slice) CBCT (Rotational, biplane)	Single slice CT: 100kVp, 100mAs MDCT (16-slice): 120kVp, 120mAs CBCT (rotational): kVp and mAs not specified.	Scalar position	Unspecified	Scalar position could be determined on a CBCT (rotational, Biplane) (1/1) with small amount of metallic electrode artefacts. Single slice CT and MDCT could not determine scalar position (0/1 respectively), only intra- vs. extracochlear electrode placement (1/1 respectively)
Bartling *et al.* (2006) [31]	MDCT (4-slice) CBCT (fpVCT)	MDCT:140kVp, 624mAs CBCT (fpVCT): 120kVp, 200mAs and 320mAs	Scalar position	2 raters (1x otolaryngologist, 1x neuroradiologist). Blinded. Independent	Electrode array was visible on both MDCT and CBCT, however MDCT produced more widening blur artefact than CBCT.
Burck *et al.* (2021) [32]	MDCT (128 slice) CBCT (Standard)	MDCT (128 slice): 120kVp, 1200mAs CBCT: 96kVp and 120kVp, 71mAs	Scalar position	2 raters (2x neuroradiologists) Blinded. Independent. Randomised.	MDCT correctly determined scalar position in 31/40 cases (77.5%) CBCT at 96kV determined scalar position in 39/40 cases (97.5%) CBCT at 120kV determined scalar position in 40/40 cases (100%) Accuracy of determining intrascalar electrode array position was higher for CBCT compared with MDCT • MDCT vs. 96kV CBCT: $p = 0.04$ • MDCT vs. 120kV CBCT: $p = 0.007$ No difference between 96kV vs. 120kV CBCT protocol in determining scalar position ($p > 0.99$)
Carlson *et al.* (2017) [33]	MDCT (64 slice) MDCT (192 slice)	MDCT (64 slice): 120kVp, 400mAs MDCT (192 slice): 120kVp, 400mAs	Scalar position	3 raters (3x neuroradiologists). Independent.	192-slice scanner provided superior (vs. 64 slice) resolution with better visualisation and identification of individual electrodes which improves diagnostic confidence ($p < 0.001$).
Cushing *et al.* (2012) [34]	CBCT (Rotational)	100kVp, mA not specified, 60s rotation	Scalar position	3 raters (2x otolaryngologist, 1x neuroradiologists). Blinded. Independent.	Scalar position correctly identified by CBCT (rotational) in all cases (11/11).
De Seta *et al.* (2016) [35]	CBCT (Standard)	110kVp, 684mAs	Scalar position	2 reviewers (2x otolaryngologist, 1x neuroradiologist)	Good concordance found between CBCT and histology for identification of electrodes in the basal turn (Cohen's k = 0.54, pairwise agreement 78.7%). Concordance was poorer identifying apical electrode position (Cohen's k = 0.31, pairwise agreement 50%)

Author (year)	CT modality(s)	CT parameters	Metric evaluated	Rater characteristic	Results
Helbig *et al.* (2012) [37]	MDCT (4-slice)	120kVp, 220mA, exposure time not specified	Scalar position	2 raters (2x neuroradiologists) Blinded.	Both radiologists correctly determined scalar position in 17/20 (85%) cases in the basal turn up to an insertion angle of 270°. Correct scalar position determination became progressively worse beyond 270°.
Husstedt *et al.* (2002) [38]	CBCT (Rotational)	kVp and mAs not specified	Scalar position Electrode to modiolus distance	Unspecified	In all cases, CBCT (rotational) gave similar information concerning the scalar position and electrode to modiolus proximity when compared with histologic analysis
Iso-Mustajärvi *et al.* (2017) [39]	CBCT (Standard)	96kVp, 105mAs	Scalar position Electrode to modiolus distance	3 raters (3x otolaryngologists) Independent.	Scalar position and translocations detectable with CBCT 3D fusion technique and histology, with both techniques confirming the only instance of scala translocation. Significant interclass correlation (0.697) between CBCT 3D fusion technique and histology measurements of electrode to modiolus distance.
Karkas *et al.* (2023) [40]	CBCT (Standard)	90kVp, 200mAs	Scalar position	2 raters (1x otolaryngologist, 1x neuroradiologist) Blinded. Independent.	Investigators comment that assessment of scalar position was permitted with both micro-CT and CBCT, however no formal/statistical comparison is made.
Kennedy *et al.* (2016) [41]	MDCT (16 slice) CBCT (Rotational)	MDCT: 120kVp, "Smart mA" CBCT: 125kVp, mAs not specified	Scalar position	5 raters (3x otolaryngologists, 2x neuroradiologists). Blinded. Independent.	CBCT (rotational) is superior to MDCT at localising the electrode within the correct scalar compartment (odds ratio = 8.96, $p < 0.001$)
Kurzweg *et al.* (2010) [42]	CBCT (Standard)	60kVp, 144mAs	Scalar position Electrode to modiolus distance	2 raters (unspecified). Independent.	Scalar position could be correctly identified in 11/13 cases (84.6%) on CBCT. Mean difference in measurement of electrode to modiolus distance between CBCT and histology was 65.40µm.
Lane *et al.* (2007) [43]	MDCT (64 slice)	120kVp, 320mAs	Scalar position	2 raters (2x neuroradiologists).	The electrode was localised to the scala tympani on MDCT throughout it's 360 degree insertion.
Lecerf *et al.* (2011) [44]	MDCT (40 slice)	140kVp, 400mAs	Scalar position	2 raters (2x neuroradiologists). Independent.	High radioanatomic correlation (94%) in determining the scalar position when using a midmodiolar reconstruction
Manrique *et al.* (2014) [45]	MDCT (64 slice)	140kVp, 400mAs	Scalar position	Unspecified	MDCT indicated correct scalar position in 4/5 implanted temporal bones when compared to histology. In one implanted bone, CT incorrectly deemed the electrode was in the scala vestibuli, but histology indicated it was in the scala tympani.
Marx *et al.* (2014) [46]	CBCT (Standard)	110kVp, 342mAs	Scalar position	2 raters (1x otolaryngologist, 1x neuroradiologist). Independent.	CBCT reached high sensitivity (100%) and specificity (90%) in determining scalar electrode position.
Mosnier *et al.* (2017) [47]	CBCT (Standard)	Not specified	Scalar position	2 raters (1x otolaryngologist, 1x neuroradiologist). Independent.	Histological analysis verified CBCT electrode scalar position in 7/8 TBs (88%)

Author (year)	CT modality(s)	CT parameters	Metric evaluated	Rater characteristic	Results
Rak *et al.* (2024) [56]	Photon counting CT	120kVp, 158mAs	Angular insertion depth Inserted electrode length	2 raters (2x otolaryngologist). Independent.	Significant difference in the accuracy of AID and IEL measurement between MDCT and PCCT ($p < 0.001$). No significant difference in accuracy of AID and IEL measurement between CBCT and PCCT.
Ramos de Miguel (2019) [55]	CBCT (Standard)	Not specified	Intracochlear position index Homogeneity factor Wrapping factor	10 raters (5x otolaryngologists, 5x radiologist).	No significant difference between CBCT and histology for: - ICPI, in 3/3 specimens → considered the most accurate measure - HF in 2/3 specimens WF in 1/3 specimens.
Razafindranaly *et al.* (2016) [48]	CBCT (Standard)	110kV, 4320mAs	Scalar position Inserted electrode length	2 raters (2x radiologists). Blinded. Independent. Randomised.	A Kappa value of 0.643 ($p = 0.002$) was found, showing good agreement between MDCT and CBCT for determining scalar localization. Mean difference in inserted electrode length measurement between MDCT and CBCT was 0.66mm
Saeed *et al.* (2014) [49]	CBCT (Standard)	95kVp, 87.5mAs	Scalar position	3 raters (3x otolaryngologists) Blinded.	In most cases, determination of scalar position on CBCT scans and histology were in agreement. One observer incorrectly judged some of the apical electrodes to be in the scala vestibuli in 2/8 temporal bones.
Schuman *et al.* (2010) [50]	CBCT (fpVCT, with MicroCT)	120kVp, 420mAs	Scalar position	Unspecified	CBCT based algorithm could discern 5/5 complete ST insertions and 3/3 intracochlear translocations from ST to SV.
Sipari *et al.* (2020) [51]	CBCT (Standard, with image fusion)	96kVp, 75 – 106.5mAs	Scalar position	Unspecified	The addition of pre/postoperative CBCT imaging fusion resulted in scalar position grading change in 40/151 (26.5%) of measurement points assessed.
Teymouri *et al.* (2011)[52]	MDCT (4 slice) MDCT (64 slice)	MDCT 4-slice: 120kVp, 315mA, 0.5mm collimation, 0.9 pitch. MDCT 64-slice: 120kVp, 360mA, 0.5mm collimation, 0.9 pitch.	Scalar position	3 raters (2x otolaryngologist, 1x audiologist). Independent.	150/158 (94.9%) concordance of electrode positions analysed via histology when with MDCT. 302/310 (97.0%) concordance of MDCT with MicroCT reference standard, with most instances of disagreement confined to the apical electrodes.
Zeitler *et al.* (2011)[53]	CBCT (fpVCT)	120kVp, 280mA, exposure time not stated	Scalar position Angular insertion depth Electrode to modiolus distance	2 raters (2x neuroradiologists). Independent.	Intrascalar position and angular insertion depth correlated well between CBCT (fpVCT) and histology. Mean electrode to modiolus distance did not differ significantly between CBCT (fpVCT) and MDCT images.
Zou *et al.* (2015)[54]	CBCT (fpVCT)	88kVp, 495mAs	Scalar position Electrode to medial wall distance	Unspecified	Scalar position within the scala tympani was confirmed on CBCT in all samples. Mean difference in electrode to medial wall distance as measured between CBCT and MicroCT = 0.154mm

Table 4.

Descriptive statistics of metrics of intracochlear electrode position as measured by the primary rater (AT).

Metric	Modality	n	Mean ± SD	Min	Max	95% CI
Angular insertion depth (°)	MicroCT	12	386.8 ± 55.5	275.0	450.3	351.5 – 422.0
	CBCT	12	389.3 ± 58.8	271.4	467.5	352.0 – 426.7
	MDCT	12	391.7 ± 63.8	268.5	474.0	351.1 – 432.2
Inserted electrode length (mm)	MicroCT	11	15.7 ± 1.9	13.89	18.89	14.4 – 17.0
	CBCT	11	16.5 ± 1.8	14.5	18.9	15.3 – 17.7
	MDCT	11	16.8 ± 2.1	14.7	19.9	15.4 – 18.2
Lateral wall length (mm)	MicroCT	11	20.5 ± 1.9	15.89	22.86	19.2 – 21.7
	CBCT	11	22.0 ± 1.9	18.0	25.1	20.8 – 23.3
	MDCT	11	22.5 ± 1.3	19.5	24.1	21.5 – 23.5
Wrapping factor	MicroCT	11	0.77 ± 0.12	0.62	0.93	0.69 – 0.85
	CBCT	11	0.76 ± 0.11	0.61	0.89	0.68 – 0.93
	MDCT	11	0.75 ± 0.07	0.64	0.83	0.70 – 0.80
Medial wall to electrode distance (mm)	MicroCT	247	1.12 ± 0.49	0.37	2.42	1.06 – 1.18
	CBCT	247	1.15 ± 0.55	0.34	2.83	1.08 – 1.22
	MDCT	0	-	-	-	-
Medial wall to lateral wall distance (mm)	MicroCT	247	1.97 ±0.32	0.82	3.05	1.93 – 2.01
	CBCT	247	2.13 ± 0.38	1.05	3.03	2.08 – 2.18
	MDCT	0	-	-	-	-
Modiolus to lateral wall distance (mm)	MicroCT	248	3.26 ± 0.79	1.06	5.74	3.16 – 3.36
	CBCT	248	3.51 ± 0.89	1.18	6.27	3.40 – 3.62
	MDCT	0	-	-	-	-
Electrode to modiolus distance (mm)	MicroCT	255	2.47 ± 0.92	0.61	6.08	2.35 – 2.58
	CBCT	255	2.61 ± 1.00	0.69	6.52	2.49 – 2.73
	MDCT	0	-	-	-	-
$ICPI_{i,\ RdM}$	MicroCT	247	0.57 ± 0.21	0.23	0.95	0.54 – 0.59
	CBCT	247	0.53 ± 0.20	0.15	0.94	0.51 – 0.56
	MDCT	0	-	-	-	-
$\overline{ICPI}_{RdM}$	MicroCT	12	0.58 ± .18	0.39	0.84	0.46 – 0.69
	CBCT	12	0.54 ± 0.18	0.36	0.78	0.42 – 0.65
	MDCT	0	-	-	-	-
$ICPI_{i,\ Lee}$	MicroCT	248	0.73 ± 0.15	0.44	0.97	0.71 – 0.75
	CBCT	248	0.71 ± 0.14	0.39	0.95	0.70 – 0.73
	MDCT	0	-	-	-	-
$\overline{ICPI}_{Lee}$	MicroCT	12	0.73 ± .18	0.39	0.84	0.62 – 0.84
	CBCT	12	0.72 ± .11	0.56	0.88	0.64 – 0.79
	MDCT	0	-	-	-	-

Table 5.
Bland–Altman analysis of pairwise modality comparisons for intracochlear electrode position metrics, including mean bias and 95% limits of agreement.

Metric	Modality comparison	*p value*[*]	Bias	Bias as percentage[**]	Limits of agreement (lower – upper)
AID (°)	MicroCT vs. CBCT	.18	-2.58	0.7	-14.91 – 9.76
	MicroCT vs. MDCT	.16	-4.90	1.3	-26.08 – 16.28
	CBCT vs. MDCT	.41	-2.33	0.6	-20.01 – 15.36
IEL (mm)	MicroCT vs. CBCT	*.005*	-0.85	5.4	-1.76 – 0.07
	MicroCT vs. MDCT	*.003*	-1.15	7.3	-2.31 – 0.01
	CBCT vs. MDCT	*.036*	-0.30	1.9	-1.23 – 0.63
LWL (mm)	MicroCT vs. CBCT	*.01*	-1.54	7.5	-2.86 – -0.22
	MicroCT vs. MDCT	*.01*	-2.02	9.9	-4.81 – 0.77
	CBCT vs. MDCT	.30	-0.48	2.3	-3.31 – 2.35
WF	MicroCT vs. CBCT	.09	0.02	2.6	-0.04 – 0.07
	MicroCT vs. MDCT	.29	0.02	2.6	-0.08 – 0.13
	CBCT vs. MDCT	.72	0.01	1.3	-0.07 – 0.09
Medial wall to electrode distance (mm)	MicroCT vs. CBCT	*.027*	-0.03	2.7	-0.44 – 0.38
Medial wall to lateral wall distance (mm)	MicroCT vs. CBCT	<*. 001*	-0.16	8.1	-0.70 – 0.37
Modiolus to lateral wall distance (mm)	MicroCT vs. CBCT	< *.001*	-0.24	7.4	-0.81 – 0.32
Electrode – modiolus distance (mm)	MicroCT vs. CBCT	< *.001*	-0.14	5.7	-0.60 – 0.32
$ICPI_{i,\ RdM}$	MicroCT vs. CBCT	< *.001*	0.04	7.0	-0.08 – 0.16
$\overline{ICPI}_{RdM}$	MicroCT vs. CBCT	*.003*	0.04	6.9	-0.01 – 0.08
$ICPI_{i,\ Lee}$	MicroCT vs. CBCT	< *.001*	0.02	2.7	-0.08 – 0.11
$\overline{ICPI}_{Lee}$	MicroCT vs. CBCT	*.06*	0.02	2.7	-0.04 – 0.08

* *p*-value for pairwise comparison. Statistically significant values highlighted.

**Bias presentation as a percentage of the mean value of the corresponding metric as measured on the gold standard (i.e. microCT)

Table 6.
Measurement concordance of intracochlear electrode position metrics by electrode array type (perimodiolar vs lateral wall).

Metric	Modality comparison	Mean absolute difference ± SD (perimodiolar vs. lateral wall)	*p* value
AID (°)	MicroCT vs. CBCT	8.2 ± 6.1° vs 3.3 ± 2.7°	.07
	MicroCT vs. MDCT	15.0 ± 12.6° vs 5.3 ± 3.6°	.06
	CBCT vs. MDCT	8.8 ± 8.5° vs. 7.1 ± 4.3°	.65
IEL (mm)	MicroCT vs. CBCT	1.06 ± 0.40mm vs. 0.72 ± 0.49mm	.27
	MicroCT vs. MDCT	1.25 ± 0.73mm vs. 0.98 ± 0.18mm	.50
	CBCT vs. MDCT	0.27 ± 0.30mm vs. 0.52 ± 0.36mm	.27
LWL (mm)	MicroCT vs. CBCT	1.96 ± 0.43mm vs. 1.30 ± 0.70mm	.13
	MicroCT vs. MDCT	2.59 ± 1.48mm vs. 1.03 ± 0.58mm	*.03*
	CBCT vs. MDCT	1.29 ± 1.16mm vs. 0.93 ± 0.31mm	< *.01*
WF	MicroCT vs. CBCT	0.03 ± 0.03 vs. 0.01 ± 0.01	.09
	MicroCT vs. MDCT	0.06 ± 0.05 vs 0.02 ± 0.01	.1
	CBCT vs. MDCT	0.03 ± 0.01 vs. 0.04 ± 0.03	.65
Medial wall to electrode distance (mm)	MicroCT vs. CBCT	0.14 ± 0.13mm vs. 0.17 ± 0.15mm	.62
Medial wall to lateral wall distance (mm)	MicroCT vs. CBCT	0.20 ± 0.17mm vs. 0.28 ± 0.21mm	*.001*
Modiolus to lateral wall distance (mm)	MicroCT vs. CBCT	0.29 ± 0.16mm vs. 0.32 ± 0.26mm	.39
Electrode to modiolus distance (mm)	MicroCT vs. CBCT	0.20 ± 0.19mm vs. 0.21 ± 0.17mm	.49
$ICPI_{i,\ RdM}$	MicroCT vs. CBCT	0.06 ± 0.05 vs. 0.05 ± 0.04	.23
$\overline{ICPI}_{RdM}$	MicroCT vs. CBCT	0.05 ± 0.01 vs. 0.03 ± 0.02	.35
$ICPI_{i,\ Lee}$	MicroCT vs. CBCT	0.04 ± 0.03 vs, 0.04 ± 0.03	.62
$\overline{ICPI}_{Lee}$	MicroCT vs. CBCT	0.02 ± 0.01 vs. 0.03 ± 0.03	.21

Table 7.
Spearman's correlation of measurement concordance along the electrode array.

Metric	Spearman's ρ*	*p*-value	Interpretation
Medial wall to electrode distance (mm)	-0.086	.18	No significant variation in discrepancy along the array
Medial wall to lateral wall distance (mm)	0.009	.89	No significant variation in discrepancy along the array
Modiolus to lateral wall distance (mm)	-0.183	*0.004*	Weak trend toward greater basal discrepancy
Electrode to modiolus distance (mm)	-0.157	*0.012*	Weak trend toward greater basal discrepancy
ICPI$_{i,\ RdM}$	0.198	*0.002*	Weak trend toward greater apical discrepancy
ICPI$_{i,\ Lee}$	0.396	*< 0.001*	Weak-moderate trend toward apical discrepancy

* Positive Spearman's ρ reflects increasing discrepancy at more apical electrode positions; negative values reflect increasing discrepancy at more basal electrode positions.

Table 8.
Spearman's correlation of measurement concordance along the electrode array, stratified by electrode array type

Metric	Array	Spearman's ρ	*p*-value	Interpretation
Medial wall – electrode distance (mm)	PM	0.044	.43	No significant variation in discrepancy along the array for either PM or LW arrays
	LW	0.700	.15	
Medial wall – lateral wall distance (mm)	PM	0.072	.19	Weak apical trend in discrepancy for LW arrays; no significant variation for PM arrays
	LW	0.138	*.004*	
Modiolus – lateral wall distance (mm)	PM	-0.152	*0.006*	PW and LW arrays show a weak-moderate tend toward greater basal discrepancy
	LW	-0.273	*< .001*	
Electrode – modiolus distance (mm)	PM	-0.199	*< .001*	
	LW	-0.276	*< .001*	
ICPI$_{i,\ RdM}$	PM	0.123	*0.026*	PW and LW arrays show a weak-moderate tend toward greater apical discrepancy.
	LW	0.102	*.036*	
ICPI$_{i,\ Lee}$	PM	0.290	*< .001*	
	LW	0.209	*< .001*	

LW – lateral wall; PM – perimodiolar.

Table 9.
Interobserver agreement across three raters for intracochlear electrode position metrics.

Metric	Modality	ICC (3,1) (95 % CI)	Degree of interobserver reliability
AID	MicroCT	0.94 (0.83 – 0.98)	Excellent
	CBCT	0.93 (0.81 – 0.98)	Excellent
	MDCT	0.92 (0.78 – 0.97)	Excellent
IEL	MicroCT	0.87 (0.66 – 0.96)	Excellent
	CBCT	0.87 (0.68 0 0.96)	Excellent
	MDCT	0.56 (0.14 – 0.85)	Moderate
LWL	MicroCT	0.79 (0.54–0.93)	Good
	CBCT	0.60 (0.25–0.86	Moderate
	MDCT	0.54 (0.11–0.84)	Moderate
WF	MicroCT	0.94 (0.85 – 0.98)	Excellent
	CBCT	0.93 (0.82 – 0.98)	Excellent
	MDCT	0.76 (0.48 – 0.92)	Good
Medial wall to electrode distance	MicroCT	0.79 (0.74 – 0.82)	Good
	CBCT	0.86 (0.83 – 0.88)	Excellent
Medial wall to lateral wall distance	MicroCT	0.62 (0.56 – 0.68)	Moderate
	CBCT	0.66 (0.60 – 0.71)	Moderate
Electrode to modiolus distance	MicroCT	0.96 (0.95 – 0.97)	Excellent
	CBCT	0.96 (0.95 – 0.97)	Excellent
Modiolus to lateral wall distance	MicroCT	0.94 (0.92 – 0.95)	Excellent
	CBCT	0.92 (0.90 – 0.93)	Excellent
$ICPI_{i,\ RdM}$	MicroCT	0.78 (0.74 – 0.82)	Good
	CBCT	0.85 (0.82 – 0.88)	Excellent
$ICPI_{i,\ Lee}$	MicroCT	0.93 (0.91 – 0.94)	Excellent
	CBCT	0.82 (0.80 – 0.86)	Excellent
$\overline{ICPI}_{RdM}$	MicroCT	0.91 (0.79 – 0.97)	Excellent
	CBCT	0.93 (0.81 – 0.98)	Excellent
$\overline{ICPI}_{Lee}$	MicroCT	0.99 (0.96 – 1.00)	Excellent
	CBCT	0.96 (0.89 – 0.99)	Excellent

ICC (3,1) reflects a two-way mixed-effects model for absolute agreement.

ICC interpretation followed conventional thresholds: poor (< 0.50), moderate (0.50 – 0.74), good (0.75 – 0.89) and excellent (≥ 0.90).
All ICC values were statistically significant at $p > 0.001$

Figure 8.
Transmodiolar view of specimen 7 on microCT.
The medial cochlea wall (yellow arrow) is a porous bony matrix subject to metallic and partial volume artefact. It is difficult define as a single location on CT. This confers inherent uncertainty in metrics requiring the identification of this landmark, such as $ICPI_{i, RdM}$.

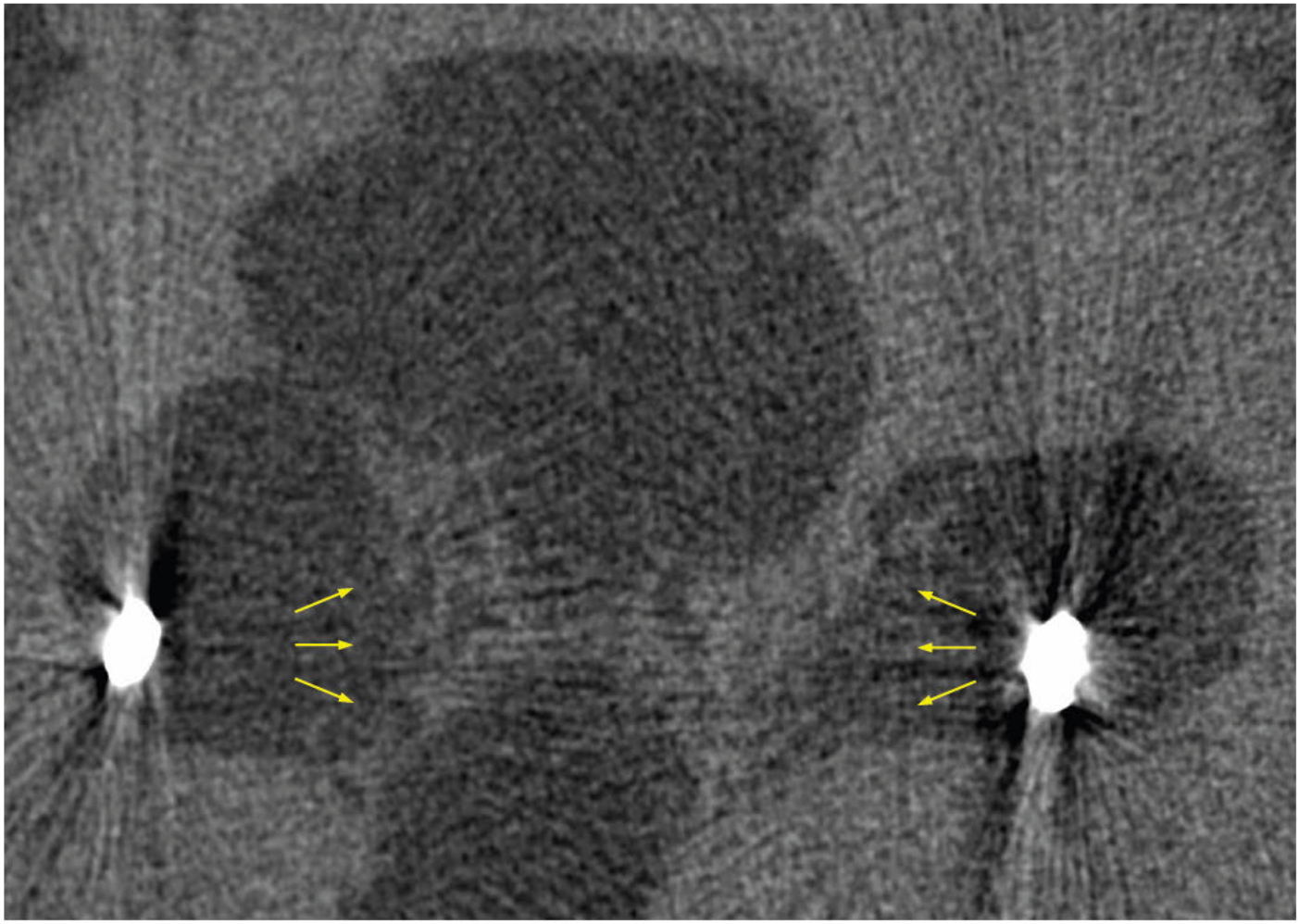

Appendix 2. Metrics of intracochlear electrode position

Measurement protocol for metrics of intracochlear electrode position

After import into 3D Slicer and appropriate windowing, multiplanar reconstruction was performed to define the *basal turn plane*. This plane was defined as the axial plane through the lowermost turn of the cochlea in which the maximum number of individual electrode contacts were visible (Figure 9). Subsequently, a *modiolar axis* was defined by constructing a straight line between the helicotrema and the centre of the lamina cribosa (Figure 10). Following this, each individual electrode contact was marked with a single point placed at the best approximation of its geometric centre (Figure 11).

Once the modiolar axis and individual electrode contacts had been defined, the below straight-line distances were measured for each of the 22 electrode contacts. Measurements were performed in the basal turn plane for contacts visible within this plane. Electrode contacts located above or below this plane were measured in planes parallel to the basal turn plane.

1. **Electrode to modiolar distance**: the radial, straight line distance between a given electrode contact and the modiolar axis (Figure 12, 13).
2. **Lateral wall to modiolus distance**: the radial, straight line distance between the modiolar axis and the lateral cochlear wall. This direction of this distance is coincident to the direction of the electrode to modiolar distance. (Figure 13, 14)
3. **Medial wall to electrode distance:** the straight line distance between a given electrode contact and the medial cochlear wall. This distance was measured in a direction perpendicular to the face of the electrode contact (Figure 13)
4. **Lateral wall to medial wall distance:** the straight line distance between the medial and lateral cochlear walls. This distance of this distance is coincident with the medial wall to electrode distance. (Figure 13, 14)

Following this the angular insertion depth was measured using the 3D angular measurement tool in 3D Slicer (Figure 15).

Finally, the inserted electrode length and lateral wall lengths were drawn in 3D using the curvilinear drawing tool in 3D Slicer (Figure 16).

Table 10.
Definitions of metrics of intracochlear electrode positions measured in this study.

Metric	Definition	Reference
Angular insertion depth (AID)	Angle (in degrees) through which the intracochlear portion of the electrode has been inserted into the cochlea. The angle is measured as follows: • A 0-degree reference line is drawn in the plane of the basal turn in which the maximal number of electrode contacts are visible. This 0-degree reference line passes from the centre of the round window to the modiolus. • An angular measurement is made from the modiolus, over the 0-degree reference line and through the most apical point on the apical most electrode pad.	Verbist *et al.* (2010)[25] Heutink *et al.* (2019)[105]
Wrapping factor (WF)	Dimensionless factor describes the proximity of the intracochlear portion of the electrode to the medial/lateral wall of the cochlea. It is averaged over the length of the entire electrode and is an indirect measure of electrode to modiolus proximity. $\text{Wrapping factor (WF)} = \frac{\text{Inserted electrode length (IEL)}}{\text{Lateral wall length (LWL)}}$ Where, • IEL = length along the electrode trajectory, running from the point at which the electrode array traverse the round window, to the apical most point of the electrode array • LWL = length of the lateral cochlear wall, running from the from the level of round window to the apical most point of the electrode array. The length is measured along the same trajectory as the inserted electrode length. A WF approaching 1.0 suggests an array closely adhered to the lateral wall (i.e. loosely wrapped around the medial wall/modiolar axis).	Holden *et al.* (2013)[8] Ramos de Miguel *et al.* (2019)[55]

Intracochlear position index, per Ramos de Miguel *et al.* ($ICPI_{RdM}$)	$ICPI_{RdM}$ is defined as the ratio between the distance from the medial wall to a given electrode contact and the distance between the modiolus and the lateral wall. It is defined for each individual electrode contact as follows: $$ICPI_{RdM,\,i} = \frac{\text{Medial wall to electrode distance }_i}{\text{Lateral wall to medial wall distance }_i}$$ Where: - i = electrode number (i.e. 1 – 22)	**Figure 17.** Diagrammatic representation of intracochlear position index (ICPI) as defined by Ramos de Miguel *et al.* (2019)[55] 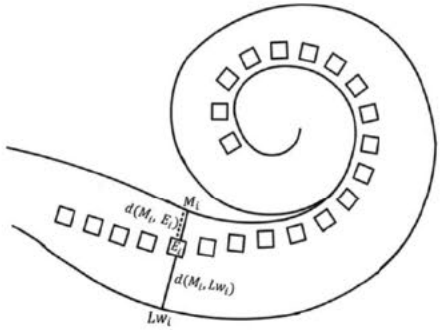 $$\overline{ICPI} = \frac{\sum_{i=1}^{n} ICPI_i}{n} \qquad ICPI_i = \frac{dist(M_i, E_i)}{dist(M_i, L_{wi})}$$	Ramos de Miguel *et al.* (2019)[55]
Intracochlear position index, per Lee *et al.* ($ICPI_{Lee}$)	$ICPI_{Lee}$ is defined as the ratio between the electrode to modiolus distance, and the lateral wall to modiolus distance. The latter is measured along a line concurrent with the electrode to modiolar distance. It is defined for each individual electrode contact as follows: $$ICPI_{Lee,\,i} = \frac{\text{electrode to modiolus distance }_i}{\text{lateral wall to modiolus distance }_i}$$ Where: - i = electrode number (i.e. 1 – 22)	**Figure 18.** Diagrammatic representation of intracochlear position index (ICPI) as defined by Lee *et al.* (2020)[61] 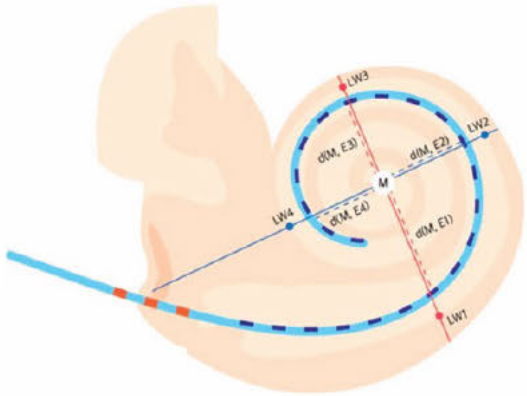 $$ICPI(i) = \frac{\text{dist (M, Ei)}}{\text{dist (M, LWi)}}$$	Lee *et al.* (2020)[61]

Mean intracochlear position index ($\overline{\text{ICPI}}$)	Calculated as the mean ICPI taken over all electrodes: $$\overline{\text{ICPI}} = \sum_{i=1}^{n} \text{ICPI}_i$$ Where, • n = 22, for CI622 and CI632 Given there are two methods by which the ICPI is defined (i.e. ICPI_{RdM} and ICPI_{Lee}), there is an associated mean for each.	Ramos de Miguel *et al.* (2019)[55] Lee *et al.* (2020)[61]

Figure 9.
Depiction of the *basal turn plane* on specimen 11 on microCT.
The basal turn plane is defined as that in which a maximum number of individual electrode pads were visible in the lowermost turn of the cochlea.

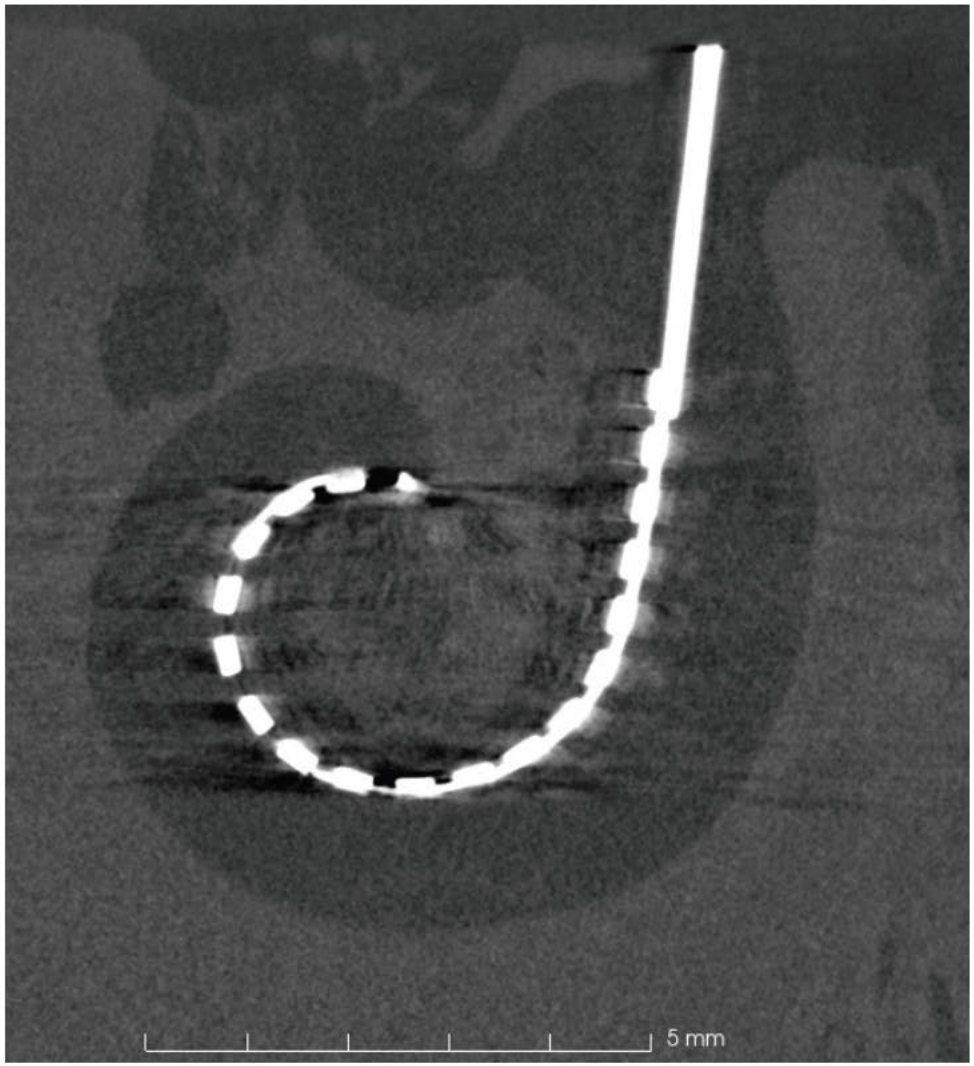

Figure 10.
Transmodiolar view of specimen 11.
Yellow line: *modiolar axis*, defined as the straight line joining the helicotrema to the centre of the tractus spiralis foraminosus.
Blue line: *electrode to modiolar distance*, defined as the radial, straight line distance between a given electrode contact and the modiolar axis.

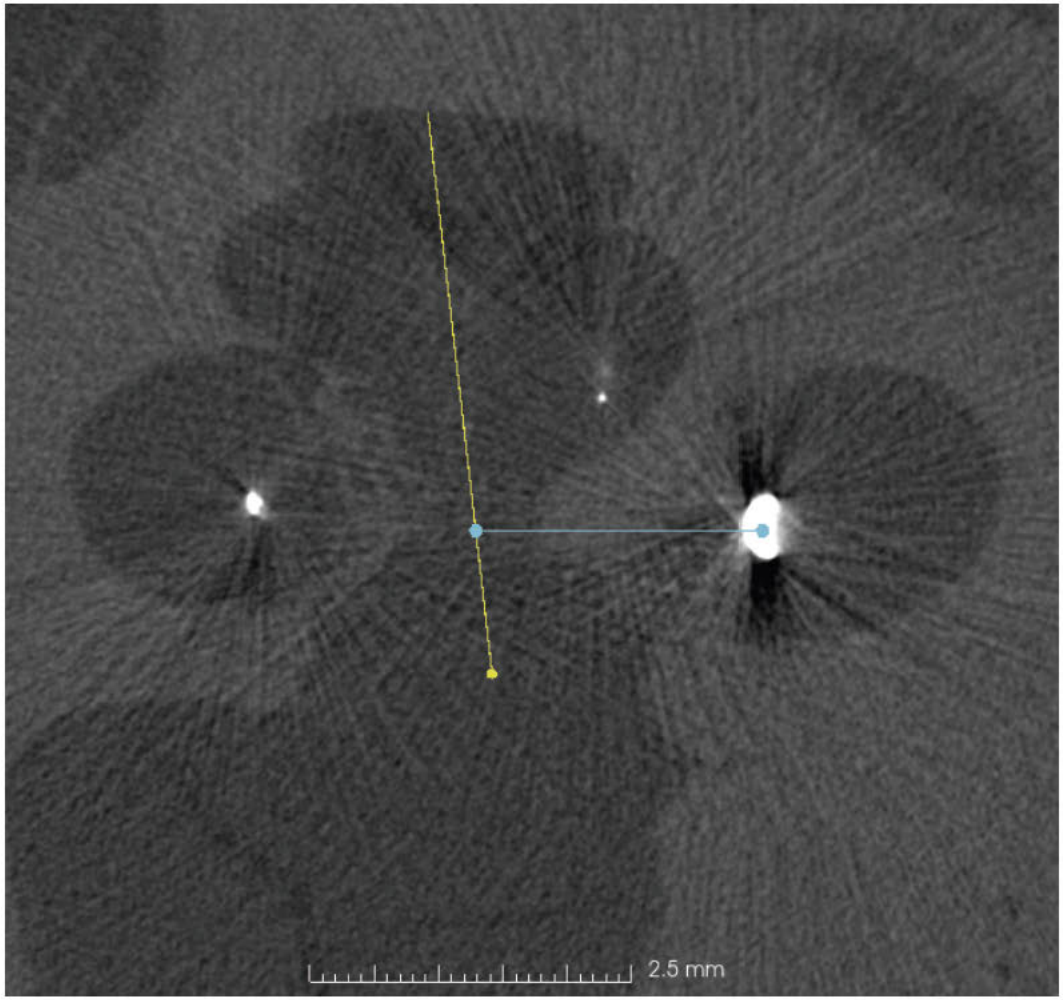

Figure 11.
Basal turn plane view of specimen 4 on microCT.
The geometric centres of each electrode contact visible in the basal turn plane view are marked in green. Electrode contacts not visible in this plane (above or below the basal turn plane), were marked in a plane parallel to the basal turn plane.

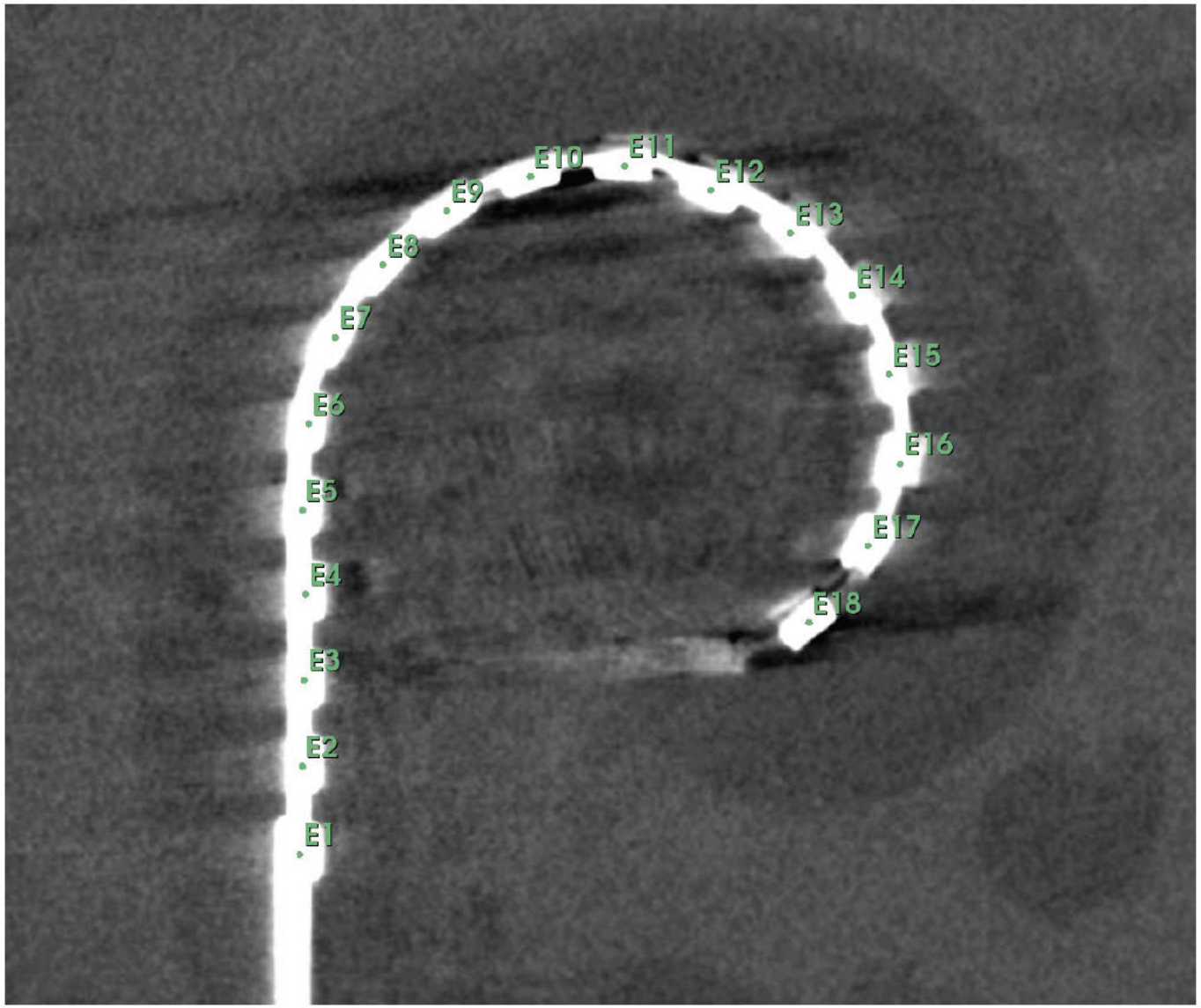

Figure 12.
(A): Basal turn plane view of specimen 4 on microCT.
The geometric centres of each electrode contact visible in the basal turn plane view are marked in green. Electrode contacts not visible in this plane (above or below the basal turn plane), were marked in a plane parallel to the basal turn plane.
(B) and **(C)**: 3D rendering of the electrode array, modiolar axis and electrode to modiolus distance.

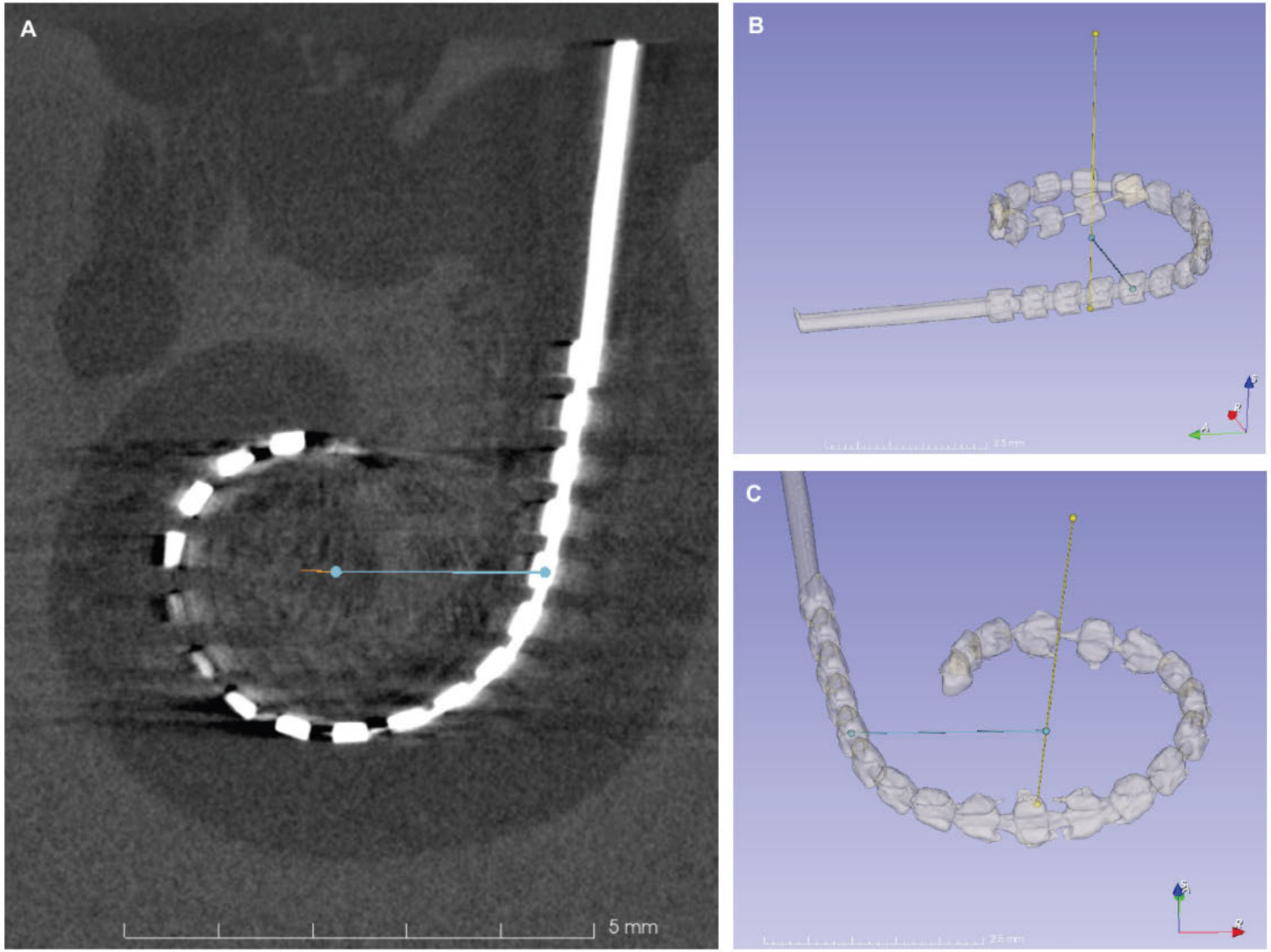

Figure 13.
Basal turn plane view of specimen 3 on microCT.
Green line: medial wall to electrode distance.
Red line: lateral wall to medial wall distance. This line is drawn coincident to the medial wall to electrode distance for a given electrode contact.
Purple line: lateral wall to modiolus distance. This line is drawn coincident to the electrode to modiolus distance for a given electrode contact.

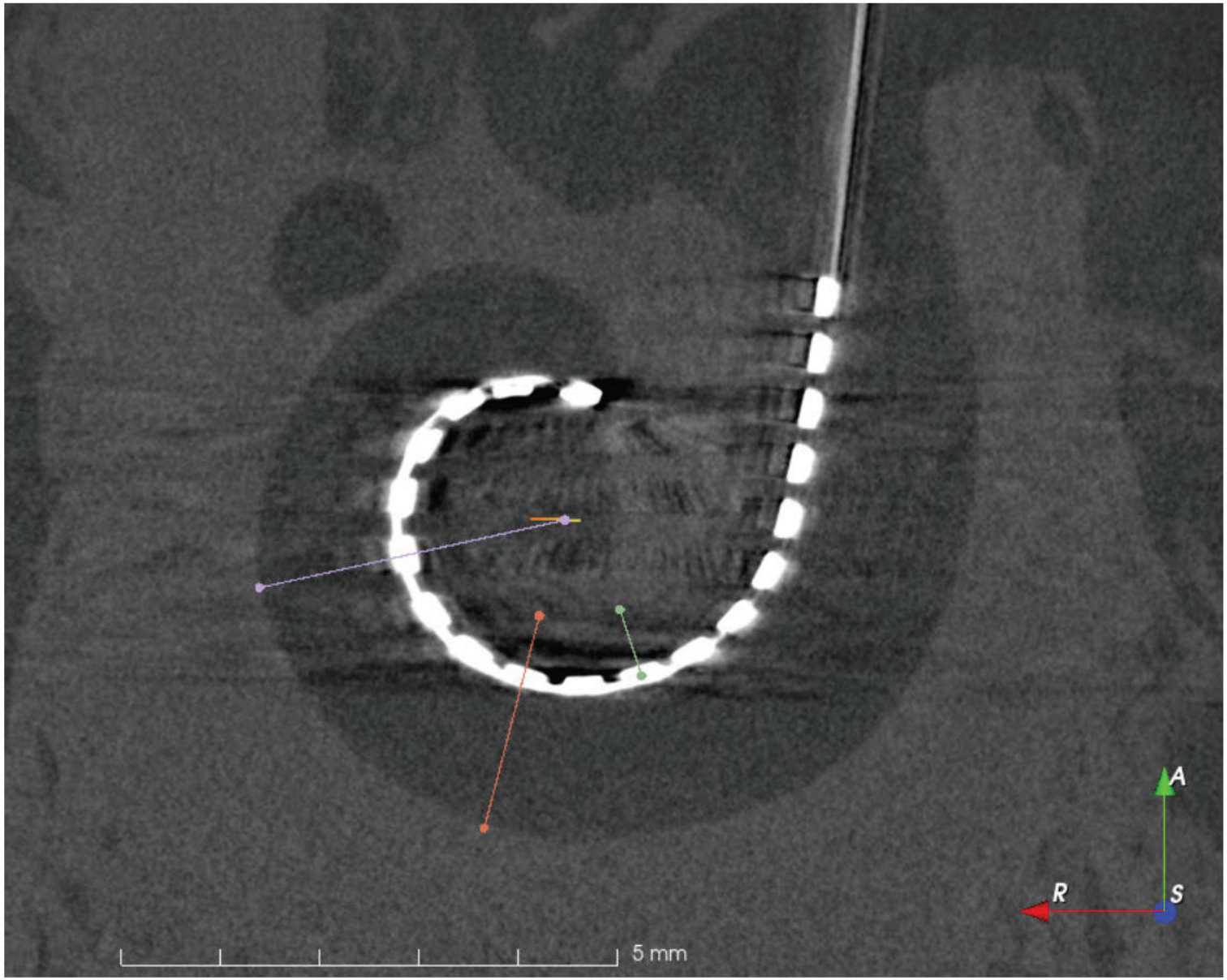

Figure 14.
Depiction of the measurement of medial wall to electrode (purple line) and lateral wall to medial wall (blue line) distances. These distances were measured in a direction perpendicular to the face of their respective individual electrode contact.
Appropriate windowing allowed for identification of the geometric centre of the electrode contact (A) as well we the bony cochlear walls (B)

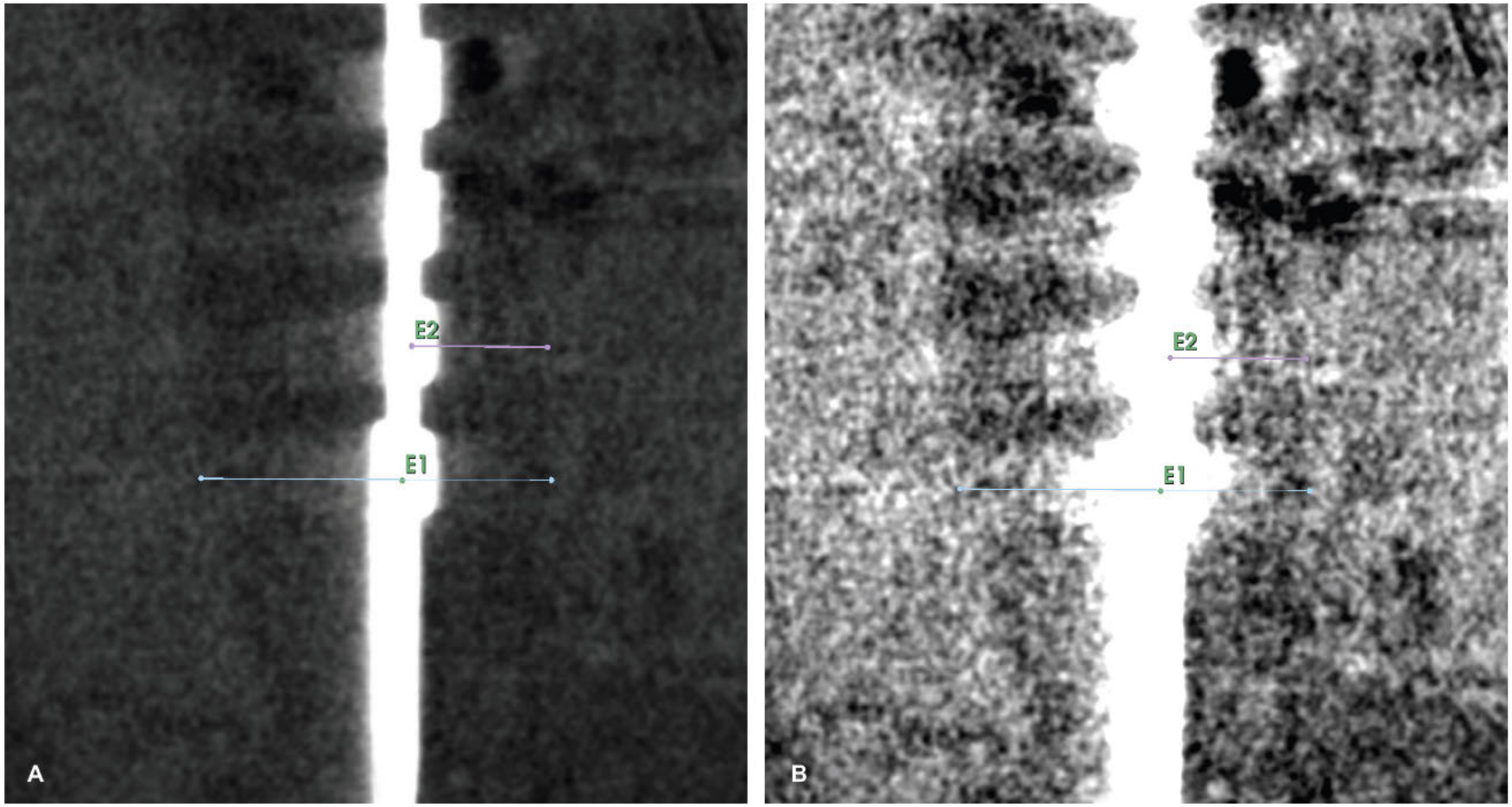

Figure 15.
Measurement of angular insertion depth (AID) in specimen 4 on MDCT.
A: oblique view of the electrode array with the relevant landmarks required for measurement of AID.
B: 3D rendering of the electrode array and AID measurement.

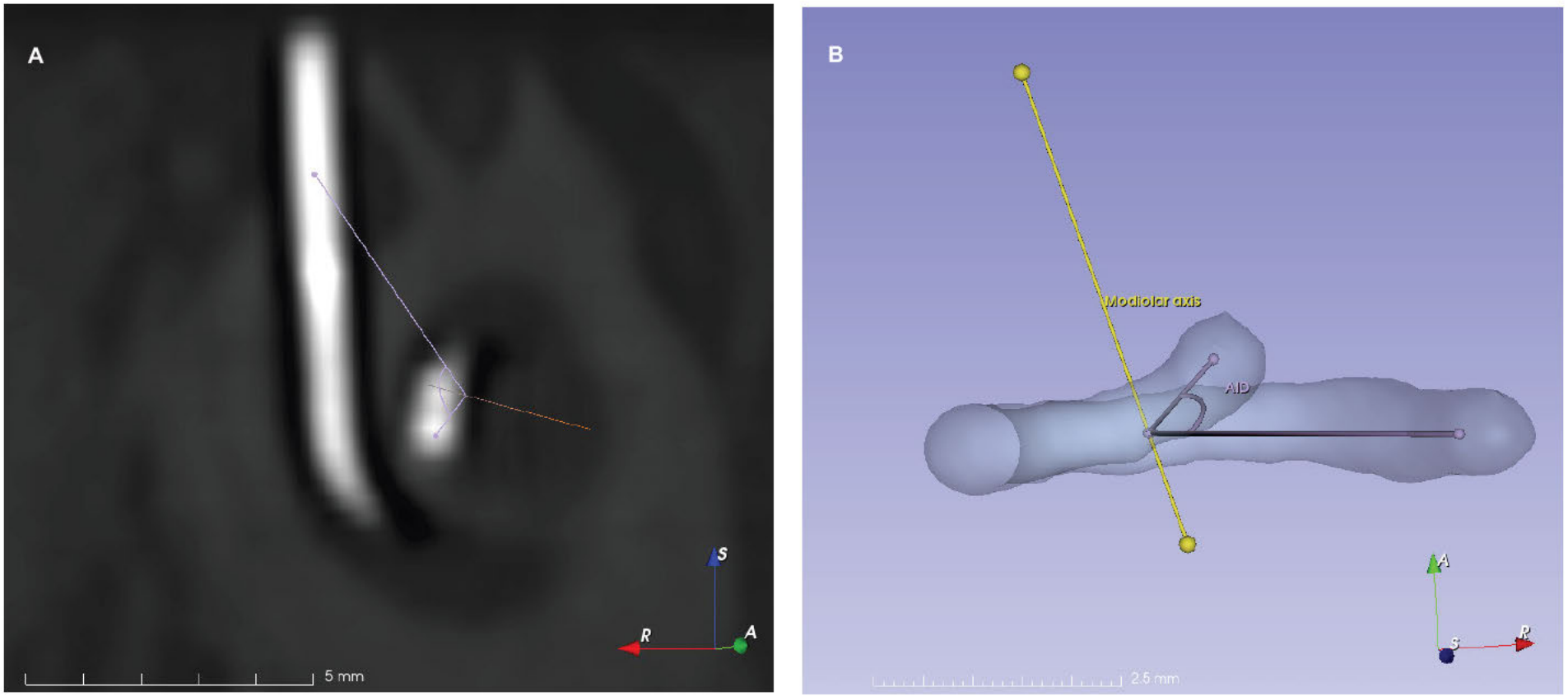

Figure 16.
Measurement of inserted electrode length (IEL) and lateral wall length (LWL) and in specimen 5 on CBCT.
A: IEL and LWL as measured on CBCT
B: 3D rendering of the IEL and LWL

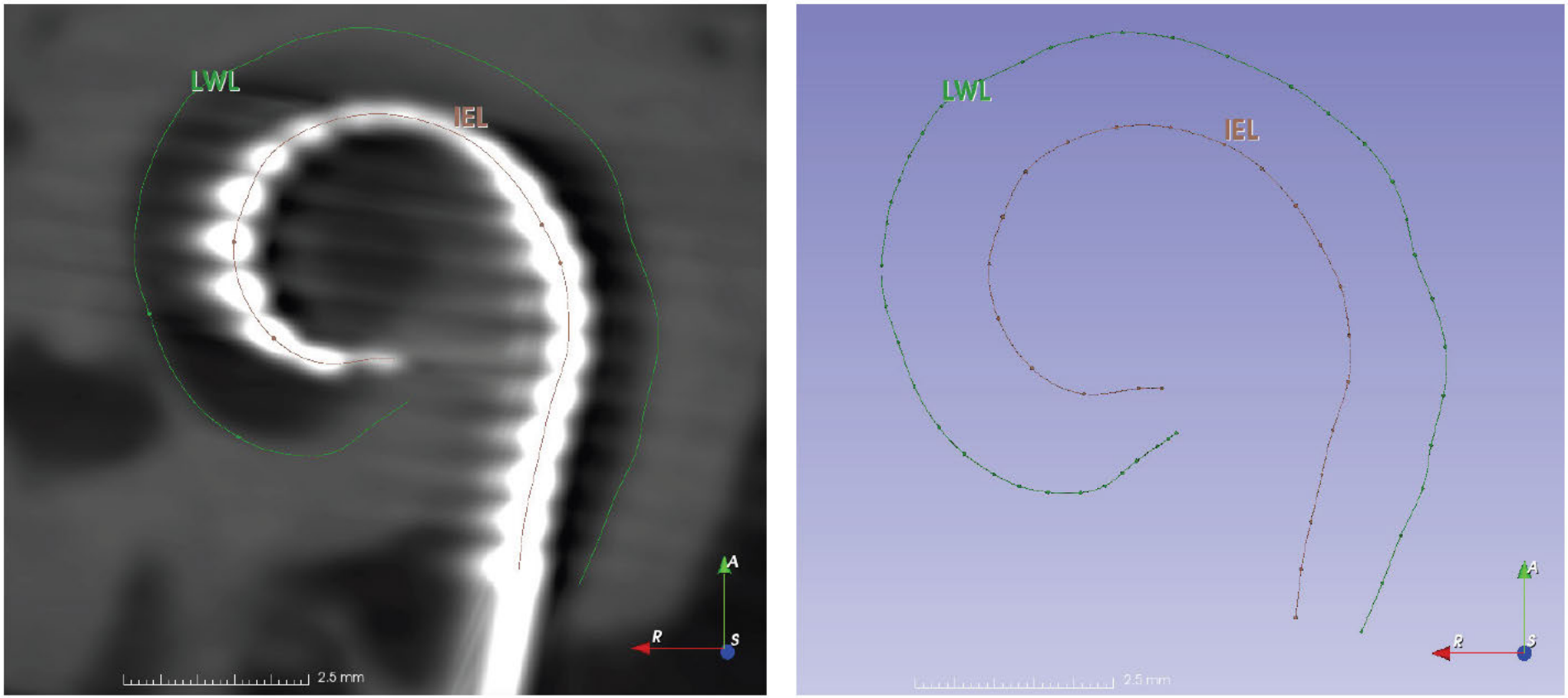

Appendix 3. Supplementary Documentation

Ethics approval submission to WSHLD HREC

Validation of cochlear implant electrode position measures derived from clinical imaging against histology and microCT reference standards.

HREC proposal to WSLHD

22nd November 2022

Study Title

Validation of cochlear implant electrode position measures derived from clinical imaging against histology and microCT reference standards.

Affiliations

1. Department of Otolaryngology-Head and Neck Surgery, Westmead Hospital
2. Cochlear Limited (Sydney, Australia; cochlear.com)

This research project will have an industry partner in Cochlear Limited (Sydney, Australia; cochlear.com)

Investigators

Coordinating Principal Investigator	**A/Professor Melville Da Cruz** Senior Staff Specialist, Department of Otolaryngology-Head and Neck Surgery Westmead Hospital, Sydney A/Professor, Department of Surgery, Western Clinical School University of Sydney e: melville.dacruz@sydney.edu.au [redacted]
Principal Investigators	**Dr. Irfan Durmo** Senior Surgery and Anatomy Specialist Cochlear Limited, Sydney [redacted]
	Mark Allen Senior Radiographer Castlereagh Imaging, Mons Rd Westmead [redacted]
Researchers	**Dr Alon Taylor** Registrar, Department of Otolaryngology-Head and Neck Surgery Prince of Wales Hospital, Sydney E: alon.taylor@gmail.com [redacted]
	Dr Zachary Smith Director of Algorithms and Applications Cochlear Limited, Sydney [redacted]
	Dr. Nick Pawsey Principal Research Engineer, Advanced Innovation Cochlear Limited, Sydney [redacted]
	A/Prof Kerry Hitos Medical Statistician Executive Director, Westmead Research Centre for the Evaluation of Surgical Outcomes, Westmead Hospital Department of Surgery, University of Sydney kerry.hitos@sydney.edu.au

Proposed mode of research

This is an experimental, basic sciences research study in the field of otolaryngology, specifically in otology and cochlear implantation. The experimental modes of research will be radiological and histological analysis of human cadaveric temporal bone tissue blocks implanted with intracochlear electrodes, from which measurements will be derived and computational and numerical analysis will be performed.

Research synopsis and aims

Intracochlear electrode position is a key determinant of the electrode-neural interface in cochlear implant (CI) surgery. As such, it forms a modifiable determinant of outcome following cochlear implantation[1-4]. Current clinical methods used to determine post implantation electrode position rely on imaging studies – plain x-ray, spiral computed tomography (CT) and cone beam computed tomography (CBCT) (Figure 1 – 3)[5]. These studies are limited by availability (such as in CBCT), time-constraints, need for manual measurements by trained experts and poor image quality (such as with plain x-ray or CT in which image quality can be poor due to movement or metal artefact, and the error margins in determining cochlea measurements can be large). In particular, a lack of validation against reference standards (microCT and histology) has limited useful interpretation of currently obtained clinical images by the above imaging modalities. Present and future outcomes studies following CI, as well as engineering of the next generation of electrodes, require validated and standardised measures of intracochlear electrode position that are easily accessible for clinicians and engineers[2,6].

The aim of this project is to validate clinical measurements of cochlear implant electrode positioning which are normally derived from postoperative imaging studies - plain X-ray, spiral CT and CBCT. This will be performed by comparing these radiological measurements with a reference gold standard. This reference standard will be provided by 3D microCT and histological measurements taken from cadaveric temporal bones implanted with a variety of cochlear implant electrodes.

3D MicroCT and histology are suitable reference studies for several reasons:

a. Both provide high fidelity images from which accurate measurements can be derived.
b. Histology is likely to be the most refined source of intracochlear measurements. It provides images with high resolution and a lack of metal artefact which are seen on CT imaging modalities. The fixation process in histological processing eliminates electrode migration which can occur during transportation, imaging studies and archiving. This makes it an excellent reference modality for a research study such as this one. However practically, it is expensive, time consuming and requires specialised skills and laboratories. From a clinical perspective it is only useful post-mortem.
c. Micro CT is also likely to be a refined source of intracochlear measurements and is relatively available in the first world. 3D microCT offers non-destructive, slice-by-slice scanning that can be reconstructed into 3D volumetric objects for quantitative analysis or visualisation. It provides high throughput and high-resolution imaging to a quality that cannot be obtained by other non-destructive imaging techniques. For the testing samples size and imaging capabilities used in this project, 3D microCT analysis can obtain image resolution on a scale of 4 - 10µm, which will provide excellent image quality and useful and novel results [7].

With regards to current clinical measures of intracochlear electrode position, these are acquired via standard postoperative imaging studies, and include

1. Angular insertion depths[8].

2. Number of electrodes inserted as a fixed point (i.e. the round window).
3. Wrapping factor (defined as the ratio of implanted electrode length to the corresponding outer wall length)[3].
4. Intracochlear position index (ICPI) and its derivatives such as modified ICPI, homogeneity factor and electrode to modiolus, medial–lateral (EMML)[2].
5. Qualitative observations such as the presence and number of electrode translocations, bends, kinks and tip fold overs.

These measurements have not been validated against actual implanted/histological reference standards. As such these current clinical measurements remain approximations of true electrode positions. With ongoing refinements in electrode design and the importance of the spatial interaction between the electrode and the functional neural elements of the hearing apparatus (i.e. auditory nerve ganglion cells, dendrites, axons and inner and out hair cells) a more focused understanding of electrode position is required with the aim of obtaining better post-implantation hearing outcomes.

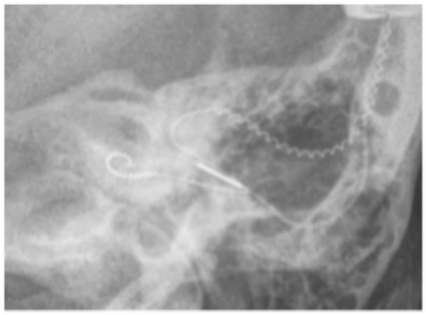

Figure 1 – Postoperative plain X-ray demonstrating the normal position of a cochlear electrode array medial to the expected location of the cochleostomy. (Case courtesy of A/Prof. Craig Hacking, Radiopeadia.org, rID: 36899)

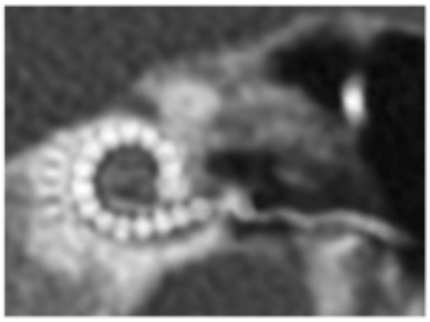

Figure 2 – Postoperative spiral CT (CT) imaging reformatted in the oblique coronal plane demonstrating the intracochlear electrode array (Connor et al., 2018)

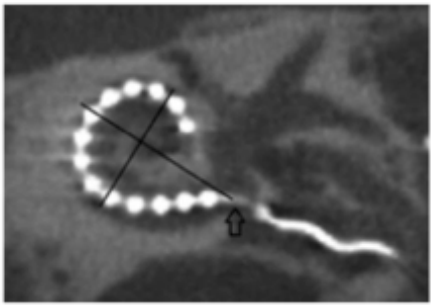

Figure 3 – Postoperative cone beam CT (CBCT) imaging reformatted in the oblique coronal plane demonstrating the intracochlear electrode array (Connor et al., 2018)

Aim

The primary objective of this study is to validate traditional measures of intracochlear electrode position by quantifying post implantation measures against histology in implanted cadaveric human temporal bones. The validated imaging studies would then allow electrode position (on an electrode-by-electrode basis) to be considered as an independent variable in functional outcomes, thereby quantifying one of the factors determining the diversity of observed CI outcomes seen in all clinics[1,3,4,9]. Furthermore, with a set of normative data provided by this project, the secondary objective of this project is to derive novel radiological measures of intracochlear electrode position which better represent the true position of the electrode with the cochlea.

The study will compare:

1. histology vs micro CT to determine our best reference standard
2. CBCT vs histology and micro CT
3. CT vs histology and micro CT
4. plain xray vs histology and micro CT

As such, we aim to identify and quantify the strengths and limitations of each available imaging modality and make recommendations of how useful each is in various settings.

Background

To date, there are different approaches to measure the electrode position relative to the modiolar wall. The modiolus is the conical central axis of the cochlea and is located near the spiral ganglion (the bipolar neurons which innervate the hair cells of the Organ of Corti). The lateral wall of the cochlea duct is more clearly seen than the modiolar wall on radiological studies and represents a limitation of our current clinical imaging techniques. However, the modiolar wall is a visible landmark on histology. There are several measurable aspects of the final position of a CI electrode which impact postoperative outcomes. These include:

1. The scalar position of the electrode.
2. The depth of insertion of the electrode.
3. The position of the electrode in relation to the modiolar wall.
4. Damage to the neural and membranous elements of the Organ of Corti due to electrode trauma[1,2].

Below are descriptions of several common radiologically derived clinical measurements of electrode position.

Wrapping factor

The wrapping factor (WF) provides a metric of how tightly or loosely wrapped an electrode array is relative to the modiolar wall. This is an important metric to know, as studies suggests that electrode positioning is a key factor in predicting postoperative hearing outcomes and accounts for about 20% of the variability in speech outcomes[3,4,9,11-17]. Because the modiolar wall is not seen as clearly as the lateral wall on spiral CT scans, the metric is indirectly based on measurements of electrode position relative to the visible lateral wall. The formula to derive the wrapping factor is given below:

$$WF = \frac{L_{EL}}{L_{LW}}$$ (see Figure 4)[3]

Where,

- L_{EL} = the length along the electrode trajectory from the basal to apical electrode
- L_{LW} = the lateral wall length from the insertion angle of the most basal electrode to the insertion angle of the most apical electrode

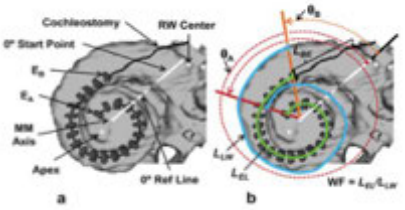

Figure 4 - CT derived images of a participant's electrode array (Contour Advance) and corresponding markers used to measure array position (Holden et al. 2013)

A WF ratio of 0 indicates a tightly wrapped array perfectly applied to the modiolar wall. This is the design goal for all perimodiolar electrode arrays – placing the array in the closest possible position to the spiral ganglion cells. A WF ratio of 1 indicates a loosely wrapped array perfectly applied to the lateral wall. This is the design goal for all straight lateral wall electrode arrays – placing them in close proximity to the Organ of

Corti (Figure 5). WF has become a standard in postoperative radiological testing. Studies have shown that better post cochlear implantation hearing outcomes, such as the consonant-nucleus-consonant (CNC) scores, are inversely proportional to the WF (Figure 6)[3].

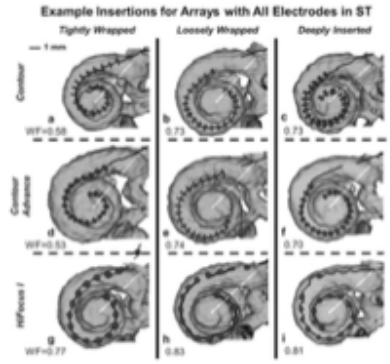

Figure 5 - Examples of tightly-wrapped, loosely wrapped and deeply inserted electrode arrays positioned in the scala tympani for the Nucleus Contour, Nucleus Contour Advance and AB HiFocus I electrodes (Holden et al. 2013)

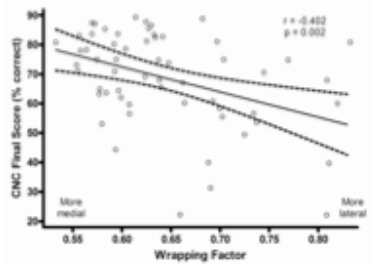

Figure 6 - A scatter plot of Wrapping Factor vs. CNC Final Score for 59 participants with electrode arrays positioned in the scala tympani (Holden et al. 2013)

However the WF has been reported to yield inconsistency to determine the relative relationship of the electrode array against the lateral wall between the cone-beam CT and histologic finding, requiring a more accurate and refined radiological value for modular proximity.[18] WF provides a "summary" parameter for overall electrode position. Focused data concerning each electrode position is not possible with the WF. This is a key limitation of this parameter as it cannot be used for electrode-electrode measurements or correlations with individual electrode physiology. The development of EMML and ICPI (and its modifications) provides more granular data which looks at individual electrode positions. This can be correlated with electrophysiological responses to stimulation at multiple positions across the cochlear.

Intracochlear position index

The intracochlear position index (ICPI) is another measure used to describe electrode-modiolar proximity. In contrast to the WF, the ICPI indicates the distance of each contact relative to the modiolar wall. The formula to derive the ICPI is given below[18]:

$$\overline{ICPI} = \frac{\sum_{i=1}^{n} ICPI_i}{n}$$

$$ICPI_i = \frac{dist(M_i, E_i)}{dist(M_i, L_{wi})}$$

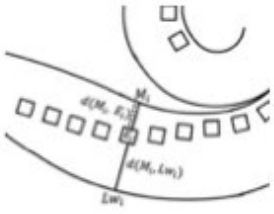

Figure 7
(de Miguel *et al.* 2019)

The ICPI is normalised to a number from 0 to 1; with 0 being closest to the modiolus and 1 being closest to the lateral wall and n representing the number of electrodes. The validity of the ICPI has been evaluated in a single, small cadaveric study (3 temporal bones, with 3 different electrode positions using the same electrode (CI532)) which deem it to be most accurate radiological technique6.

Homogeneity factor

The homogeneity factor (HF) can be derived from the ICPI. It indicates the degree to which there is uniformity of the electrode-modiolus distance across all electrode channels. The formula for the homogeneity factor is given below[18]:

$$HF = \frac{\sqrt{\sum_{i=1}^{n} \left(\overline{ICPI} - ICPI_i\right)^2}}{n}$$

The HF increases when the positions of the electrodes are not uniform (i.e. some perimodiolar, some near the lateral wall) (Figure 8, B) and approaches 0 when all electrodes placed at the same distance (Figure 8, A and C). It requires cone-beam CT to be calculated.

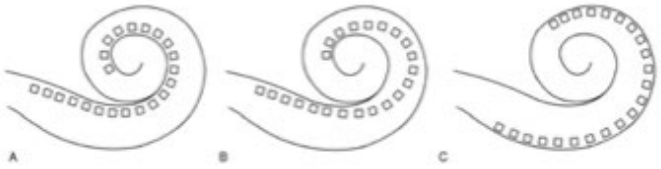

Figure 8 (de Miguel et al. 2019)

Expected Research Contribution

This project is expected to provide the following research contributions:

a) It will provide the first robust validation of commonly used radiological measures of cochlear implant electrode positioning measurements. To date, the largest sample size for a study of this nature is 3 cadaveric temporal bones. No validation studies exist for the radiological measures listed in Section 9. This study will significantly extend beyond 3 temporal bones, such that we will be able to confidently evaluate how well the radiological measurements in Section 9 correlate with a gold standard i.e. histology and MicroCT. We anticipate the use of 12 – 16 temporal bones.

b) As a result, we may have the opportunity to develop a series of novel radiological ways in which to more appropriately and accurately measure intracochlear electrode positioning, by comparing it to our gold standard data set (i.e. histological and MicroCT images), thereby filling an identified knowledge gap in the understanding of the electrode-neural interface.

Hypothesis

We hypothesise that measures of intracochlear electrode position derived from preclinical (i.e. 3D microCT) and clinical imaging modalities (i.e. plain X-ray, cone beam CT and spiral CT) are equivalent with those derived from temporal bone histology

There are three hypotheses to test:

1. That measures of intracochlear electrode position derived from histology and microCT are equivalent.
2. That measures of intracochlear electrode position derived from clinical imaging studies and histology are equivalent.
3. That measures of intracochlear electrode position derived from clinical imaging studies and microCT are equivalent.

Methodology

Type of study

This project is a basic science, observational cadaveric study

Study sites

This project will be undertaken at the following sites:

Site:	Tasks undertaken
Westmead Public Hospital (Westmead 2145)	- Project conception, planning - Data analysis - Thesis writing
Temporal bone laboratory at Cochlear Ltd (Macquarie Park 2113)	- Implantation of CI electrodes into cadaveric specimens - Fixation of temporal bones - Storage of cadaveric temporal bones
Castlereagh Imaging Westmead) (Westmead 2145)	- Plain XR imaging of cadaveric temporal bones (CTBs) - Cone beam CT imaging of CTBs - Spiral CT imaging of CTBs
The University of Sydney (Camperdown 2006)	- 3D MicroCT imaging of CTBs

Length of study

This study will be undertaken as a project fulfilling the degree requirements of a Master of Philosophy (MPhil) at The University of Sydney. The candidate is Dr. Alon Taylor (Principal Investigator). The MPhil will be undertaken part-time. It is estimated to span from 2022 to 2024/2025 (inclusive) i.e. 3 – 4 years. A more detailed outline of the study timeline is found in Appendix 1.

Study size

We aim to obtain approximately 12 – 16 cadaveric human temporal bones for this study. This will significantly expand on the largest pre-existing data set (3 cadaveric temporal bones[18]) used to validate radiological measures of cochlear electrode positioning against histological gold standard.

Recruitment methodology

The cadaveric temporal bones used in this study will be supplied by Cochlear Ltd. Cochlear has an established, verified and lawful pathway in place for acquiring cadaveric temporal for research purposes from consenting donors. This pathway is adherent to the requirements of the Human Tissue Act 1983 in relation to research and use of tissue. The appropriate measures to ensure confidentiality of the donors are taken by Cochlear Ltd during the acquisition, storage and testing phases of research on temporal bones.

Specific information about the pathway via with Cochlear Ltd acquires cadaveric temporal bones for research purposes is found in the 'Ethical Considerations' section of this protocol in the 'Consent' subsection.

Randomisation

This is study is an observational human cadaver study with in-subject controls. As such, randomisation will not be required.

Visit schedules and proposed study timeline

As the study material is human cadaveric temporal bones no regimented visited schedule are required. The bones are fixed and stored in formalin allowing for indefinite study period.

The proposed study timeline for this project is found in Appendix 1.

Study protocol

The study protocol will be divided into 6 subsections as below:

a. Temporal bone registration and surgical implantation
b. Data acquisition
    1. Radiological assessment
    2. Histological assessment
c. Post-processing of derived data
d. Analysis and reflection
e. Dissemination of knowledge
f. Consideration of next steps

a. Implantation

Each bone will be registered with a unique tracking number that will be visible on anatomical specimens and radiological images. Implantation of the cochlear electrodes into the cadaveric temporal bones will take place in the Cochlear Ltd campus TBL. The temporal bones will be implanted with several different types of the most commonly use electrodes. These electrodes will be supplied by Cochlear Ltd. The electrodes will include some, or all, of the following[19]:

a) Slim Straight (CI622, Cochlear Ltd)
b) Slim Modiolar (CI632, Cochlear Ltd)
c) Contour advance (CI612, Cochlear Ltd)

The surgical implantation will be performed by A/Prof Melville da Cruz and Dr Alon Taylor with histological processing of the tissue block performed by Irfan Durmo, Senior Surgery and Anatomy Specialist, Cochlear Limited, Sydney Australia), who has extensive experience in cochlear implant electrode implantation and temporal bone histological techniques[18,20,21]. After implantation, the electrodes are fixed as their proximal end at the level of either the facial recess or round window with cyanoacrylate glue. This prevents the

electrode from any scalar translocation which may occur in the process of transporting or processing the specimen.

b. Data acquisition

Once the implanted specimens have been fixed, the data collection process will take place. There will be two data sources: radiological and histological assessment of the specimens.

b. 1 Radiological assessment

The implanted temporal bones, fixed in a tissue block (see *'Histological assessment'* for details of the fixation process), will then be subject to radiological assessment, using 4 imaging modalities.

i. Plain X-ray – Castlereagh Imaging, Westmead[•] and/or Cochlear Limited Laboratory
ii. Cone beam CT – Castlereagh Imaging, Westmead and/or Cochlear Limited Laboratory
iii. Spiral CT – Castlereagh Imaging, Westmead
iv. 3D MicroCT – this will be performed at the University of Sydney MicroCT facilities (https://www.sydney.edu.au/research/facilities/sydney-imaging/preclinical-imaging.html).

A known challenge in imaging metallic structures using computed tomography is image interpretation in the presence of metallic artefact. The presence of 'metallic bloom' is more evident in spiral CT compared with cone beam CT. Fortunately several scanner setting templates and postprocessing algorithms have been developed which reduce metallic artefacts generated by CI electrodes and improve CT image quality[22-25].

b. 2 Histological assessment

Ex-vivo histological studies are the 'gold standard' technique for accurately localising CI electrodes. Once radiological assessment has been performed with the modalities listed in *'Radiological assessment'*, the specimens will undergo histological preparation, sectioning, and photography. This will occur after radiological assessment as it is a destructive process.

A General Data Entry Sheet template in which the relevant radiological and histological measures will be entered, has been uploaded to the HREA proposal titled 'General Data Entry Sheet'

Cochlear Ltd maintains a standard procedure for preparing, sectioning, and photographing CI electrode implanted temporal bones for histological analysis. This procedure has been documented in several peer-reviewed studies conducted in conjunction with Cochlear Ltd which use this method to assess features of CI electrode positioning using histological and radiological methods[20,25-29].

For this project, this process will occur at the Cochlear Ltd campus TBL (Sydney, Australia). It will be performed by one of the Research Associates (Irfan Durmo), who has extensive experiences in temporal bone histological techniques[18,20,21].

[•] Castlereagh Imaging is a private facility with extensive expertise in imaging cochlear implants following routine CI surgery. Transfer of cadaveric human tissue blocks to and from the facility for the purpose of imaging will be governed by the Human Tissue Act 1983 with prior approval by the HREC at Western Sydney Local Health District.

An overview of this process is detailed below:

1. Surgical implantation of the temporal bone with the cochlear implant electrode (as detailed in the previous section).
2. The proximal electrode is fixed at the level of either the facial recess or the round window with cyanoacrylate glue. This prevents the electrode from any scalar translocation which may occur in the process of transporting or processing the specimen.
3. Excess cryanoacrylate glue within the facial recess and around the stapes footplate is removed with a surgical drill and a 0.5mm burr.
4. The relevant imaging as outlined in Section in 11.4.a is undertaken.
5. The stapes footplate is removed.
6. The specimens are dehydrated in ethanol using serial concentrations from 70% to 100% to remove moisture whilst preventing tissue distortion.
7. Specimens are immersed in degassed epoxy resin to achieve acrylic fixation.
8. A vacuum is applied to ensure the epoxy infiltrates the cochlea completely and to remove any air bubbles.
9. After embedding, excess portions of the temporal bone specimen within the epoxy block are trimmed to leave only the cochlea.
10. Specimens are reoriented and reembedded such that the modiolus axis is oriented parallel to the plane of sectioning, which is perpendicular to the electrode array.
11. Specimens are then sectioned with a thickness of 200 – 500µm using a grinding technique with sections capturing the round window through to the ascending basal turn.
12. Each section is then polished and stained with toluidine blue.
13. Sections are then placed under light microscopy and photographed.
14. High quality micrographs (such as those in Figure 6) will be produced which can then be examined to assess various features of electrode position.

Figure 6 - Histologic sections taken in Stenver's view showing a human cochlea implanted with a slim periomodiolar (CI532) electrode. (de Miguel et al. 2019)

c. Post-processing

A range of high-quality micrographs (such as those in Figure 6) will be produced for the implanted temporal bones in the study. Following this, measures of intracochlear electrode position (i.e. angle of rotation, depth of insertion, EMML, ICPI, HF) will be calculated from both imaging modalities (i.e. X-ray, CBCT, spiral CT and microCT) and the 'reference standard' (i.e. histology)

c. 1 Derivation of measures from imaging modalities

Once imaged, all data obtained from radiological analysis will be obtained issued by the imaging facilities to the study investigators in DICOM format. This is the standard format in which all imaging data is exported. Subsequently, this data will then be analysed using standard radiology analysis software which can resolve distances on the submillimetre scale. The abovementioned measures of intracochlear electrode position will then be calculated from the derived images.

c. 2 Derivation of measures from histology

The high-resolution histological micrographs will be analysed using standard histological analysis software which is also able to resolve distances on the submillimetre scale. The abovementioned measures of intracochlear electrode position will then be calculated from the derived micrographs.

For both c.1 and c. 2, multiple and repeated measures of each study parameter will be collected by at least two researchers independently, in order to determine inter- and intra-observer measurement error rates.

d. Data analysis

Following this, a comparison of these measures will be made between those derived from imaging and histology. Statistical analysis will be performed in conjunction with a medical statistician (A/Prof Kerry Hitos) using standard statistical software (such a SPSS) in order to draw conclusions about the validity, relevance and usefulness of existing measures of cochlear electrode positioning, and potentially derive novel, clinically useful measures.

The results of this comparison, and specifically how closely the imaging measures compare to those obtained from histology will form the major finding of this project.

This data set will provide the most robust validation study of radiological measures of cochlear implant electrode position available in the literature.

e. Dissemination of knowledge

This study will be written up in the form of a manuscript for submission to high-impact, peer-reviewed scientific journals in the field of otology and cochlear implantation. It will be submitted to national and international otology conferences for presentation to a wide audience who is likely to benefit from this knowledge. Furthermore the results will be submitted by Alon Taylor to the University of Sydney in the form

of a the thesis to satisfy the requirements of his candidacy for a Masters of Philosophy (Health and Medicine).

f. Reflection and consideration of next steps

This data set will provide a robust validation of currently used measures of intracochlear electrode position. There are several possible expected responses to the generated conclusions. This may include more widespread use of one or more specific electrode position measures analysed in this study, which are shown to be particularly valid and clinically relevant. This will have implications for both cochlear implant surgeons and radiologists. Other electrode position measures may be shown to be less accurate and their use and application may diminish.

There are several possible future avenues for research which may be generated from this study. The most obvious is the derivation of novel measures of intracochlear electrode position which are formulated and created based on our data set and used in future analysis of cochlear implant electrode position. Furthermore, the contribution that electrode position makes to hearing outcomes through variations in the electrode-neural interface in cochlear implant recipients is a critical missing part of current understanding of outcome variability. This knowledge is relevant to current uses of cochlear implants and the engineering of future designs.

Resources

This project will require several resources and, as mentioned will be undertaken in conjunction with an industry partner, Cochlear Limited.

Intellectual property and data ownership

Data ownership and publication rights will be shared between Cochlear and the Investigators listed on the ethics approval application. The outcome of this study will be submitted for peer-review with the aim to publish in high impact otology and otolaryngology journals. A mutually agreed upon arrangement will be made between the Candidate (AT), Research Supervisor (MDC), Industry Collaboratory (Cochlear Ltd) and the University of Sydney prior to the commencement of the research project as to intellectual property rights and data ownership stemming from this project.

Human cadaveric temporal bone specimens

The preliminary estimate is of 12 – 16 human temporal bones which will be provided by Cochlear Ltd. Storage, implantation, histological preparation, and analysis of the implanted temporal bones will all occur at Cochlear Ltd.

Temporal bone laboratory

Implantation, fixation, sectioning, staining and microscopic photography of the temporal bones will occur at the Cochlear Ltd Temporal Bone Laboratory (Macquarie Park, 2113).

Individual/expertise to implant the cochlear electrodes

This will be performed by three of the principal investigators at the temporal bone laboratory at the Cochlear Ltd campus:

1. Melville Da Cruz (Staff Specialist in ENT Surgery (Westmead Hospital, Sydney) and A/Professor in Department of Surgery (Western Clinical School, USyd).
2. Alon Taylor (MPhil Candidate (USyd) and ENT Surgery registrar (Prince of Wales Hospital, Sydney)
3. Irfan Durmo (Research Associate, Cochlear Ltd).

Cochlear implant electrodes

Approximately 12 - 16 cochlear implant electrodes will be required. See Section 11.2 for more information about the types of electrodes which will be used. These electrodes are made by Cochlear Ltd and will be supplied by Cochlear Ltd

Imaging capabilities

The imaging modalities required for this process are:

I. Xray
II. Cone beam
III. Spiral CT
IV. MicroCT

See Section 11.4.1 for further information regarding imaging.

Histological capabilities

The technology, technical expertise and site for histological assessment of the implanted temporal bones will be provided by Cochlear Ltd by staff with specialist knowledge at Cochlear Ltd (Irfan Durmo).

Funding

As a part of this collaboration, funding in kind will be provided by Cochlear Ltd. These costs will cover those for the CI electrodes, temporal bone implantation/fixation/processing, lab facility and staff, MicroCT imaging, clinical imaging feeds and ethics submission costs. Costs incurred for the ethics approval application fees payable to the WSLHD will be covered by the Westmead Hospital Department of Otolaryngology-Head and Neck Surgery Research Department.

Statistical analysis

- All measures of electrode position (angle of rotation, depth of insertion, EMML, ICPI) will be obtained by visual observation of X-ray/CT and histological images on a computer screen viewed in appropriate software equipped with validated measuring tools.
- Multiple and repeated measures of each study parameter will be undertaken by at least two researchers to determine inter- and intra-observer measurement error rates.
- Comparisons of these measures will be made between those derived from X-ray/CT and histology (the reference standard) to determine the validity of visually acquired measures derived from clinically available X-ray and CT imaging.
- In a limited number of cases, opportunities for acquiring measurements using automated machine learning will be investigated.

We will consult with a medical statistician (A/Prof Kerry Hitos) to ensure appropriate and accurate statistical analysis is undertaken.

Ethical considerations

Privacy

- As determined by the details of the donor patient consent form (See 'Consent' section below and Appendix 2), the identify of the donors is unknown to both the study investigators and Cochlear Ltd.

Storage, retention and destruction of data

- Storage of cadaveric temporal bones for this project will be at the Cochlear Ltd campus in Sydney (1 University Ave, Macquarie Park NSW 2113) within the site's licenced Temporal Bone Laboratory (TBL). The TBL is a purpose-built surgical laboratory designed for testing, storage and implantation of cochlear electrodes into cadaveric temporal bones.
- All data derived from imaging and histology acquired from multiple sites (Cochlear Ltd., USyd Imaging Centre and Castlereagh Imaging Westmead) will be stored on a REDCap[1] centralised, password

[1] Account provided by the University of Sydney (https://redcap.sydney.edu.au/)

protected study database. Access to the stored data will only be granted to the CPI and PIs listed in the 'Investigators' section of this proposal.

- Data sets will only be identified by a unique study identified number allocated to each temporal bone at the commencement of the study. The donor identity of the study temporal bones is unknown to the study investigators and to Cochlear Ltd (see Appendix 2). In this way donor privacy is protected.
- The study database will be held for a period of 5 years following publication of the study findings and then will be securely destroyed.
- The disposal of the temporal bones at the conclusion of the study will be determined by the donor consent (See Appendix 2) and standard operating procedures in the Cochlear Ltd TBL which is governed by its licence agreement with NSW Health. Specifically this is by cremation of all tissues derived from the tissue block at the North Sydney Crematorium using standard techniques governed by the Human Tissue Act 1983[30]. This will be performed at 5 years after the publication of the study results, with the specimens being securely archived at the Cochlear Ltd campus TBL during the intervening period.

Consent

- This project will make use of cadaveric temporal bones which will be provided by Cochlear Ltd.
- The organisation from which Cochlear Ltd acquires cadaveric temporal bones is Science Care, Inc. (Phoenix, AZ, USA). Appendix 2 contains all pertinent documentation relating to Science Care and Cochlear Ltd's acquisition of cadaveric temporal bones from Sciene Care
- Science Care (www.sciencecare.com) is a whole body donation organisation based in Arizona, USA that is accredited by the American Association of Tissue Banks (AATB) (https://www.aatb.org/science-care-inc; Accreditation number 00124/7; Accreditation Expiry March 7th 2024) for the acquisition, preparation, storage, distribution and authorisation of non-transplant anatomical material (See Appendix 2 – 'Science Care – Statement of purpose and standards documentation' and 'Science Care – Statement of Accreditation by the AATB (American Association of Tissue Banks)'
- Informed consent is obtained for all donors accepted into the program in the form of authorisation for Donation and Cremation (see 'Donation and Cremation Consent' forms in Appendix 2).
- All legal consents obtained from donors and Next of Kin are retained indefinitely.In accordance with AATB Standards, monetary inducement or other valuable consideration (including goods or services) are never offered to a donor, authorising person, donor's estate or any 3rd party. Science Care protocols require that all donor information remains anonymous. Confidential donor information is not permitted to be released to the end user, or the general public. See Appendix 2.
- The 'Donation and Cremation Consent' form is sufficiently broad such that it satisfies the consent requirements of the Human Tissue Act.

Custodianship

For this project, we will assign a specimen custodian under the anatomy licence (Dr. Irfan Durmo) who will be responsible for each specimen during the course of the research process, whilst it is taken to an offsite imaging centre and until it is returned back to the primary licenced authority.

- A letter written by the NSW Chief Health Officer has been issued to Dr. Durmo to approve the transfer of the human tissue blocks from Cochlear Limited to the participating offsite imaging centres. This letter is contained in Appendix 2.

Should the specimen custodian (Dr. Irfan Durmo) be unable to physically accompany a specimen to an offsite imaging centre (due to logistical reasons), an authority letter written by the specimen custodian will be issued to the individual accompanying the specimen to the offsite imaging centre. This individual will be either the Principal Investigator (Dr. Alon Taylor) or the Coordinating Principal Investigator (A/Prof. Melville Da Cruz) who will transport and accompany the specimens to and from the locations and act as specimen custodian during this time.

Conclusions/Outcomes

The successful completion of this study will form the most robust validation study of radiological measurements of intracochlear electrode position available in the literature. The study outcomes are likely to fill a knowledge gap in the many aspects of cochlear implant research. The validity and accuracy of available imaging methods to quantified measures of intracochlear electrode position, will be better understood. The contribution electrode position makes to hearing outcomes through variations in the electrode-neural interface in cochlear implant recipients is a critical missing part of current understanding of outcome variability. This knowledge is relevant to current uses of cochlear implants and the engineering of future designs.

References

1. Ramos de Miguel Á, Durmo I, Falcón González JC, Borkoski Barreiro S, Ramos Macias A. Evaluation of Intracochlear Position of a Slim Modiolar Electrode Array, by Using Different Radiological Analyses. Otol Neurotol. 2019;40(5S Suppl 1):S10-S17.
2. Long CJ, Holden TA, McClelland GH, et al. Examining the electro-neural interface of cochlear implant users using psychophysics, CT scans, and speech understanding. JARO J Assoc Res Otolaryngol. 2014;15(2):293-304.
3. Holden LK, Finley CC, Firszt JB, et al. Factors affecting open-set word recognition in adults with cochlear implants. Ear Hear. 2013;34(3):342-360.
4. Blamey P, Artieres F, Başkent D, et al. Factors affecting auditory performance of postlinguistically deaf adults using cochlear implants: An update with 2251 patients. Audiol Neurotol. 2012;18(1):36-47.
5. Connor SEJ. Contemporary imaging of auditory implants. Clin Radiol. 2018;73(1):19-34.
6. Lee SY, Han JH, Carandang M, Bae YJ, Choi BY. Simpler and effective radiological evaluations for modiolar proximity of a slim modiolar cochlear implant electrode. Sci Rep. 2020;10(1).
7. The University of Sydney. Preclinical imaging. https://www.sydney.edu.au/research/facilities/sydney-imaging/preclinical-imaging.html. Published 2022. Accessed.
8. Heutink F, De Rijk SR, Verbist BM, Huinck WJ, Mylanus EAM. Angular Electrode Insertion Depth and Speech Perception in Adults with a Cochlear Implant: A Systematic Review. Otology and Neurotology. 2019;40(7):900-910.
9. Chakravorti S, Noble JH, Gifford RH, et al. Further Evidence of the Relationship Between Cochlear Implant Electrode Positioning and Hearing Outcomes. Otol Neurotol. 2019;40(5):617-624.
10. Eshraghi AA, Yang NW, Balkany TJ. Comparative study of cochlear damage with three perimodiolar electrode designs. Laryngoscope. 2003;113(3):415-419.
11. Sturm JJ, Patel V, Dibelius G, Kuhlmey M, Kim AH. Comparative Performance of Lateral Wall and Perimodiolar Cochlear Implant Arrays. Otology & neurotology : official publication of the American Otological Society, American Neurotology Society [and] European Academy of Otology and Neurotology. 2021;42(4):532-539.
12. Ramos Macias A, Perez Zaballos MT, Ramos de Miguel A, Cervera Paz J. Importance of Perimodiolar Electrode Position for Psychoacoustic Discrimination in Cochlear Implantation. Otology & neurotology. 2017;38(10):e429-e437.
13. Garaycochea O, Manrique-Huarte R, Lazaro C, et al. Comparative study of two different perimodiolar and a straight cochlear implant electrode array: surgical and audiological outcomes. Eur Arch Oto-Rhino-Laryngol. 2020;277(1):69-76.
14. Holder JT, Yawn RJ, Nassiri AM, et al. Matched Cohort Comparison Indicates Superiority of Precurved Electrode Arrays. Otol Neurotol. 2019;40(9):1160-1166.

15. Ramos de Miguel Á, Argudo AA, Borkoski Barreiro SA, Falcón González JC, Ramos Macías A. Imaging evaluation of electrode placement and effect on electrode discrimination on different cochlear implant electrode arrays. Eur Arch Oto-Rhino-Laryngol. 2018;275(6):1385-1394.
16. Shaul C, Weder S, Tari S, Gerard JM, O'Leary SJ, Briggs RJ. Slim, Modiolar Cochlear Implant Electrode: Melbourne Experience and Comparison with the Contour Perimodiolar Electrode. Otol Neurotol. 2020;41(5):639-643.
17. Holden LK, Firszt JB, Reeder RM, Uchanski RM, Dwyer NY, Holden TA. Factors affecting outcomes in cochlear implant recipients implanted with a perimodiolar electrode array located in scala tympani. Otol Neurotol. 2016;37(10):1662-1668.
18. De Miguel ÁR, Durmo I, González JCF, Barreiro SB, Macías AR. Evaluation of Intracochlear Position of a Slim Modiolar Electrode Array, by Using Different Radiological Analyses. Otology and Neurotology. 2019;40(4):S10-S17.
19. Cochlear Ltd Nucleus® implant portfolio. https://www.cochlear.com/us/en/professionals/products-and-candidacy/nucleus/implant#:~:text=spiral%20ganglion%20cells.-,Slim,industry's%20thinnest%20full%20length%20electrode.&text=A%20soft%20tip%20combined%20with,protect%20the%20delicate%20cochlear%20structures. Published 2022. Accessed.
20. Marx M, Risi F, Escudé B, et al. Reliability of cone beam computed tomography in scalar localization of the electrode array: A radio histological study. Eur Arch Oto-Rhino-Laryngol. 2014;271(4):673-679.
21. Needham K, Stathopoulos D, Newbold C, et al. Electrode impedance changes after implantation of a dexamethasone-eluting intracochlear array. Cochlear Implants International. 2020;21(2):98-109.
22. Wei F, Li J, Zhou C, et al. Combined application of single-energy metal artifact reduction and reconstruction techniques in patients with Cochlear implants. J Otolaryngol Head Neck Surg. 2020;49(1).
23. Kennedy TA, Connell N, Szczykutowicz T, et al. Flat-Panel CT for cochlear implant electrode imaging: Comparison to multi-detector CT. Otology and Neurotology. 2016;37(10):1646-1653.
24. Bamberg F, Dierks A, Nikolaou K, Reiser MF, Becker CR, Johnson TRC. Metal artifact reduction by dual energy computed tomography using monoenergetic extrapolation. European Radiology. 2011;21(7):1424-1429.
25. Iso-Mustajärvi M, Matikka H, Risi F, et al. A New Slim Modiolar Electrode Array for Cochlear Implantation: A Radiological and Histological Study. Otology and Neurotology. 2017;38(9):e327-e334.
26. Cushing SL, Daly MJ, Treaba CG, et al. High-resolution cone-beam computed tomography: A potential tool to improve atraumatic electrode design and position. Acta Oto-Laryngol. 2012;132(4):361-368.

27. Saeed SR, Selvadurai D, Beale T, et al. The use of cone beam imaging to determine cochlear implant electrode position in human temporal bones. Cochlear Implants International. 2013;14(SUPPL. 4):S14-S15.
28. Saeed SR, Selvadurai D, Beale T, et al. The use of cone-beam computed tomography to determine cochlear implant electrode position in human temporal bones. Otology and Neurotology. 2014;35(8):1338-1344.
29. Mosnier I, Célérier C, Bensimon JL, et al. Cone beam computed tomography and histological evaluations of a straight electrode array positioning in temporal bones. Acta Oto-Laryngol. 2017;137(3):229-234.
30. NSW Government Human Tissue Act 1983 No 164. In.

References

1. Skarżyński H, Lorens A, Matusiak M, Porowski M, Skarżyński PH, James CJ. Cochlear implantation with the nucleus slim straight electrode in subjects with residual low-frequency hearing. Article. *Ear and Hearing*. 2014;35(2):e33-e43. doi:10.1097/01.aud.0000444781.15858.f1

2. Snels C, In't Hout J, Mylanus E, Huinck W, Dhooge I. Hearing Preservation in Cochlear Implant Surgery: A Meta-Analysis. Article. *Otology and Neurotology*. 2019;40(2):145-153. doi:10.1097/MAO.0000000000002083

3. Varadarajan VV, Sydlowski SA, Li MM, Anne S, Adunka OF. Evolving Criteria for Adult and Pediatric Cochlear Implantation. Editorial. *Ear, Nose and Throat Journal*. 2021;100(1):31-37. doi:10.1177/0145561320947258

4. Blamey P, Arndt P, Brimacombe J, et al. Factors affecting auditory performance of postlinguistically deaf adults using cochlear implants. Article. *Audiol Neuro-Otol*. 1996;1(5):293-306. doi:10.1159/000259212

5. Blamey P, Artieres F, Başkent D, et al. Factors affecting auditory performance of postlinguistically deaf adults using cochlear implants: An update with 2251 patients. Article. *Audiol Neurotol*. 2012;18(1):36-47. doi:10.1159/000343189

6. Lazard DS, Vincent C, Venail F, et al. Pre-, Per- and Postoperative Factors Affecting Performance of Postlinguistically Deaf Adults Using Cochlear Implants: A New Conceptual Model over Time. Article. *PLoS ONE*. 2012;7(11)e48739. doi:10.1371/journal.pone.0048739

7. Zhao EE, Dornhoffer JR, Loftus C, et al. Association of Patient-Related Factors with Adult Cochlear Implant Speech Recognition Outcomes: A Meta-analysis. Article. *JAMA Otolaryngology - Head and Neck Surgery*. 2020;146(7):613-620. doi:10.1001/jamaoto.2020.0662

8. Holden LK, Finley CC, Firszt JB, et al. Factors affecting open-set word recognition in adults with cochlear implants. Research Support, N.I.H., Extramural. *Ear Hear*. May-Jun 2013;34(3):342-60. doi:https://dx.doi.org/10.1097/AUD.0b013e3182741aa7

9. Giraud AL, Lee HJ. Predicting cochlear implant outcome from brain organisation in the deaf. Article. *Restor Neurol Neurosci*. 2007;25(3-4):381-390.

10. Lazard DS, Lee HJ, Gaebler M, Kell CA, Truy E, Giraud AL. Phonological processing in post-lingual deafness and cochlear implant outcome. Article. *NeuroImage*. 2010;49(4):3443-3451. doi:10.1016/j.neuroimage.2009.11.013

11. Nguyen S, Cloutier F, Philippon D, Côté M, Bussières R, Backous DD. Outcomes review of modern hearing preservation technique in cochlear implant. Review. *Auris Nasus Larynx*. 2016;43(5):485-488. doi:10.1016/j.anl.2016.02.014

12. Santa Maria PL, Gluth MB, Yuan Y, Atlas MD, Blevins NH. Hearing preservation surgery for cochlear implantation: A meta-analysis. Article. *Otology and Neurotology*. 2014;35(10):e256-e269. doi:10.1097/MAO.0000000000000561

13. O'Connell BP, Cakir A, Hunter JB, et al. Electrode Location and Angular Insertion Depth Are Predictors of Audiologic Outcomes in Cochlear Implantation. *Otology and Neurotology*. 2016;37(8):1016-1023. doi:10.1097/MAO.0000000000001125

14. Wanna GB, Noble JH, Carlson ML, et al. Impact of electrode design and surgical approach on scalar location and cochlear implant outcomes. Article. *Laryngoscope*. 2014;124(S6):S1-S7. doi:10.1002/lary.24728

15. Chakravorti S, Noble JH, Gifford RH, et al. Further Evidence of the Relationship Between Cochlear Implant Electrode Positioning and Hearing Outcomes. *Otology & neurotology : official publication of the American Otological Society, American Neurotology Society [and] European Academy of Otology and Neurotology*. 2019;40(5):617-624. doi:10.1097/MAO.0000000000002204

16. O'Connell BP, Hunter JB, Haynes DS, et al. Insertion depth impacts speech perception and hearing preservation for lateral wall electrodes. Research Support, N.I.H., Extramural. *Laryngoscope*. 10 2017;127(10):2352-2357. doi:https://dx.doi.org/10.1002/lary.26467

17. Skinner MW, Ketten DR, Holden LK, et al. CT-derived estimation of cochlear morphology and electrode array position in relation to word recognition in Nucleus-22 recipients. Research Support, Non-U.S. Gov't

Research Support, U.S. Gov't, P.H.S. *J Assoc Res Otolaryngol*. Sep 2002;3(3):332-50. doi:https://dx.doi.org/10.1007/s101620020013

18. Buchman CA, Dillon MT, King ER, Adunka MC, Adunka OF, Pillsbury HC. Influence of cochlear implant insertion depth on performance: A prospective randomized trial. *Otology and Neurotology*. 2014;35(10):1773-1779. doi:10.1097/MAO.0000000000000541

19. Canfarotta MW, Dillon MT, Brown KD, Pillsbury HC, Dedmon MM, O'Connell BP. Insertion Depth and Cochlear Implant Speech Recognition Outcomes: A Comparative Study of 28- and 31.5-mm Lateral Wall Arrays. *Otology and Neurotology*. 2022;43(2):183-189. doi:10.1097/MAO.0000000000003416

20. Verberne J, Risi F, Campbell L, Chambers S, O'Leary S. The effect of scala tympani morphology on basilar membrane contact with a straight electrode array: A human temporal bone study. Article. *Otology and Neurotology*. 2017;38(1):47-53. doi:10.1097/MAO.0000000000001259

21. Risi F. Considerations and Rationale for Cochlear Implant Electrode Design - Past, Present and Future. *J*. 2018;14(3):382-391. doi:10.5152/iao.2018.6372

22. Wanna GB, O'Connell BP, Francis DO, et al. Predictive factors for short- and long-term hearing preservation in cochlear implantation with conventional-length electrodes. Article. *Laryngoscope*. 2018;128(2):482-489. doi:10.1002/lary.26714

23. Vohra V, Andresen NS, Carver C, et al. Cochlear Implant Electrode Array Design and Speech Understanding. Article. *Otology and Neurotology*. 2024;45(2):136-142. doi:10.1097/MAO.0000000000004083

24. Sturm JJ, Patel V, Dibelius G, Kuhlmey M, Kim AH. Comparative Performance of Lateral Wall and Perimodiolar Cochlear Implant Arrays. *Otol Neurotol*. 2021;42(4):532-539. doi:10.1097/MAO.0000000000002997

25. Verbist BM, Skinner MW, Cohen LT, et al. Consensus panel on a cochlear coordinate system applicable in histologic, physiologic, and radiologic studies of the human cochlea. Article. *Otology and Neurotology*. 2010;31(5):722-730. doi:10.1097/MAO.0b013e3181d279e0

26. McInnes MDF, Moher D, Thombs BD, et al. Preferred Reporting Items for a Systematic Review and Meta-analysis of Diagnostic Test Accuracy Studies The PRISMA-DTA Statement. Article. *JAMA*. 2018;319(4):388-396. doi:10.1001/jama.2017.19163

27. Agency for Healthcare Research and Quality. *Methods Guide for Effectiveness and Comparative Effectiveness Reviews*. 2014. 10(14)-EHC063-EF. https://effectivehealthcare.ahrq.gov/topics/cer-methods-guide/overview

28. Whiting PF. QUADAS-2: A Revised Tool for the Quality Assessment of Diagnostic Accuracy Studies. *Annals of Internal Medicine*. 2011;155(8):529-536. doi:10.7326/0003-4819-155-8-201110180-00009

29. McGuinness LA, Higgins JPT. Risk-of-bias VISualization (robvis): An R package and Shiny web app for visualizing risk-of-bias assessments. John Wiley and Sons Ltd; 2021:55-61.

30. Aschendorff A, Kubalek R, Hochmuth A, et al. Imaging procedures in cochlear implant patients--evaluation of different radiological techniques. *Acta Otolaryngol Suppl (Stockh)*. May 2004;(552):46-9.

31. Bartling SH, Gupta R, Torkos A, et al. Flat-panel volume computed tomography for cochlear implant electrode array examination in isolated temporal bone specimens. Comparative Study. *Otol Neurotol*. Jun 2006;27(4):491-8. doi:https://dx.doi.org/10.1097/01.mao.0000194816.15298.50

32. Burck I, Schneider SV, Balster S, et al. Radiohistologic Comparison Study of Temporal Bone Specimens After Cochlear Implant Electrode Array Insertion: Is Cone-Beam CT Superior to MDCT? Comparative Study

Research Support, Non-U.S. Gov't. *AJR Am J Roentgenol*. 03 2021;216(3):752-758. doi:https://dx.doi.org/10.2214/AJR.20.23157

33. Carlson ML, Leng S, Diehn FE, et al. Cochlear Implant Electrode Localization Using an Ultra-High Resolution Scan Mode on Conventional 64-Slice and New Generation 192-Slice Multi-Detector Computed Tomography. *Otol Neurotol*. 08 2017;38(7):978-984. doi:https://dx.doi.org/10.1097/MAO.0000000000001463

34. Cushing SL, Daly MJ, Treaba CG, et al. High-resolution cone-beam computed tomography: a potential tool to improve atraumatic electrode design and position. Research Support, Non-U.S. Gov't. *Acta Otolaryngol (Stockh)*. Apr 2012;132(4):361-8. doi:https://dx.doi.org/10.3109/00016489.2011.644805

35. De Seta D, Mancini P, Russo FY, et al. 3D curved multiplanar cone beam CT reconstruction for intracochlear position assessment of straight electrodes array. A temporal bone and clinical study. *Acta Otorhinolaryngol Ital*. Dec 2016;36(6):499-505. Ricostruzione multiplanare 3D di immagini cone beam per l'idenficazione della posizione degli impianti cocleari. doi:https://dx.doi.org/10.14639/0392-100X-1279

36. Eisenhut F, Taha L, Manhart M, et al. High-speed flat-detector computed tomography for temporal bone imaging and postoperative control of cochlear implants. *Neuroradiology*. Jul 2022;64(7):1437-1445. doi:https://dx.doi.org/10.1007/s00234-022-02940-x

37. Helbig S, Mack M, Schell B, Bratzke H, Stöver T, Helbig M. Scalar localization by computed tomography of cochlear implant electrode carriers designed for deep insertion. Article. *Otology and Neurotology*. 2012;33(5):745-750. doi:10.1097/MAO.0b013e318259520c

38. Husstedt HW, Aschendorff A, Richter B, Laszig R, Schumacher M. Nondestructive three-dimensional analysis of electrode to modiolus proximity. *Otol Neurotol*. Jan 2002;23(1):49-52. doi:https://dx.doi.org/10.1097/00129492-200201000-00012

39. Iso-Mustajarvi M, Matikka H, Risi F, et al. A New Slim Modiolar Electrode Array for Cochlear Implantation: A Radiological and Histological Study. *Otol Neurotol*. 10 2017;38(9):e327-e334. doi:https://dx.doi.org/10.1097/MAO.0000000000001542

40. Karkas A, Boureille P, Laroche N, Vico L, Bergandi F, Marotte H. Imaging of the human cochlea using micro-computed tomography before and after cochlear implantation: comparison with cone-beam computed tomography. *Eur Arch Otorhinolaryngol*. Jul 2023;280(7):3131-3140. doi:https://dx.doi.org/10.1007/s00405-022-07811-y

41. Kennedy TA, Connell N, Szczykutowicz T, et al. Flat-Panel CT for Cochlear Implant Electrode Imaging: Comparison to Multi-Detector CT. *Otol Neurotol*. 12 2016;37(10):1646-1653. doi:https://dx.doi.org/10.1097/MAO.0000000000001216

42. Kurzweg T, Dalchow CV, Bremke M, et al. The value of digital volume tomography in assessing the position of cochlear implant arrays in temporal bone specimens. Validation Study. *Ear Hear*. Jun 2010;31(3):413-9. doi:https://dx.doi.org/10.1097/AUD.0b013e3181d3d6b6

43. Lane JI, Driscoll CLW, Witte RJ, Primak A, Lindell EP. Scalar Localization of the Electrode Array After Cochlear Implantation: A Cadaveric Validation Study Comparing 64-Slice Multidetector Computed Tomography With Microcomputed Tomography. *Otol Neurotol*. 2007;28(2):191-194. doi:10.1097/01.mao.0000247817.31572.ed

44. Lecerf P, Bakhos D, Cottier JP, Lescanne E, Trijolet JP, Robier A. Midmodiolar reconstruction as a valuable tool to determine the exact position of the cochlear implant electrode array. *Otol Neurotol*. Sep 2011;32(7):1075-81. doi:https://dx.doi.org/10.1097/MAO.0b013e318229d4dd

45. Manrique M, Picciafuoco S, Manrique R, et al. Atraumaticity study of 2 cochlear implant electrode arrays. *Otol Neurotol*. Apr 2014;35(4):619-28. doi:https://dx.doi.org/10.1097/MAO.0000000000000284

46. Marx M, Risi F, Escude B, et al. Reliability of cone beam computed tomography in scalar localization of the electrode array: a radio histological study. *Eur Arch Otorhinolaryngol*. Apr 2014;271(4):673-9. doi:https://dx.doi.org/10.1007/s00405-013-2448-6

47. Mosnier I, Célérier C, Bensimon J-L, et al. Cone beam computed tomography and histological evaluations of a straight electrode array positioning in temporal bones. *Acta Otolaryngol (Stockh)*. 2017;137(3):229-234. doi:10.1080/00016489.2016.1227477

48. Razafindranaly V, Truy E, Pialat JB, et al. Cone Beam CT Versus Multislice CT: radiologic Diagnostic Agreement in the Postoperative Assessment of Cochlear Implantation. Journal article. *Otol Neurotol*. 2016;Vol.37(9):1246-1254p.

49. Saeed SR, Selvadurai D, Beale T, et al. The use of cone-beam computed tomography to determine cochlear implant electrode position in human temporal bones. *Otol Neurotol*. Sep 2014;35(8):1338-44. doi:https://dx.doi.org/10.1097/MAO.0000000000000295

50. Schuman TA, Noble JH, Wright CG, Wanna GB, Dawant B, Labadie RF. Anatomic verification of a novel method for precise intrascalar localization of cochlear implant electrodes in adult temporal bones using clinically available computed tomography. Comparative Study

Research Support, N.I.H., Extramural

Research Support, Non-U.S. Gov't. *Laryngoscope*. Nov 2010;120(11):2277-83. doi:https://dx.doi.org/10.1002/lary.21104

51. Sipari S, Iso-Mustajarvi M, Kononen M, Lopponen H, Dietz A. The Image Fusion Technique for Cochlear Implant Imaging: A Study of its Application for Different Electrode Arrays. Research Support, Non-U.S. Gov't. *Otol Neurotol*. 02 2020;41(2):e216-e222. doi:https://dx.doi.org/10.1097/MAO.0000000000002479

52. Teymouri J, Hullar TE, Holden TA, Chole RA. Verification of computed tomographic estimates of cochlear implant array position: A micro-CT and histologic analysis. Review. *Otology and Neurotology*. 2011;32(6):980-986. doi:10.1097/MAO.0b013e3182255915

53. Zeitler DM, Wang KH, Prasad RS, Wang EY, Roland JT. Flat-panel computed tomography versus multislice computed tomography to evaluate cochlear implant positioning. Comparative Study. *Cochlear implants int*. Nov 2011;12(4):216-22. doi:https://dx.doi.org/10.1179/146701011X12962268235742

54. Zou J, Hannula M, Lehto K, et al. X-ray microtomographic confirmation of the reliability of CBCT in identifying the scalar location of cochlear implant electrode after round window insertion. Research Support, Non-U.S. Gov't. *Hear Res*. Aug 2015;326:59-65. doi:https://dx.doi.org/10.1016/j.heares.2015.04.005

55. Ramos de Miguel A, Durmo I, Falcon Gonzalez JC, et al. Evaluation of Intracochlear Position of a Slim Modiolar Electrode Array, by Using Different Radiological Analyses. *Otol Neurotol*. 2019;40:S10-S17. doi:10.1097/MAO.0000000000002213

56. Rak K, Spahn B, Muller-Graff FT, et al. The Photon-Counting CT Enters the Field of Cochlear Implantation: Comparison to Angiography DynaCT and Conventional Multislice CT. Comparative Study. *Otol Neurotol*. Jul 01 2024;45(6):662-670. doi:https://dx.doi.org/10.1097/MAO.0000000000004221

57. James CJ, Karoui C, Laborde M-L, et al. Early Sentence Recognition in Adult Cochlear Implant Users. *Ear & Hearing (01960202)*. 2019;40(4):905-917. doi:10.1097/AUD.0000000000000670

58. Shaul C, Dragovic AS, Stringer AK, O'Leary SJ, Briggs RJ. Scalar localisation of peri-modiolar electrodes and speech perception outcomes. Observational Study. *J Laryngol Otol*. Nov 2018;132(11):1000-1006. doi:https://dx.doi.org/10.1017/S0022215118001871

59. Zelener F, Majdani O, Roemer A, et al. Relations between Scalar Shift and Insertion Depth in Human Cochlear Implantation. Article. *Otology and Neurotology*. 2020;41(2):178-185. doi:10.1097/MAO.0000000000002460

60. Hasan Z, Key S, Lee M, Da Cruz M. Systematic Review of Intracochlear Measurements and Effect on Postoperative Auditory Outcomes after Cochlear Implant Surgery. *Otol Neurotol*. 2024;45(1)

61. Lee SY, Han JH, Carandang M, Bae YJ, Choi BY. Simpler and effective radiological evaluations for modiolar proximity of a slim modiolar cochlear implant electrode. Research Support, Non-U.S. Gov't. *Sci*. 10 19 2020;10(1):17714. doi:https://dx.doi.org/10.1038/s41598-020-74738-x

62. Widmann G, Dejaco D, Luger A, Schmutzhard J. Pre- and post-operative imaging of cochlear implants: a pictorial review. Review. *Insights Imaging*. 2020;11(1)93. doi:10.1186/s13244-020-00902-6

63. Barrett JF, Keat N. Artifacts in CT: Recognition and avoidance. Review. *Radiographics*. 2004;24(6):1679-1796. doi:10.1148/rg.246045065

64. Scarfe WC, Farman AG, Sukovic P. Clinical applications of cone-beam computed tomography in dental practice. Review. *J Can Dent Assoc*. 2006;72(1):75-80.

65. Helal RA, Jacob R, Elshinnawy MA, et al. Cone-beam CT versus Multidetector CT in Postoperative Cochlear Implant Imaging: Evaluation of Image Quality and Radiation Dose. Multicenter Study. *AJNR Am J Neuroradiol*. 01 2021;42(2):362-367. doi:https://dx.doi.org/10.3174/ajnr.A6894

66. Miracle AC, Mukherji SK. Conebeam CT of the Head and Neck, Part 2: Clinical Applications. *American journal of neuroradiology : AJNR*. 2009;30(7):1285-1292. doi:10.3174/ajnr.A1654

67. Ruivo J, Mermuys K, Bacher K, Kuhweide R, Offeciers E, Casselman JW. Cone beam computed tomography, a low-dose imaging technique in the postoperative assessment of cochlear implantation. Case Reports. *Otol Neurotol*. Apr 2009;30(3):299-303. doi:https://dx.doi.org/10.1097/MAO.0b013e31819679f9

68. Theunisse HJ, Joemai RM, Maal TJ, Geleijns J, Mylanus EA, Verbist BM. Cone-beam CT versus multi-slice CT systems for postoperative imaging of cochlear implantation--a phantom study on image quality and radiation exposure using human temporal bones. Research Support, Non-U.S. Gov't. *Otol Neurotol*. Apr 2015;36(4):592-9. doi:https://dx.doi.org/10.1097/MAO.0000000000000673

69. Guberina N, Dietrich U, Arweiler-Harbeck D, Forsting M, Ringelstein A. Comparison of radiation doses imparted during 128-, 256-, 384-multislice CT-scanners and cone beam computed tomography for intra- and perioperative cochlear implant assessment. Comparative Study. *Am J Otolaryngol*. Nov - Dec 2017;38(6):649-653. doi:https://dx.doi.org/10.1016/j.amjoto.2017.09.005

70. Willemink MJ, Persson M, Pourmorteza A, Pelc NJ, Fleischmann D. Photon-counting CT: Technical principles and clinical prospects. Review. *Radiology*. 2018;289(2):293-312. doi:10.1148/radiol.2018172656

71. Tian X, Huang Y, Tong J, et al. Photon counting CT versus multi-slice CT for radiographic evaluation of postoperative cochlear implantation: Electrode characteristics and image-quality analysis. *Eur J Radiol*. 2025;191:112331. doi:10.1016/j.ejrad.2025.112331

72. Canfarotta MW, Dillon MT, Buss E, Pillsbury HC, Brown KD, O'Connell BP. Frequency-To-Place Mismatch: Characterizing Variability and the Influence on Speech Perception Outcomes in Cochlear Implant Recipients. Article. *Ear and Hearing*. 2020;41(5):1349-1361. doi:10.1097/AUD.0000000000000864

73. Landsberger DM, Svrakic M, Roland JT, Svirsky M. The Relationship between Insertion Angles, Default Frequency Allocations, and Spiral Ganglion Place Pitch in Cochlear Implants. Article. *Ear and Hearing*. 2015;36(5):e207-e213. doi:10.1097/AUD.0000000000000163

74. Davis TJ, Zhang D, Gifford RH, Dawant BM, Labadie RF, Noble JH. Relationship between electrode-To-modiolus distance and current levels for adults with cochlear implants. Article. *Otology and Neurotology*. 2016;37(1):31-37. doi:10.1097/MAO.0000000000000896

75. Boas FE, Fleischmann D. CT artifacts: Causes and reduction techniques. Review. *Imaging Med*. 2012;4(2):229-240. doi:10.2217/iim.12.13

76. Bevis N, Effertz T, Beutner D, Gueldner C. Evaluation of artifacts of cochlear implant electrodes in cone beam computed tomography. *Eur Arch Otorhinolaryngol*. May 2021;278(5):1381-1386. doi:https://dx.doi.org/10.1007/s00405-020-06198-y

77. Diogo I, Franke N, Steinbach-Hundt S, et al. Differences of radiological artefacts in cochlear implantation in temporal bone and complete head. Article. *Cochlear implants int*. 2014;15(2):112-117. doi:10.1179/1754762813Y.0000000035

78. Shibata T, Matsumoto S, Agishi T, Nagano T. Visualization of Reissner membrane and the spiral ganglion in human fetal cochlea by micro-computed tomography. Article. *American Journal of Otolaryngology - Head and Neck Medicine and Surgery*. 2009;30(2):112-120. doi:10.1016/j.amjoto.2008.07.012

79. Ltd. C. Slim Straight Electrode (CI622). Accessed 5th August, 2025. https://www.cochlear.com/us/en/professionals/products-and-candidacy/nucleus/implant/electrodes/slim-straight

80. Ltd. C. Slim Modiolar Electrode (CI632). Accessed 5th August, 2025. https://www.cochlear.com/us/en/professionals/products-and-candidacy/nucleus/implant/electrodes/slim-modiolar

81. Sismono F, Mancini L, Leblans M, et al. Synchrotron radiation X-ray microtomography for the visualization of intra-cochlear anatomy in human temporal bones implanted with a perimodiolar cochlear implant electrode array. *J Synchrotron Radiat*. Jan 01 2021;28(Pt 1):327-332. doi:https://dx.doi.org/10.1107/S1600577520014952

82. Le Breton A, Jegoux F, Pilet P, Godey B. Micro-CT scan, electron microscopy and optical microscopy study of insertional traumas of cochlear implants. Comparative Study. *Surg Radiol Anat*. Sep 2015;37(7):815-23. doi:https://dx.doi.org/10.1007/s00276-015-1469-9

83. Kikinis R, Pieper SD, Vosburgh KG, Jolesz FA. 3D Slicer: A Platform for Subject-Specific Image Analysis, Visualization, and Clinical Support. Springer New York; 2014:277-289.

84. Al-Dhamari I, Helal R, Abdelaziz T, Waldeck S, Paulus D. Automatic cochlear multimodal 3D image segmentation and analysis using atlas–model-based method. Article. *Cochlear implants int*. 2024;25(1):46-58. doi:10.1080/14670100.2023.2274199

85. Liu GS, Cooperman SP, Neves CA, Blevins NH. Estimation of Cochlear Implant Insertion Depth Using 2D-3D Registration of Postoperative X-Ray and Preoperative CT Images. Article. *Otology and Neurotology*. 2024;45(3):E156-E161. doi:10.1097/MAO.0000000000004100

86. Al-Dhamari I, Helal R, Morozova O, et al. Automatic intra-subject registration and fusion of multimodal cochlea 3D clinical images. Article. *PLoS ONE*. 2022;17(3 March)e0264449. doi:10.1371/journal.pone.0264449

87. Rolfe S, Pieper S, Porto A, et al. SlicerMorph: An open and extensible platform to retrieve, visualize and analyse 3D morphology. Article. *Methods Ecol Evol*. 2021;12(10):1816-1825. doi:10.1111/2041-210X.13669

88. *IBM SPSS Statistics for Windows, Version 31.0*. Version 31.0. IBM Corp; 2025.

89. Schober P, Mascha EJ, Vetter TR. Statistics From A (Agreement) to Z (z Score): A Guide to Interpreting Common Measures of Association, Agreement, Diagnostic Accuracy, Effect Size, Heterogeneity, and Reliability in Medical Research. *Anesthesia and analgesia*. 2021;133(6):1633-1641. doi:10.1213/ANE.0000000000005773

90. Wurfel W, Lanfermann H, Lenarz T, Majdani O. Cochlear length determination using Cone Beam Computed Tomography in a clinical setting. *Hear Res*. Oct 2014;316:65-72. doi:https://dx.doi.org/10.1016/j.heares.2014.07.013

91. Hussain R, Frater A, Calixto R, et al. Anatomical Variations of the Human Cochlea Using an Image Analysis Tool. *J Clin Med*. Jan 8 2023;12(2)doi:10.3390/jcm12020509

92. Schraivogel S, Aebischer P, Wagner F, et al. Postoperative Impedance-Based Estimation of Cochlear Implant Electrode Insertion Depth. Article. *Ear and Hearing*. 2023;44(6):1379-1388. doi:10.1097/AUD.0000000000001379

93. Brüllmann D, Schulze RKW. Spatial resolution in CBCT machines for dental/maxillofacial applications - What do we know today? Review. *Dentomaxillofac Radiol*. 2015;44(1)20140204. doi:10.1259/dmfr.20140204

94. Maret D, Peters OA, Galibourg A, et al. Comparison of the accuracy of 3-dimensional cone-beam computed tomography and micro-computed tomography reconstructions by using different voxel sizes. Article. *J Endod*. 2014;40(9):1321-1326. doi:10.1016/j.joen.2014.04.014

95. Patro A, Moberly AC, Freeman MH, et al. Investigating the Minimal Clinically Important Difference for AzBio and CNC Speech Recognition Scores. Article. *Otology and Neurotology*. 2024;45(9):e639-e643. doi:10.1097/MAO.0000000000004319

96. Whitmer WM, McShefferty D, Akeroyd MA. On detectable and meaningful speech-intelligibility benefits. Article. *Advances in Experimental Medicine and Biology*. 2016;894:447-455. doi:10.1007/978-3-319-25474-6_47

97. Suri N. *Imaging Handbook on Anatomy of Cochlea*. 1st ed. Thieme Medical Publishers; 2024.

98. Christensen GE, He J, Dill JA, Rubinstein JT, Vannier MW, Wang G. Automatic measurement of the labyrinth using image registration and a deformable inner ear atlas. Article. *Acad Radiol*. 2003;10(9):988-999. doi:10.1016/S1076-6332(03)00121-1

99. Geerardyn A, Zhu M, Klabbers T, et al. Human Histology after Structure Preservation Cochlear Implantation via Round Window Insertion. Article. *Laryngoscope*. 2024;134(2):945-953. doi:10.1002/lary.30900

100. Ishiyama A, Ishiyama G, López IA, Linthicum FH. Temporal Bone Histopathology of First-Generation Cochlear Implant Electrode Translocation. Article. *Otology and Neurotology*. 2019;40(6):E581-E591. doi:10.1097/MAO.0000000000002247

101. Elfarnawany M, Alam SR, Rohani SA, Zhu N, Agrawal SK, Ladak HM. Micro-CT versus synchrotron radiation phase contrast imaging of human cochlea. Article. *J Microsc*. 2017;265(3):349-357. doi:10.1111/jmi.12507

102. Li H, Helpard L, Ekeroot J, et al. Three-dimensional tonotopic mapping of the human cochlea based on synchrotron radiation phase-contrast imaging. Article. *Sci*. 2021;11(1)4437. doi:10.1038/s41598-021-83225-w

103. Li H, Schart-Moren N, Rajan G, et al. Vestibular Organ and Cochlear Implantation–A Synchrotron and Micro-CT Study. Article. *Frontiers in Neurology*. 2021;12663722. doi:10.3389/fneur.2021.663722

104. Rohani SA, Iyaniwura JE, Zhu N, Agrawal SK, Ladak HM. Effects of object-to-detector distance and beam energy on synchrotron radiation phase-contrast imaging of implanted cochleae. Article. *J Microsc*. 2019;273(2):127-134. doi:10.1111/jmi.12768

105. Heutink F, De Rijk SR, Verbist BM, Huinck WJ, Mylanus EAM. Angular Electrode Insertion Depth and Speech Perception in Adults with a Cochlear Implant: A Systematic Review. *Otology and Neurotology*. 2019;40(7):900-910. doi:10.1097/MAO.0000000000002298